Characterization of *Bacillus* Spore Membrane Proteomes and Investigation of Their Roles in the Spore Germination Process

Yan Chen

Dissertation submitted to the faculty of the Virginia Polytechnic Institute and State University in partial fulfillment of the requirements for the degree of

Doctor of Philosophy
In
Biological Sciences

David L. Popham, Chair
Stephen B. Melville
Richard F. Helm
Birgit E. Scharf

Sep 5th, 2014
Blacksburg, VA

Keywords: *Bacillus*, *subtilis*, *anthracis*, germination, membrane proteins, proteome, spore, SleB, YpeB, HtrC, protease

Characterization of *Bacillus* Spore Membrane Proteomes and Investigation of Their Roles in the Spore Germination Process

Yan Chen

ABSTRACT

Components of the bacterial spore germination apparatus are crucial for survival and for initiation of infection by some pathogens. While some components of the germination apparatus are well conserved in spore-forming species, such as the *spoVA* operon, each species may possess a different and possibly unique germinant recognition mechanism. The significance of several individual proteins in the germination process has been characterized. However, the mechanisms of how these proteins perform their functions and the network connecting these proteins in the complete germination process are still a mystery.

In this study, we characterized a *Bacillus subtilis* superdormant spore population and investigated the abundance of 11 germination-related proteins. The relative quantities of these proteins in dormant, germinating and superdormant spores suggested that variation in the levels of proteins, other than germinant receptor proteins may result in superdormancy. Specifically, variation in the abundance of the GerD lipoprotein may contribute to heterogeneity of spore germination rates.

Spore membrane proteomes of *Bacillus anthracis* and *B. subtilis* were characterized to generate a candidate protein list that can be further investigated. Proteins that were not

previously known to be spore-associated were identified, and many of these proteins shared great similarity in both *Bacillus* species. A significant number of these proteins are implicated in functions that play major roles in spore formation and germination, such as amino acid or inorganic ion transport and protein fate determination.

By analyzing the *in vivo* and *in vitro* activity of HtrC, we proved that the protease is responsible for YpeB proteolytic processing at specific sites during germination. However, without HtrC present in the spore, other proteases appear to degrade YpeB at a reduced rate. The activity of purified HtrC *in vitro* was stimulated by a relatively high concentration of Mn^{2+} or Ca^{2+} ions, but the mechanism behind the stimulation is not clear. We also demonstrated that YpeB and SleB, in the absence of their partner protein, were degraded by unknown proteases other than HtrC during spore formation. Identification and characterization of these unknown proteases would be a future direction for revealing the roles of proteases in spore germination.

DEDICATION

This dissertation is dedicated to my lovely wife Hualan for encouraging me to start this journey, also to each member of my family who have supported me and loved me unconditionally through my life.

ACKNOWLEDGEMENTS

First of all, I want express my deepest gratitude to my advisor, Dr. David Popham, for his enthusiastic mentorship and his invaluable role model during my PhD study at his lab. I could not have gotten this far without his excellent guidance, remarkable patience, constant encouragement and support. I am thankful to him for shaping up my academic interests, offering great career advices, and spending countless time on editing my conference abstracts, posters, presentation slides, and manuscripts etc. He is a brilliant, extraordinary and genuine scientist whom I respect and admire as both a scientist and a person.

I would also like to thank my committee members, Dr. Stephen Melville, Dr. Richard Helm, and Dr. Birgit Scharf for guiding my research for the past several years. Their tough questions and incisive insights constantly motivated me to maintain high standards for my work. I am grateful for their advice, support, and encouragements when my research faced challenges.

I always feel so fortunate that I could finish my PhD in the Popham lab and the microgroup in VT. I thank Jared and Emily for recommending me into the Popham lab and providing great examples of successful graduate students. Casey and Sean, two lab members and also life friends I have pleasure to know and work with for the majority of my time in the Popham lab. I will never forget the many wonderful lab dinners and fun talks and activities we have done together. Their generous supports not only on my research but also on my English improvement are deeply appreciated. They are a key reason that makes the Popham lab "sporific". I also like to thank Cameron, the newest lab member, for taking over the future directions of this work. I look forward to hearing his journey in the Popham lab. I also must thank Hannah for her valuable support and diligent work as my undergraduate research assistant.

I also thank the rest of Micro Group faculty, staff, and graduate students for creating such a remarkable friendly and collaborative environment. My thanks also goes to staff in the teaching labs over the years, Katie, Katrina, Carla and Ranee for their help and support during my GTA semesters. My special thanks to Andrea, Tim, Ben, and Craig for their friendship during the hardest time when we first arrived in the United States.

ATTRIBUTION

Several colleagues aided in research projects that presented as part of this dissertation. A brief description of their contributions is included here.

Chapter 2: Levels of Germination Proteins in *Bacillus subtilis* Dormant, Superdormant, and Germinating Spores.

W. Keith Ray, PhD (Department of Biochemistry) is currently a research scientist in Mass Spectrometry Incubator at Virginia Tech. Dr. Ray contributed on performing the LC-MS/MS analysis, and editorial comments of manuscript.

Richard F. Helm, PhD (Department of Biochemistry) is currently a professor in biochemistry at Virginia Tech. Dr Helm contributed on conceiving and designing the experiments, and editorial comments of manuscript.

Stephen B. Melville, PhD (Department of Biological Sciences) is currently a professor in microbiology at Virginia Tech. Dr. Melville contributed on conceiving and designinig the experiments, and editorial comments of manuscript.

David L. Popham, PhD (Department of Biological Sciences) is currently a professor in microbiology at Virginia Tech. Dr. Popham was the principle investigator of this project.

Chapter 3: Membrane Proteomes in *Bacillus anthracis* and *Bacillus subtilis* Dormant and Germinating Spores.

W. Keith Ray, PhD (Department of Biochemistry) is currently a research scientist in Mass Spectrometry Incubator at Virginia Tech. Dr. Ray contributed on performing the LC-MS/MS analysis, and editorial comments of manuscript.

Richard F. Helm, PhD (Department of Biochemistry) is currently a professor in biochemistry at Virginia Tech. Dr Helm contributed on conceiving and designing the experiments, and editorial comments of manuscript.

Stephen B. Melville, PhD (Department of Biological Sciences) is currently a professor in microbiology at Virginia Tech. Dr. Melville contributed on conceiving and designinig the experiments, and editorial comments of manuscript.

David L. Popham, PhD (Department of Biological Sciences) is currently a professor in microbiology at Virginia Tech. Dr. Popham was the principle investigator of this project.

Chapter 4: HtrC is involved in proteolysis of YpeB during germination of *Bacillus anthracis* and *Bacillus subtilis* spores.

Casey B. Bernhards, PhD (Department of Biological Sciences) was a graduate student in Dr. Popham's lab. Dr. Bernhards is responsible for the work presented in Figures 4.1, 4.2, 4.3, 4.4, and 4.9.

Hannah K. Toutkoushian is an undergraduate student in Virginia Tech. Hannah performed germination rate assays involving *htrC* mutants and provided laboratory assistance.

David L. Popham, PhD (Department of Biological Sciences) is currently a professor in microbiology at Virginia Tech. Dr. Popham was the principle investigator of this project.

TABLE OF CONTENT

LIST OF FIGURES

LIST OF TABLES

CHAPTER 1

Introduction and Review of Literature

Bacteria of several genera are capable of transitioning between two cellular morphologies: vegetative cells and endospores. When they detect environmental conditions are becoming unfavorable for their survival, they form endospores. Dormant spores are resistant to most agents that would normally kill the vegetative cells, such as heat, oxidizing agents and even ultraviolet and ionizing radiation (1). Due to their high resistance, spores cause much trouble in food sterilization, hospital decontamination, and medical treatment, and some are potent bioweapons (2). These resistance characteristics enable spores to persist for a long period of time until the environment is changed to a favorable condition. The spores then germinate into vegetative living cells. Once a dormant spore begins germination, the integral spore structures which maintain the intrinsic resistance, dormancy and germination properties are degraded, and the spore simultaneously loses its heat resistance and becomes much more susceptible to most antimicrobial treatments (3).

Bacterial endospore structure. A full copy of the bacterial chromosome DNA and essential metabolic enzymes such as ribosomes are embedded in the spore core, also known as protoplast. A high concentration of calcium dipicolinic acid (Ca^{2+}-DPA) and relatively dehydrated conditions protect proteins and nucleic acids from denaturation (4). There is also a large family of small, acid-soluble proteins (SASPs) that package the chromosome DNA into a toroid-like structure, therefore protecting it against many types of DNA damage (5). The spore dehydration is maintained by several surrounding layers, which also isolate and protect the core from other damaging agents, such as acid, organic chemicals and digestive enzymes. The significantly compressed and immobile inner forespore membrane (IFM) provides the major permeable barrier that restricts passage of small molecules into the spore core (6). The low permeability is critical for spore resistance to heat and chemicals. In contrast, the outer forespore membrane (OFM) is not an effective permeability barrier, but it plays important role in spore coat assembly and spore cortex formation (7). Between the two

membranes there are two layers of peptidoglycan (PG). The germ cell wall is a thin layer peptidoglycan that has structure similar to vegetative cell wall. It will serve as initial cell wall after spore germination. Another much thicker layer of PG is called cortex, which is a unique, spore-specific structure that fulfills a role in maintaining spore dormancy, core dehydration and heat resistance (8, 9). Outside of the OFM are the spore coats, which are composed of layers of spore-specific proteins (10, 11). Though the specific functions of many of these proteins are unknown, the integrity of the spore coat is important for spore resistance against chemicals and exogenous lytic enzymes (12, 13). In the case of *Bacillus subtilis*, the spore coat is the outmost structure. Spores of some species, such as *Bacillus anthracis*, contain another loose-fitting structure called the exosporium. One role of the exosporium is to serve as a permeability barrier against enzymes and antibodies (14).

Bacterial endospore formation. Endospore formation is a seven to eight hour process that includes seven stages. It involves three cell types known as the predivisional cell, the forespore and the mother cell (15). When the vegetative cell commits to undergo the sporulation process, it forms a predivisional cell, and then undergoes an asymmetric division (stage II). This creates dissimilar-sized progeny cells: The smaller cell termed the forespore and the larger cell termed the mother cell. Engulfment of the forespore by the mother cell characterizes stage III. Cortex peptidoglycan is created between the inner and outer membranes of the engulfed forespore during stage IV. Dipicolinic acid (DPA) synthesized in the mother cell is transported into the spore core during this stage. Coat layers are added to the forespore in Stage V. Spore maturation, including acquisition of heat resistance, other resistance characteristics, and refractivity, occurs during stage VI. When morphogenesis is complete, the mature spore is released by lysis of the mother cell (stage VII) (16, 17).

More than 100 genes are involved in the sporulation and it is a highly regulated process. Gene expression in the forespore is governed by RNA polymerase sigma factors, σ^F and σ^G,

and the DNA-binding proteins RsfA and SpoVT (18). Comparative genomic studies reveal a core of genes under the σ^F and σ^G regulons that are widely conserved among endospore-forming species but are absent from closely related, non-spore-forming species (15). Most known germination related genes that localized in the IFM are under σ^F and σ^G regulons, for instance, all known germinant receptor genes, most of spore germination specific lytic enzyme genes and DPA transport genes. Notably, the functions of more than one third of σ^F and σ^G regulated genes have not been characterized (15). Characterizing these genes will help us better understand bacteria endospore structure and functional apparatus, therefore helping in the development of improved decontamination methods.

Spore germination. Germination can be stimulated by nutrient or nonnutrient germinants. Nutrient germinants are normally amino acids and sugars, such as L-alanine and glucose, and purine nucleosides, such as inosine. The interaction of these germinants with their respective germinant receptors triggers germination initiation. However, the molecular mechanism following the receptor interactions with germinants is not clear (19). Nonnutrient germinants include dipicolinic acid (DPA), lysozyme, salts, cationic surfactants and high pressure.

The current model of the spore germination process includes germination activation, stage I, stage II and outgrowth as shown in Figure 1.2 (20). Briefly, nutrient germinants travel through the outer layers of dormant spore via an undefined pathway until they reach the inner membrane and interact with their specific germinant receptors. Once the interaction happens, germination activation is accomplished, and the spore becomes committed to proceed through germination, even if the germinant is subsequently removed (20). During germination stage I, the activated spore releases ions and calcium DPA rapidly from the core, coupled with uptake of water. The core is partially rehydrated and the spore loses some resistance properties. In germination stage II, rehydration and the large amount of released Ca^{2+}-DPA triggers

activation of germination-specific lytic enzymes, followed by degradation of the cortex and release of cortical fragments into the surrounding environment. At this point, the spore is fully rehydrated and loses its dormancy and all resistance characteristics. Metabolism and protein synthesis resume in the spore core, followed by a period of outgrowth (21).

Superdormant spore. A subpopulation of dormant spores, termed superdormant spores has been recently investigated in *B. subtilis* (22). The definition of spore superdormancy is dependent on the germinant used for isolation of these spores. Superdormant spores are germination defective to the germinant used for isolation, and more interestingly, in some cases they also show a poor response to germinants that are recognized by other germinant receptors (22). This subpopulation also has been reported in other *Bacillus* species (23) such as *Bacillus cereus,* which is closely related to *B. anthracis*. Investigating the presence of superdormant spores in *B. anthracis* will be a requirement for developing further methods to control its spore contamination. Since superdormant spores germinate as well as other dormant spores with a nonnutrient germinant, such as Ca^{2+}-DPA, and vegetative cells that grow out from the superdormant spores can sporulate naturally, a genetic defect is not considered as the reason causing the germination defect (22). A later publication from the same research group showed that low level of germinant receptor proteins could be the reason for spore superdormancy (24). Previous evidences showed that altering other germination-related proteins, such as SpoVA proteins, could also affect the spore germination rate (25, 26). Perhaps there may be other mechanisms that could result in the production of superdormant spores.

Spore germination apparatus. As discussed above, components of the germination apparatus, such as germinant receptors, play an important role in the process of triggering spore germination, and therefore are crucial for initiation of infection by some pathogens. Some of the germination apparatus is well conserved across species, whereas each species

may possess unique class of germinant recognition mechanisms. The previously characterized germination apparatus in *B. subtilis* and *B. anthracis* are shown in Table 1.1, including germinant receptors, germination specific lytic enzymes, and DPA transporters. The localization of these germinant proteins has been investigated either by using specific antibodies to detect their presence in various spore fractions or by using fluorescent tags to demonstrate their locations during sporulation (27-29).

To sum up, Figure 1.1 illustrates the possible locations of these proteins (20). The fact that most germination proteins are located in the IFM focuses attention on research into this particular membrane and its associated proteins.

Germinant receptors and other Ger proteins. *B. subtilis* spore germinant receptors (GRs) have been widely studied. Three germinant receptors have been identified by isolating germination defective mutants for particular germinants. GerA, GerB, and GerK receptors are composed of three proteins encoded by homologous tricistronic operons, termed as *gerA* operon homologs (30-33). All receptor genes are expressed in the developing forespore and belong to the σ^G regulons (20). The GerA receptor recognizes L-alanine, whereas GerB and GerK cooperate together for germination with nutrient mixture of asparagine, glucose, fructose and potassium ions (AGFK) (34). Two other *gerA* operon homologs have been identified by genome sequencing: *yndDEF* and *yfkQRT* (35). A previous study suggested that the expression of these two gene clusters is low and their products had no observable contribution on nutrient-triggered spore germination (19).

GerD is a lipoprotein expressed in the forespore under control of the forespore-specific σ^G (36). There are conflicting reports about the GerD location in spores, but the commonly accepted model is that GerD is located at the inner membrane of dormant spores (37, 38). *B. subtilis gerD* mutation spores have germination defects in response to both types of

germinant, which suggested that GerD may be involved in downstream activation of nutrient-mediated germination events (26).

The *gerF* gene was first characterized in *B. subtilis*, and it is the only gene in its operon that affects spore germination (39). Mutations in *gerF* result in failure of germination in respose to both amino acids and sugars (39, 40). GerF has high similarity to Lgt proteins, which are prolipoprotein diacylglyceryl-transferases, enzymes catalyzing the transfer of a diacylglyceride group to the N-terminal cysteine of bacterial membrane lipoproteins (41). GerF may contribute in correct localization or assembly of a number of Ger proteins by catalyzing lipid attachment (39). Blast analysis of Lgt homologues indicated that GerF is a unique candidate to perform the enzymic function in *B. subtilis*.

The categorization of germinant receptors and their response germinants in *B. anthracis* is more complicated than in *B. subtilis* due to the complex combination of germinants. Five distinct germination pathways have been recognized (42-44). Briefly, the alanine germination pathway is the only pathway that triggers spore germination with a sole amino acid. However, the concentration of L-alanine needs to be above 30 mM, which is much higher than the physiological level in the host (43) . The alanine and proline (AP) response requires only physiologically relevant concentration of L-alanine in combination with L-proline. The physiologically relevant concentration of L-alanine can also cooperate with L-histidine, L-tyrosine or L-tryptophan to active the aromatic amino acid-enhanced alanine (AEA) pathway (43). Purine ribonucleosides, in cooperation with a cogerminant, have been demonstrated as effective germinants for *B. anthracis* spore (43). Binary combination of inosine with L-alanine, L-serine, L-valine, L-methionine, or L-proline can active amino acid and inosine-dependent (AAID) 1 pathway (44). A combination of inosine with L-histidine, L-tyrosine, L-tryptophan, or L-phenylalanine is required to active AAID-2 pathway (44). Similar to *B. subtilis*, specific germinant receptors are required to response to these germinants

combinations. Seven *gerA* operon homologs have been identified in *B. anthracis*: *gerA*, *gerH*, *gerK*, *gerL*, *gerS*, *gerY* and *gerX* (45). Only *gerX* is found within a pathogenicity island on the pX01 virulence plasmid, while other operons are located on the chromosome (44, 46). Various single germinant receptor locus mutants were constructed to study the roles of each germinant receptor in the five signal pathways (42). The alanine and AP pathway showed a requirement for both the GerK and GerL receptors. GerK apparently could sense both L-alanine and L-pronine, whereas GerL can only sense L-alanine. The AEA pathway required GerL, GerS and GerH. GerS and GerH seem to cooperate to recognize the aromatic amino acid. GerH is involved in the AAID-1 pathway for its recognition of an aromatic amino acid. Within the AAID-1 pathway, GerL is required when using L-serine or L-valine as cogerminant, whereas GerK is required when using L-proline or L-methionine as cogerminant. Finally, the AAID-2 pathway requires only the GerH and GerS receptors. *gerA* and *gerY* may not encode functional receptors due to multiple frameshift mutations within their coding regions and nonfunctional promoter (42). Previous studies suggested that *gerX* encoded proteins may involve in macrophage-associated germination, and therefore are important for the establishment of anthrax infection and disease progression (46, 47). However, it is still not clear what specific ligand this receptor recognizes.

A completely different class of germinant receptor, the PrkC protein, has been reported to be functional in *B. anthracis* and *B. subtilis* (48). PrkC has a Ser/Thr kinase domain inside of the membrane and an extracytoplasmic domain that responds to soluble peptidoglycan fragments. PrkC function in triggering downstream steps in germination is not clear.

The Ger proteins are not universal in all endospore-forming species. For example, *Clostridium* bacteria do not encode GerD protein homologues, either clostridia do not need them, or the GerD function is met by an alternative, undefined protein. *Clostridium difficile* is the only spore-forming species that does not have any known classic germinant receptor gene

in its genome. This result is consistent with the fact that *C. difficile* spores do not respond to classic nutrient germinants, such as L-alanine, AGFK, or rich undefined medium. *C. difficile* spores do respond to glycine and bile salts (49), which are not common germinants for other species. Therefore, there must be some unknown germinant recognition mechanism that is unique for *C. difficile*.

DPA and ion channels. Several features of the spore core play major roles in spore resistance. The high DPA content in the spore core is one such feature. DPA, predominantly chelated with Ca^{2+}, comprises nearly 25% of the dry weight of the core (50). DPA less spores are more sensitive to wet heat, hydrogen peroxide and dry heat (51). Besides its role in spore resistance, the large amount of DPA released during early germination is essential for triggering the activation of a germination specific lytic enzyme. Thus, the DPA channel and its releasing pattern are another activity need to be unveiled for a complete understanding of the overall process of spore germination.

DPA synthesis starts with an intermediate in the lysine biosynthetic pathway in a sporulating mother cell. DPA synthetase, which is coded by *spoVF*, catalyzes the sole DPA-specific synthetic step (52). DPA is then transported through both the OFM and IFM into the spore core (53). It has been demonstrated that the proteins encoded by the *spoVA* operon are involved in DPA uptake into the developing spore (54). In addition, the involvement of SpoVA proteins in DPA release during during nutrient-triggered spore germination has been reported (55). The localization of SpoVAD in the spore inner membrane is consistent with the role of SpoVA proteins in transporting DPA into and out of the spore core (27). Recent genome sequence data have shown that at least SpoVAC, SpoVAD and SpoVAE are well conserved in *Bacillus* and *Clostridium* species.

Examining the germination of individual spores of a number of *Bacillus* species by using integrated phase contrast microscopy, Raman spectroscopy, and optical tweezers have

revealed a specific DPA release pattern during spore germination (56). Spores experienced different time for completion of Ca^{2+}-DPA release during germination, termed as $T_{release}$. The difference is due to a various initial time of slower rate of Ca^{2+}-DPA release in advance, termed as $T_{lag.}$ Within a germinating spore population, although spores have different T_{lag} times, they have consistent ΔT, which equals $T_{release}$-T_{lag} (56). This finding indicates that no matter how long the spore prepares for DPA release, once it starts, it will finish rapidly in a consistent amount of time. The diversity of spore T_{lag} may explain the germination heterogeneity of individual spores. Germinant receptor level, germinant concentration and heat activation are factors affecting variability in time of initiation of rapid DPA release (56-59).

Besides DPA channels, some other ion channels are also considered to be important in the germination process. The first event of germination is an efflux of monovalent ions, such as Na^+, K^+ and H^+. The release of hydrogen ions is essential for allowing the internal pH increase from 6.6 to 7, and therefore making the internal environment suitable for metabolic resumption (20, 34). These ions cannot diffuse freely through the IFM, so how germination triggers specific ion release is important to better understanding the signal transduction pathway during germination. The GerN protein has been reported as a Na^+/H^+-K^+ antiporter in *B. cereus* spores, which may be one example of an ion transporter that participates in cation movement during spore germination (60).

Germination specific lytic enzymes (GSLEs). Studies suggest that *B. subtilis* GSLEs have at least two types of hydrolytic activity: lytic transglycosylase and N-acetylglucosaminidase (61, 62). These GSLEs can be subclassified as either spore cortex lytic enzymes (SCLEs) or cortical fragment lytic enzymes (CFLEs). SCLEs are thought to be responsible for the initial disruption of the cortex, then CFLEs act on SCLE products to

further dissolve the peptidoglycan (63) . Although these lytic enzymes have different substrates and functions they cooperate in the overall hydrolysis of the cortex (64, 65).

SleB and its homologs are SCLEs found in their mature form in the dormant spores of *B. cereus* (66), *B. subtilis* (64), and *B. anthracis* (67). Its function is characterized as lytic transglycosylase in *B. anthracis* (61). Expression of *sleB* is controlled by σ^G in the forespore (68). Immunoelectron microscopic localization of SleB just inside the spore coat layer suggested that SleB is translocated across the IFM by a secretion signal peptide and is translocated into the intermembrane space of the developing spore (68). However, further investigations should be conducted because SleB could be detected both at the outer edge of the spore cortex and inner spore membrane (64). *ypeB* is the downstream gene in the bicistronic operon with *sleB*. The fact that SleB could not be detected immunochemically in the spores of a *ypeB* mutant suggested that YpeB might be required for the localization and/or stabilization of SleB (64, 69).

When either the *sleB* or *ypeB* mutant spores are plated on nutrient medium, the spores are able to germinate indicating that there are other components involved in germination to bypass *sleB*/*ypeB* pathway (70). The discovery of CwlJ, another SCLE which is localized at the inner surface of the coat layers revealed the alternative pathway (71, 72). Unlike *sleB*, which is regulated by σ^G in the forespore, *cwlJ* is regulated by σ^E in the mother cell. Mutants lacking *cwlJ* germinate more slowly than wild-type cells, like *sleB* mutants (72). A previous study also suggested that high concentration of Ca^{2+}-DPA can trigger spore germination as nutrient germinants do by first activating CwlJ-dependent cortex hydrolysis (73). When both SleB and CwlJ are nonfunctional, the spore's peptidoglycan is not depolymerized and the spore cannot complete germination (74).

The 48 kDa CFLE SleL was firstly reported in *B. cereus*. It is localized at the outer periphery of the spore cortex with a function characterized as N-acetylglucosaminidase (75).

It plays the major role in hydrolyzing the large products of SCLEs into small, rapidly released muropeptides (63). The enzyme homologues, which are coded by *yaaH*, was reported in *B. subtilis* and *B. anthracis* (62, 64). The SleL enzymatic activity in *B. anthracis* is the same as that of *B. cereus* (62), while it was characterized to have epimerase activity in *B. subtilis* (64).

Previous proteomic studies on *Bacillus* species. Gel-based and gel-free mass spectrometry has been a powerful tool for identification and even quantification of entire proteomes of *Bacillus* vegetative cells (76-78). In 2002, Kuwanna *et al*. performed the first comprehensive analysis of the protein composition of *B. subtilis* spores using a combination of SDS-PAGE and LC-MS/MS (79). A total of 69 novel proteins were identified, and 26 of these were expressed under the control of sporulation-specific sigma factors. Taking advantage of the two-dimensional polyacrylamide gel electrophoresis and better separation of proteins, the protein profile of *B. subtilis* spores was further expanded by Mao *et al* (80). Similar proteomic analyses were carried out on *B. anthracis*, *B. cereus* and *B. thuringiensis* in 2004 and 2006 (81-83). Subproteomes of *Bacillus* spore coat protein fractions were carried out due to the requirement for solubilization of tightly associated coat proteins (84, 85). To identify potential protein targets for rapid detection of *Bacillus* and *Clostridium* spores, a subproteome of the coat and the exosporium layers of *Bacillus* and *Clostridium* species spores was carried out by Abhyankar *et al* in 2013 (86). These proteomic studies contributed toward a comprehensive understanding of how species differentially express the genome sequence under nutrient depletion stress, what proteins are specifically produced during the sporulation process, and what the fates of these spore-specific proteins are.

Objectives of this work. Traditional spore decontamination methods require the use of harsh chemicals. Research has been focused on developing methods and reagents that could prematurely trigger spore germination, potentially permitting decontamination using common antimicrobial disinfectants. The presence of extremely germination resistant but viable

superdormant spores make such method development problematic. In Chapter 2, we investigated the quantity of germination-related proteins in dormant, germinating and superdormant spores. A Multiple Reaction Monitoring Mass Spectrometry (MRM-MS) approach was established, and the relative abundance of 11 germination-related proteins was determined between spore samples. It was discovered that a deficiency in the GerD lipoprotein, besides low levels of germinant receptor proteins (24), may result in superdormancy. Specifically, variation in the abundance of the GerD lipoprotein may contribute to heterogeneity of spore germination rates.

In chapter 3 we investigate the identities of *Bacillus* spore membrane proteins by carrying out shot-gun proteomic studies on *B. subtilis* and *B. anthracis* spore membrane fractions. A total of 104 and 87 membrane-associated proteins were identified in *B. subtilis* and *B. anthracis*, respectively. These proteins were further characterized with regard to membrane association, cellular function, and conservation across species. Proteins that were not previously known to be spore associated were identified, and many of these proteins shared great similarity in both *Bacillus* species. A significant number of these proteins are implicated in functions that play major roles in spore formation and germination. This study generated a candidate protein list that can be further investigated in future studies.

HtrC, a membrane serine protease identified in our spore membrane proteome, is the major focus in Chapter 4. This study revealed that YpeB was proteolytically processed at specific sites during germination, and that HtrC is the protease responsible for specific cleavage events using both *in vivo* and *in vitro* methods. The proteolytic processing of YpeB during spore germination is proposed to be the signal that terminates the relationship between SleB and YpeB, which have been demonstrated to be co-dependent and co-localized in the inner forespore membrane.

The results of these studies provide a better understanding of spore membrane protein content and their roles in the spore germination process. This body of work begins to uncover the framework of the mysterious and complex network in the early steps of spore germination.

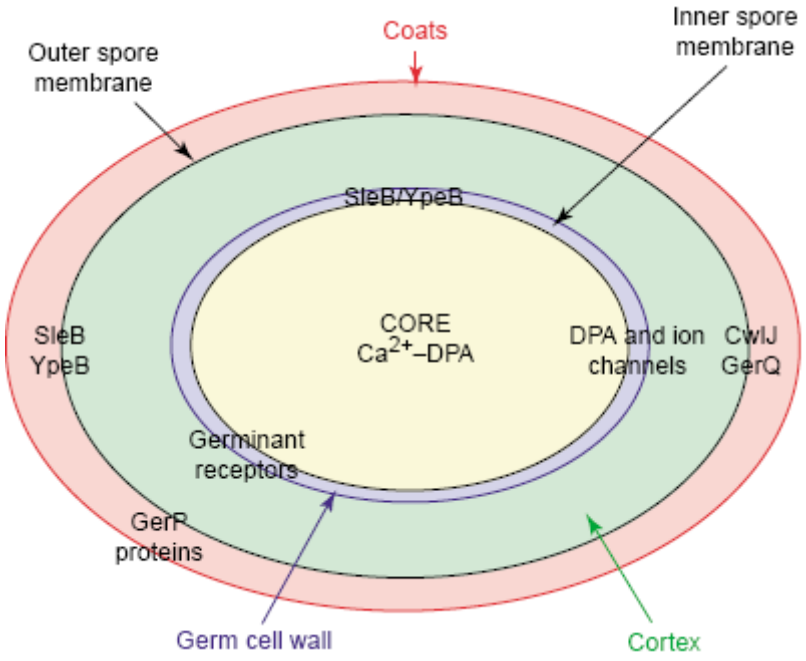

Figure 1.1. Bacterial endospore structure and components of spore germination apparatus (20). General structures of bacterial endospore are indicated in the illustration. Exosporium, an outmost additional spore structure of some spore forming species, is not included in the illustration. The localization of some major germination apparatus proteins are indicated as well. (Used with permission from RightsLink in 2014)

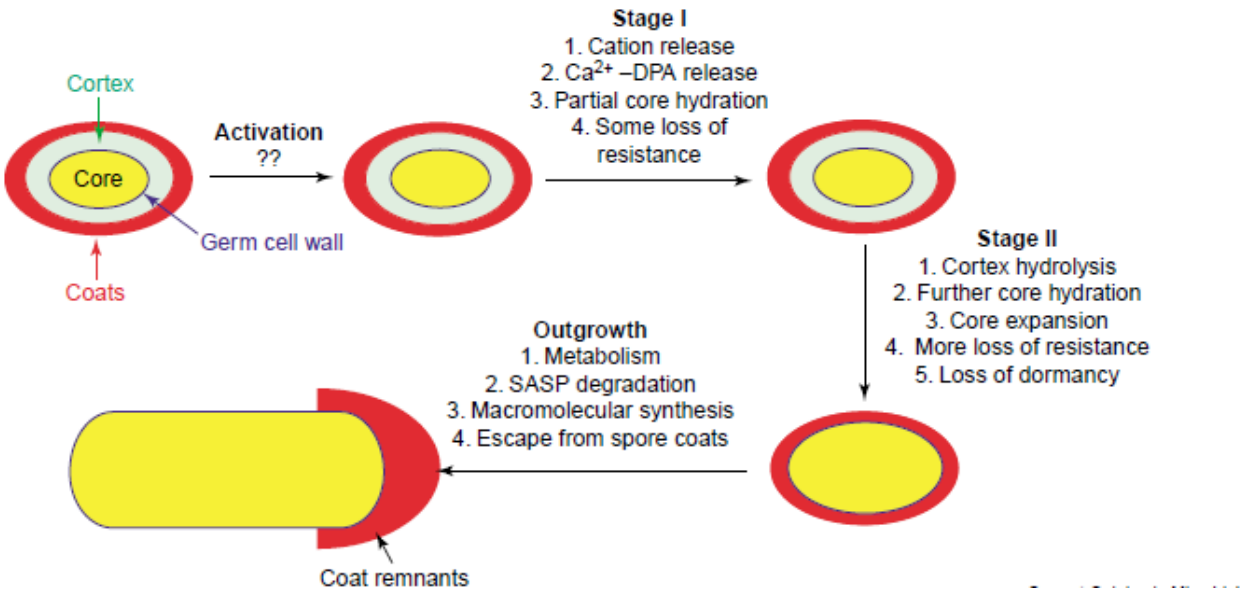

Figure 1.2. Spore germination (20). Four germination events were characterized as indicated in the illustration. The germination activation is initiated by the interaction between germinants and their corresponding germinant receptors. The downstream germination signal pathway is unknown. The characteristics of the following three stages based on current opinion in Microbiology are listed in the illustration. (Used with permission from RightsLink in 2014)

Table 1.1. Germinant apparatus reported in spores of *Bacillus* species

Species	Germinant apparatus	Functions
B.subtilis	GerA	Response to L-alanine
	GerB &GerK	Response to AGFK (L-asparagine, glucose, fructose and K^+)
	YndDEF & YfkQRT	Unknown germinant receptors
	GerF	Add diacylglycerol to membrane proteins
	GerC	Probably an enzyme of menaquinone biosynthesis
	GerD	Unknown function in nutrient germination
	CwlJ	lytic Lytic enzyme, degrade Degrades cortex peptidoglycan
	GerQ	Essential for the presence of CwlJ
	SleB	Lytic transglycosylase, degrade Degrades cortex peptidoglycan
	YpeB	Essential for the presence of SleB
	SpoVA	Proteins involved in DPA transport
B.anthracis	GerK&GerL	Alanine and AP* pathway
	GerL, GerS & GerH	AEA* pathway
	GerH, GerL &GerK	AAID-1* pathway
	GerH&GerS	AAID-2* pathway
	GerA &GerY	Unknown or non-functional germinant receptors
	GerX	Possible role in amino acid and inosine-dependent responses and macrophage- associated germination
	CwlJ1&CwlJ2	lytic Lytic enzyme, degrade Degrades cortex peptidoglycan
	SleB	Lytic transglycosylase, degrade Degrades cortex peptidoglycan
	SleL	Further degrade cortex fragments
	YpeB	Essential for the presence of SleB

AP: Alanine and proline response;
AEA: aromatic amino acid-enhanced alanine response;
AAID: amino acid and inosine dependent response;
AAID-1: Binary combination of inosine and either L-alanine, L-serine, L-valine, L-methionine or L-proline;
AAID-2: Binary combination of inosine and either L-histidine, L-tyrosine, L-tryptophan or L-phenylalanine.

CHAPTER 2

Levels of Germination Proteins in *Bacillus subtilis* Dormant, Superdormant, and Germinating Spores

Yan Chen, W. Keith Ray, Richard F. Helm, Stephen B. Melville, and David L. Popham

PLoS ONE 9(4): e95781. doi:10.1371/journal.pone.0095781

AUTHOR CONTRIBUTIONS

Conceived and designed the experiments: Yan Chen, W. Keith Ray, Richard F. Helm, Stephen B. Melville, and David L. Popham. Performed the experiments: Yan Chen, W. Keith Ray, and David L. Popham. Analyzed the data: Yan Chen, W. Keith Ray, Richard F. Helm, Stephen B. Melville, and David L. Popham. Contributed reagents/materials/analysis tools: Yan Chen, W. Keith Ray, Richard F. Helm, and David L. Popham. Wrote the paper: Yan Chen, W. Keith Ray, Richard F. Helm, Stephen B. Melville, and David L. Popham.

ABSTRACT

Bacterial endospores exhibit extreme resistance to most conditions that rapidly kill other life forms, remaining viable in this dormant state for centuries or longer. While the majority of *Bacillus subtilis* dormant spores germinate rapidly in response to nutrient germinants, a small subpopulation termed superdormant spores are resistant to germination, potentially evading antibiotic and/or decontamination strategies. In an effort to better understand the underlying mechanisms of superdormancy, membrane-associated proteins were isolated from populations of *B. subtilis* dormant, superdormant, and germinated spores, and the relative abundance of 11 germination-related proteins was determined using multiple-reaction-monitoring liquid chromatography-mass spectrometry assays. GerAC, GerKC, and GerD were significantly less abundant in the membrane fractions obtained from superdormant spores than those derived from dormant spores. The amounts of YpeB, GerD, PrkC, GerAC, and GerKC recovered in membrane fractions decreased significantly during germination. Lipoproteins, as a protein class, decreased during spore germination, while YpeB appeared to be specifically degraded. Some protein abundance differences between membrane fractions of dormant and superdormant spores resemble protein changes that take place during germination, suggesting that the superdormant spore isolation procedure may have resulted in early, non-committal germination-associated changes. In addition to low levels of germinant receptor proteins, a deficiency in the GerD lipoprotein may contribute to heterogeneity of spore germination rates. Understanding the reasons for superdormancy may allow for better spore decontamination procedures.

INTRODUCTION

Bacterial endospores are metabolically dormant and resistant to a variety of anti-microbial treatments due to their protective structures and dehydrated spore core (87, 88). These spores can survive for decades in the absence of nutrients. However, they are able to return to a metabolically active state through a series of events termed spore germination. Once spores lose many of their resistance properties during germination, they can then be easily eliminated by routine decontamination methods (20). Since the spores of *Bacillus* and *Clostridium* species cause food spoilage and are infectious agents in several human diseases (89), the development of methods or reagents that stimulate highly efficient germination across a spore population could greatly simplify decontamination efforts and reduce morbidity and mortality.

Procedures used for triggering spore germination do not achieve 100% efficiency due to heterogeneity in germination rate within spore populations. Studies of single germinating *B. cereus* and *Clostridium* spores indicated that the spore germination heterogeneity results from the variation in time of initiation of rapid Ca^{2+}-dipicolinic acid (DPA) release (T_{lag}) (56, 90). Subpopulations of *B. subtilis* spores termed superdormant spores can be isolated following multiple rounds of germination with saturating nutrient germinant levels (22). These superdormant spores exhibit extremely poor germination response to the germinant used for isolation, but will germinate to varying degrees when triggered with germinants that utilize other germinant receptors (22, 91). Individual germinating superdormant spores exhibit longer times for initiation of rapid Ca^{2+}-DPA release relative to initial dormant spore populations (91). However, once rapid Ca^{2+}-DPA release is initiated, the rate of release is similar for all spores. Thus one may hypothesize that the state of superdormancy is related to processes occurring prior to Ca^{2+}-DPA release.

Four groups of proteins have been implicated to be involved in the early steps of germination: 1) germinant receptors; 2) DPA channel proteins; 3) germination-specific lytic enzymes (GSLEs) and their partner proteins; and 4) lipoproteins potentially involved in transducing germinant-binding signals (20, 21). In *B. subtilis*, three major germinant receptors (GRs) have been characterized: GerA, GerB, and GerK (32, 92, 93). Each GR is comprised of at least A, B, and C subunits (some receptors have D subunits encoded within or associated with the receptor operon (94)) and is localized to the spore inner membrane. The A and B subunits are believed to be integral membrane proteins with multiple transmembrane domains. The C subunits are putative lipoproteins based on their N-terminal signal peptides and on the effect of a *gerF* mutation, which eliminates the only protein diacylglycerol transferase in this species, on their function (40).

Previous genetic studies of these GRs illustrated their germinant specificity. GerA alone responds to L-alanine or L-valine, while GerB and GerK are required for germination with a mixture of L-asparagine, D-glucose, D-fructose, and potassium ions (AGFK) (93, 95). The binding of nutrient germinants to their cognate GR or GRs initiates irreversible germination activation (20), and via an unclear pathway, results in the opening of DPA channels and the rapid release of this abundant spore solute. Proteins encoded by the *spoVA* operon are involved in DPA uptake during sporulation as well as release during spore germination. Since SpoVA proteins are transcribed exclusively in the developing forespore and some appear to be integral membrane proteins, they are most likely localized to the inner spore membrane (54, 96, 97). The PrkC protein has been identified as an alternate class of germinant receptor that recognized the presence of peptidoglycan fragments in the medium (48).

Complete germination requires that the thick layer of spore cortex peptidoglycan be degraded by GSLEs (70, 71, 98). SleB is a key GSLE (70), and some evidence indicates that it and a co-expressed protein involved in SleB stabilization, YpeB, are localized to the inner

spore membrane in the dormant spore (64). Spores with a *gerD* deletion mutation had a dramatically slower response to nutrient germinants utilizing any of the Ger receptors (26). Lipoproteins involved in germination, including GerAC, GerBC, GerKC and GerD, are believed to be anchored in the spore inner membrane by a covalently attached lipid (40). Spores of a *B. subtilis gerF* null mutant also lacked both the GerAC and GerD proteins (99). This mutant exhibited a significant defect in germination with a greater effect on germination triggered through the GerA receptor relative to responses via the GerB and GerK receptors (40, 99).

Several studies have indicated that the abundance of germination-associated proteins can impact the rate of spore germination. Overexpression of the GerA receptor significantly increased the germination rate triggered by its corresponded germinants but did not affect GerB and GerK abundance or germination function (100). In contrast, overexpression of SpoVA proteins increased germination rates triggered through any germinant receptor (25). It is hypothesized, based upon quantitative Western blot analyses, that a significant reduction in the amount of a Ger receptor could be the reason for spore superdormancy (24).

In an effort to provide additional insight into the mechanisms of germination, we developed a multiple-reaction monitoring (MRM) mass spectrometry assay (101) to quantify 11 germination proteins believed to be associated with the spore inner membrane. MRM assays are based upon the analyses of peptides specific to the target protein (proteotypic peptides), which become surrogates for protein abundance. The method has high specificity and sensitivity for target protein quantification, and permits reproducible analyses of multiple samples. MRM analyses were performed on membrane preparations obtained from dormant, rapidly germinating, and superdormant spore samples. The results of these analyses indicate that the GerD lipoprotein level can contribute to the heterogeneity of spore germination rate and superdormancy.

MATERIALS AND METHODS

Spore sample preparation. The *B. subtilis* strain used was PS832, a prototrophic laboratory derivative of strain 168. Spores were prepared on 2xSG (102) agar plates without antibiotics. Spores were harvested after 72 h incubation at 37 ℃ and purified by water washing and centrifugation through a 50% sodium diatrizoate (Sigma) layer as described (103). All spores used in this work were 99% free of vegetative cells and were stored in deionized water at 4 ℃ until analysis.

A 10-ml suspension of dormant spores at an optical density at 600 nm (OD_{600}) of 20 in water were heat-activated at 75 ℃ for 30 min and cooled on ice for at least 10 min. The spores were then germinated at 37 ℃ and at an OD_{600} of 2 with 10 mM L-valine in 25 mM Tris-HCl buffer (pH 7.4). The germination of spores was terminated after the OD_{600} dropped to 50% of the initial value. Germinated spores were collected by centrifugation at 12,000 x *g* for 5 min at 4 ℃, quickly washed with cold deionized water, centrifuged again, and frozen at -80 ℃. Examination by phase-contrast microscopy indicated that >95% of the spores in these preparations had germinated.

Superdormant spores were isolated and characterized as described previously (22). Briefly, dormant spores at OD_{600} of 1 were germinated as described above for 2 h and collected by centrifugation. The pellet was washed with deionized water, suspended in 20 % w/v sodium diatrizoate, and centrifuged through a 50 % w/v sodium diatrizoate solution (13,000 x *g* for 45 min) to separate dormant spores from germinated spores. The dormant spore pellets were collected and washed thoroughly with deionized water. These dormant spores were subjected to another 2 h round of germination and were separated by density gradient centrifugation again. The final superdormant spore pellet was washed thoroughly with deionized water and stored at 4 ℃.

Superdormant spore characterization. For phenotypic studies, isolated superdormant spores as well as initial dormant spores were germinated with nutrient germinants: 10 mM L-Valine or AGFK (13 mM L-asparagine, 13 mM D-glucose, 13 mM D-fructose, 13 mM KPO_4 [pH 7.4]); or the non-nutrient germinant 60 mM Ca^{2+}-DPA [pH 7.4]. Prior to nutrient-triggered germination, spores were heat-activated in water at 75 ℃ for 30 min and then briefly cooled on ice. Germination was initiated by diluting spores to an OD_{600} of 0.2 in germination solutions and incubating at 37 ℃. Germination was monitored as the change in OD_{600} over time. Spores used for Ca^{2+}-DPA germination were not heat-activated and the germination was at 30 ℃. To assess Ca^{2+}-DPA germination, 100 spores were examined by phase-contrast microscopy at several incubation time points.

Preparation of spore membrane fractions. Spore membrane fractions were prepared by a modification of previously described methods (28, 37, 104). Dormant, germinated, and superdormant spores prepared as described above were lyophilized. The dry spores (~19 mg for germinated spores and ~24 mg for dormant and superdormant spores) were pulverized with 100 mg of glass beads in a dental amalgamator (Wig-L-Bug) at 4,600 rpm for pulses of 30 s each, with 30 s pauses on ice between pulses. Spore disruption was monitored by suspending a small sample of spore material in H_2O and observing under phase-contrast microscopy. Once >80% of spores were disrupted, the dry powder was suspended in 0.5 ml of 4 ℃ extraction buffer (10 mM Tris-HCl [pH 7.4], 1 mM EDTA, 2 mg/ml RNase A, 2 mg/ml DNase I, 1 mM phenylmethylsulfonyl fluoride (PMSF)). The suspension was centrifuged (6,000 X *g*, 10 min, 4 ℃) and the resultant supernatant was centrifuged again (13,000 X *g*, 10 min, 4 ℃) to remove insoluble material. The remaining supernatant was subjected to ultracentrifugation (100,000 X *g*, 60 min, 4 ℃). The resulting supernatant was considered the spore core soluble fraction and was stored at -80 ℃. The resulting pellet, designated the crude spore membrane fraction, was homogenized in 1 ml high salt buffer (20

mM Tris-HCl [pH 7.5], 10 mM EDTA, 1 M NaCl, and 1 mM PMSF) and was gently shaken for 30 min at 4 ℃. The homogenate was subjected to ultracentrifugation again as described above. The remaining pellet was homogenized in 1 ml alkaline buffer (100 mM Na_2CO_3-HCl [pH 11], 10 mM EDTA, 100 mM NaCl, and 1 mM PMSF) and was again subjected to ultracentrifugation. After a final wash with 1 ml TE buffer (10 mM Tris-HCl [pH 7.4], 1 mM EDTA, 1 mM PMSF), the resulting pellet was homogenized in 200 µl TE buffer, flash frozen, and stored at -80 ℃ until analysis. The protein concentration was determined by acid hydrolysis and amino acid analysis (105) with comparison to a standard set of amino acids (Sigma).

Protein digestion. Proteins in spore membrane fractions (70 µg) were precipitated with 1 mL of acetone -20 ℃ overnight and collected by centrifugation for 20 min at 12,000 g. Protein was resuspended in 250 µl of freshly-prepared 8 M urea, 20 mM Tris-HCl, pH 8.0 to give a final protein concentration of 1 mg/ml. Proteins were denatured by the addition of 27.8 µl of freshly-prepared 45 mM dithiothreitol, 20 mM Tris-HCl, pH 8.0, and incubation for 1 h at 37 ℃. Free cysteines were alkylated by the addition of 30.9 µl of freshly-prepared 100 mM iodoacetamide, 20 mM Tris-HCl, pH 8.0, incubation at room temperature in the dark for 30 min. Unreacted iodoacetamide was inactivated by the addition of 102.9 µl of freshly-prepared 45 mM dithiothreitol, 20 mM Tris-HCl, pH 8.0. Proteins were digested by the addition of 1.03 ml of 20 mM Tris-HCl, pH 8.0, and 5 µg trypsin in 10 µl 50 mM acetic acid followed by incubation overnight at 37 ℃ with shaking. Trifluoroacetic acid was added to a final concentration of 0.25% and formic acid was added to a final concentration of 1%. The pH was measured and additional formic acid was added until the pH was at or below 3. Conditioning of 0.1 ml OMIX C18 solid phase extraction cartridges used 0.2 ml methanol, followed by 0.2 ml 50% acetonitrile, 0.1% TFA and finally 0.2 ml 2% acetonitrile, 0.1% TFA. A protein sample was applied to the cartridge, which was then washed three times with

0.2 ml 2% acetonitrile, 0.1% TFA. Peptides were eluted with 0.2 ml 75% acetonitrile, dried, and resuspended in 0.02 ml solvent A (2:98 acetonitrile:water containing 0.1% formic acid).

Liquid chromatography and mass spectrometry. Thirteen germination-related membrane proteins (Table 2.1) were initially targeted for MRM method development, with a list of potential proteotypic tryptic peptides generated using the Enhanced Signature Peptide Prediction tool (106) using a cutoff value of 0.6. Peptides were synthesized by JPT Peptide Technologies GmbH Inc., and were directly infused into the mass spectrometer for determination of target fragment ions and ionization conditions. For each synthesized peptide, elution times were identified, the dominant precursor ion of predicted m/z (Q1 ion) was identified and fragmented, and dominant fragment ions of expected m/z (Q3 ions) were identified and quantified. Limits of quantification (LOQ) (Table 2.1) were determined using the established MRM methods and dilution series from 10-1500 fmol of each synthetic peptide (Fig. 2.1).

Proteins in spore membrane fractions were solubilized with 20 mM Tris-HCl [pH 8.0], 8 M urea, 45 mM dithiothreitol at a final protein concentration of 1 mg/ml, followed by a 37℃ overnight trypsin digestion at 20:1 (w/w) protein:Trypsin ratio. The tryptic peptides were desalted and concentrated using OMIX C18 microextraction pipette tips (Varian) following the manufacturer's protocol. Peptides was separated using an Eksigent Nano 2-D liquid chromatography system connected to a 100 x 0.075 mm Magic C18AQ (200Å, 3μm, Bruker) column packed in-house using an eFRIT fused silica capillary (Phoenix S&T). Ten microliters of each sample was first loaded onto a C18 trap cartridge at 10 μl/min for 15 minutes using solvent A (2:98 acetonitrile:water containing 0.1% formic acid). The trap cartridge was switched in-line with the analytical column and the trap and column were flushed with 95% solvent A, 5% solvent B (98:2 acetonitrile:water containing 0.1% formic acid) for 5 minutes at 300 nl/min. This was followed by a linear gradient to 86% solvent A

over 5 minutes then a linear gradient to 71% solvent A over 45 minutes and finally a linear gradient to 35% solvent A over 5 minutes. The column was flushed for 2 minutes with 35% solvent A and reequilibrated at the starting conditions for 13 minutes prior to the next sample injection. The eluent was introduced into an AB Sciex 4000 QTrap mass spectrometer controlled by Analyst 1.4.2 software (AB Sciex) via a nano-electrospray source (Phoenix S&T). The mass spectrometer was operated in positive ion mode utilizing an MRM method containing precursor/product ion transitions corresponding to peptides described below. Dwell time for each transition was 40 ms and the total cycle time was 6.6 seconds. The first quadrupole was operated at low resolution while the third quadrupole was set to unit resolution. Ion spray voltage was 2400V, curtain and sheath gases were 12 (arbitrary units), interface heater temperature was 120˚C and the entrance potential was 10V for all transitions. CAD gas was set to medium corresponding to a vacuum of 3.1×10^{-5} Torr.

Data collection and refining. When determining which of the identified Q3 ion peak areas were suitable for quantitative comparisons across all samples, we applied the following raw data refining criteria. 1) The retention time of a Q3 ion in all samples should be the same as that determined for the corresponding synthetic peptide. Q3 ions that did not have consistent retention times were excluded from further analysis. 2) If a quantified peptide had less than two quantifiable Q3 ions, the peptide was excluded from further analysis. 3) If the peak area of a Q3 ion was below established limited of quantification, the Q3 ion was excluded from further analysis. 4) Among all nine samples, if the Q3 ion peaks in more than three samples had S/N ratio values less than 10, then the Q3 ion was excluded from further analysis. (The end section of each Q3 ion spectrum was considered as base line (noise) when collecting the S/N ratio for limit of quantification evaluation.)

Within each biological replicate set, there were three membrane fraction samples: dormant, germinated, and superdormant. Three biological replicates were derived from three

independent spore preparations. For each quantified Q3 ion, peak area ratios between two membrane fractions were calculated only within a biological replicate set. Ratios were then compared across biological replicates. Theoretically, if a protein's abundance was the same in two different samples, the peak area ratios for the Q3 ions of its peptides would be 1. Among all Q3 ion peak area ratios calculated, those of proteins GerAA, GerBA, and GerKA were always close to 1.0. We took these proteins to represent unchanged proteins within the samples, and pooled their Q3 ion peak area ratios to represent the level of physiological variance. For each comparison group, we then evaluated the significance of a protein change by comparing peak area ratios of the protein to this unchanged protein peak area ratio pool using a two samples student t-test. In addition, for each protein, we evaluated the significance of two comparison groups using the Student's t-test. Both tests used two-tailed, unequal variance p values, and statistical significance for both t-tests was set at $p < 0.05$.

RESULTS

Isolation and characterization of spore populations. Three independent preparations of *B. subtilis* dormant spores were germinated using L-valine, with downstream processing producing rapidly germinating and superdormant spore populations. The yield of superdormant spores was 1.09 ± 0.16 % (n=3); somewhat less than the 3.8 % yield in a previous publication (22). Two reported characteristics of superdormant spore populations isolated using L-valine are that the superdormant spores germinate poorly with L-valine as well as with germinants that use a different germinant receptor, with the superdormant spores being as viable as the initial dormant spores when germinated with non-nutrient germinants (22). Our superdormant spores also germinated slowly with L-valine, in comparison with the rapid germination of the initial dormant spores (Fig. 2.2A). However, when using AGFK as germinant, which acts through different germinant receptors than does L-valine (93), the superdormant spores germinated more rapidly than the initial dormant spores (Fig. 2.2B). In addition, the superdormant spores also reached a higher efficiency of germination based on a greater OD_{600} decrease than the initial dormant spores. While our results are different from those of the original description of superdormant spores (22), similar observations were reported for superdormant spores isolated in a more recent study (91). The effect of a non-nutrient germinant on the superdormant spores was tested using Ca^{2+}-DPA, which causes activation of the GSLE CwlJ (73), bypassing part of the germination apparatus that may be deficient in superdormant spores. The superdormant spores completed Ca^{2+}-DPA-triggered germination as efficiently as the initial dormant spores after an initial lag period (Fig. 2.2C), similar to a previous report (91). In summary, the results of the phenotypic analyses support the claim that spores isolated after extensive L-valine germination can be classified as superdormant. To verify that these spores were not superdormant due to a genetic alteration, they were germinated and spread on plates, and 10 randomly selected colonies were selected,

cultured, sporulated, and tested for germination rate. Similar to a previous report (22), spore populations produced by these strains germinated equivalently to those of the wild type strain.

Quantification of spore membrane proteins by MRM assays. Membrane samples were prepared from dormant, germinated, and superdormant spores and were used to quantify the targeted germination-related proteins relative to the total protein concentration. The total protein in each sample was determined by amino acid analysis. SDS-PAGE analysis of total proteins was consistent with this quantification and revealed essentially identical protein band patterns across biological replicates (Fig. 2.3).

The MRM assays centered on the detection of 11 of the 13 proteins expected to be membrane associated and involved in spore germination (Table 2.1). As peptides of varying compositions exhibit different ionization efficiencies, we determined LOQs for each peptide. We were not able to identify any proteotypic peptides for GerAB that were even predicted to function well in an MRM assay, and we were not able to obtain quantifiable MRM data for GerBB and GerKB due to the fact that the signal for the proteotypic peptides designed for these integral membrane proteins were below the limit of detection. Nonetheless, we were able to quantify the A and C subunits of the germinant receptors. The ratios of GerAA, GerBA, and GerKA between dormant and superdormant spores were very close to 1.0. In contrast, the amounts of GerAC and GerKC in superdormant spores were 3.4 and 1.9-fold lower than the amounts in dormant spores (Fig. 2.4A). These decreases of GerAC ($p=0.002$) and GerKC ($p=0.023$) were statistically significant. GerBC, however, showed no significant difference in amount between superdormant and dormant spores (Fig. 2.4A).

GerD is a lipoprotein that is localized predominantly to the spore inner membrane (37) and functions in both GerA and GerB/K-mediated germination responses (26). GerD was 1.8-fold less abundant in membranes isolated from superdormant spores in comparison to those

from dormant spores (Fig. 2.4A). PrkC, SpoVAC, SpoVAD, and YpeB exhibited no significant difference in abundance between superdormant and dormant spore samples (Fig. 2.4A).

The relative amounts of GerAA, GerBA, and GerKA in germinated spore samples were similar to the amounts of these proteins in those from dormant spores. In contrast, the amounts of GerAC, GerBC, and GerKC in germinated spore membranes decreased 1.9, 1.6, and 2.4-fold respectively in comparison to dormant spores (Fig. 2.4B). Previous western blot results showed that membrane-associated GerD decreased during spore germination (37). This was confirmed in the MRM assays, which showed that membrane-associated GerD decreased 3.5-fold during spore germination (Fig. 2.4B). The decreases of GerAC ($p=0.009$), GerKC ($p=0.032$), and GerD ($p<0.0001$) were statistically significant.

To date, there is no report regarding PrkC function in a nutrient germinant receptor-mediated pathway. The MRM assays indicated that membrane-associated PrkC was significantly decreased 3.8-fold in amount after spore germination (Fig. 2.4B). Similarly, three proteotypic YpeB peptides decreased 6.8-fold in amount during spore germination (Fig. 2.4B). This result is consistent with a previous observation of YpeB degradation during germination (64). A fourth YpeB peptide was clearly quantifiable in dormant spore samples, but was undetectable in germinated spore membrane fractions. This peptide is near the YpeB N-terminus (residues 57-67), whereas the three detectable YpeB peptides were closer to the C terminus.

SpoVAC and SpoVAD proteins were chosen as representatives of the *spoVA*-encoded proteins. SpoVAC is predicted to be an integral membrane protein (97, 107), and SpoVAD is more likely to be a peripheral membrane protein based on its crystal structure (108). While SpoVAD could be detected in both dormant and germinated membrane fraction samples by Western-blot (data not shown), the MRM assays indicated that SpoVAC and SpoVAD

significantly increased 1.3 and 1.7-fold respectively in germinated spore membrane samples in comparison to those of dormant spores (Fig. 2.4B).

The germinant receptor A subunit amounts detected were similar in superdormant and germinated spore samples. While membranes of both superdormant and germinated spores had significantly less GerAC and GerKC proteins relative to dormant spores, the decrease in GerAC was significantly greater than that of GerKC and was 1.6-fold lower in superdormant spores in comparison to germinated spores (Fig. 2.4C). Similarly, while GerD was also less abundant in membranes from both superdormant and germinated spores than in dormant spores, the difference was greater in the germinated spores, such that GerD was 2-fold more abundant in superdormant spores than in germinated spores (Fig. 2.4C). This difference was statistically significant ($p<0.0001$). If germination-induced protein changes initiated but did not progress past GerD in superdormant spores, the difference in abundance for proteins involved in later germination events in comparison to germinated spores should be similar to a dormant/germinated spores comparison. Indeed, our results showed that YpeB and PrkC were 4.9 and 2.9-fold more abundant in samples from superdormant spores than in those from germinated spores, and SpoVAC and SpoVAD were 1.6 and 1.5-fold less abundant in superdormant spore samples than in germinated spore samples (Fig. 2.4C).

DISCUSSION

Spore germination starts at the spore inner membrane with the interaction of germinant with Ger receptor proteins and progresses through core rehydration and cortex breakdown. Deficiencies in Ger receptors and associated proteins, Ca^{2+}-DPA channels, and lytic enzymes can potentially inhibit the germination process, leading to the production of superdormant spores. In this work, L-valine superdormant spores responded poorly to valine but germinated well with AGFK; a result that is different from the initial report of superdormant spores (22) but consistent with a later report (91). In contrast to a high yield (12%) of superdormant spores isolated with AGFK in previous work (22), we were unable to isolate any superdormant spores using AGFK. The reasons for these differences are not clear, but raise the possibility that there may be multiple pathways to superdormancy, and slight differences in the method of preparation and isolation may result in significantly different superdormant spore populations.

Our quantitative MRM assays were performed on membrane samples derived from broken spores. Results published while this work was in progress indicate that these samples may represent a subset of the spore membrane fraction, as extensive chemical extraction is required to recover the full amount of several spore membrane proteins (109). While the sample analyzed here may not represent the entire spore membrane fraction, two lines of evidence indicate that the samples recovered from each spore type are similar fractions. The relative abundance of the majority of the proteins analyzed was the same in dormant and superdormant spores, and the amounts of the integral membrane A subunits of the Ger receptors were not altered in germinated spores, indicating that the membrane fractions obtained from the different spore types were comparable in their protein complements.

We interpret the similarity in Ger receptor A protein abundance in dormant and superdormant spore fractions to imply that the isolated superdormant population is not delayed in germination due to a low level of Ger receptors. These results differ from a previous publication that reported GerAA and GerAC protein levels were 7-fold lower and other GR subunits 3-fold lower in superdormant spores (24). We did find that the C subunits of the GerA and GerK receptors were decreased in samples from our superdormant spores. Germination-induced decreases in C subunit abundance, relative to dormant spores, were in one case less (GerAC) and in other cases slightly greater (GerBC and GerKC) than those observed in superdormant spores. As the C subunits are believed to be present in a stoichiometric association with the A subunits in the membranes of dormant spores (109), a decrease in the C subunits may indicate a change that takes place during early germination or may indicate a change in the maintenance of subunit association with the membrane during membrane fraction washing and isolation. Published data indicate that GerD, a lipoprotein like the C subunits, can be partially extracted by a high salt wash similar to that used in this study and is released from the membrane during germination (37). The decreased abundance of C subunits observed in superdormant spore samples could be either a cause of superdormancy or a result of the superdormant spore isolation process. Protein associations could decrease during Ger receptor activation upon germinant binding, and the membrane-association may be less stable as the spore membrane regains fluidity during germination (6). Prolonged exposure to germinants during the superdormant spore isolation may result in the loss of C subunits from the membrane, with a blockage in the germination pathway at a point downstream of the Ger receptors.

An absence of GerD was previously shown to result in a germination initiation defect (25, 26). Previous studies also indicated that the germination receptors and GerD co-localize to a discrete cluster on the membrane (110) and that SpoVA proteins can associate with Ger

receptors (111), and thus we expect that the comparable membrane factions we derived from different spore types would contain similar amounts of GerD. Superdormant spore membrane samples had 2-fold less GerD than those from dormant spores, and germinated spore samples contained even less GerD. Similar to the case for the Ger receptor C subunits, the decreased level of GerD in superdormant spores could be either a cause of superdormancy or a result of a partial germination response that is blocked at a subsequent point.

Other germination-active proteins, PrkC, SpoVAC, SpoVAD, and YpeB were present in dormant and superdormant spore membrane preparations in similar quantities, but did show changes in abundance during germination. This suggests that any early germination-related events that have taken place within the superdormant spores did not progress to later events such as SpoVA-assisted DPA release (96) or YpeB-related cortex degradation (64). Interestingly, the abundance of membrane-associated SpoVAC and SpoVAD proteins increased during germination. As this increase is taking place well before any new protein synthesis, it must represent an increased association of the proteins with the membrane or with other membrane-bound proteins, most likely other products of the SpoVA DPA-transport complex. Several studies indicate that SpoVAD localizes to the spore inner membrane (27, 112), and recent structural analyses of this protein show that it is likely to be a peripheral membrane protein (108, 113). In our western-blot analysis of SpoVAD, it was detected in both soluble and membrane fractions, suggesting a weak membrane association (data not shown). Another novel finding is that PrkC abundance decreased significantly during spore germination triggered by L-Val. Although this protein was previously demonstrated to be a germinant receptor that responds to muropeptides (48), there is no report of its activity in other germinant receptor-mediated pathways.

The most dramatic change in protein abundance during germination was that of YpeB, which is required for incorporation of SleB in spore and thus for normal cortex degradation

during germination (64). This result is consistent with a previous observation of YpeB degradation during germination. The 52 kDa YpeB is processed to a ~30 kDa product during germination (64). The 6.8-fold decrease in YpeB abundance we observed was calculated using those peptides we could detect in both dormant and germinated spore samples, all of which were in the C-terminal half of the protein. One peptide nearer the N-terminus of YpeB was detected in dormant spore samples but was undetectable in germinated spore samples, indicating a decrease of >14-fold. This differential loss of peptides indicates that the more stable 30-kDa portion of YpeB represents a C-terminal portion. Ongoing studies in our lab are consistent with this (data not shown). It is not clear if the 6.8-fold decrease in the observed YpeB peptides is due to protein degradation, a decrease in membrane association, or both. Because the N-terminus of YpeB apparently contains an uncleaved signal peptide, proteolytic removal of this domain would be expected to decrease YpeB-membrane association.

Studies of spore germination heterogeneity have shown that the major variable in kinetics of nutrient-triggered spore germination is the germination initiation time, termed T_{lag}, with the range of superdormant spores' T_{lag} times being significantly greater than that of dormant spores (91). Previous studies also showed that *gerD* spores had significantly longer T_{lag} times than wild-type spores (25). The results from our work in relation to those previous efforts lead us to propose that decreased abundance of GerD can be a contributing factor in superdormancy.

ACKNOWLEDGEMENTS

This work was supported by the National Institute of Allergy and Infectious Disease of the National Institutes of Health under award number R21AI088298. The mass spectrometry resources used in this work are maintained in part through funding by the Fralin Life Science Institute at Virginia Tech and the Agricultural Experiment Station Hatch Program at Virginia Tech (CRIS Project Number: VA-135981).

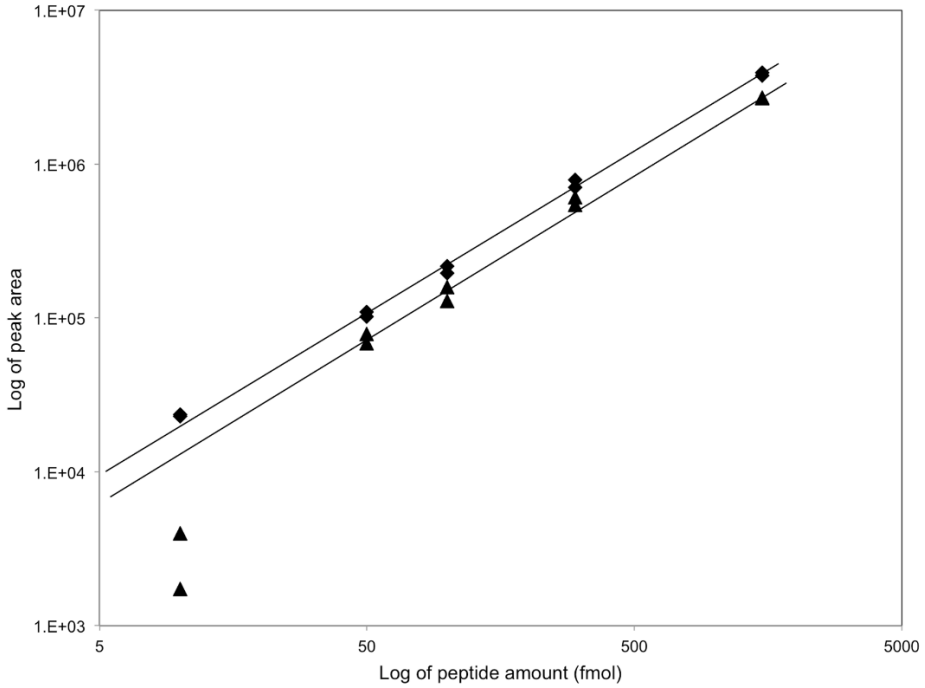

Figure 2.1. Example determinations of MRM Limit of Quantitation (LOQ) using synthetic peptides. Dilution series of peptides SLDEPSSEVVER (◆), which is proteotypic for the *B. subtilis* GerBA protein, and EAYSDDVPEGQVVK (▲), which is proteotypic for the *B. subtilis* PrkC protein, were subjected in duplicate to MRM analysis with detection of the parent ion 493.9 m/z and the fragment ion 798.3 m/z for GerBA or the parent ion 768.7 m/z and the fragment ion 1085.6 m/z for PrkC (Table 2.1). Fragment ion peak areas were plotted against peptide amount, and best-fit lines were applied. LOQ's were defined as the lowest concentration at which the response was still linear or the lowest concentration at which the contribution due to noise was such that reproducible results could be obtained (peak area $\geq 1 \times E^{+4}$).

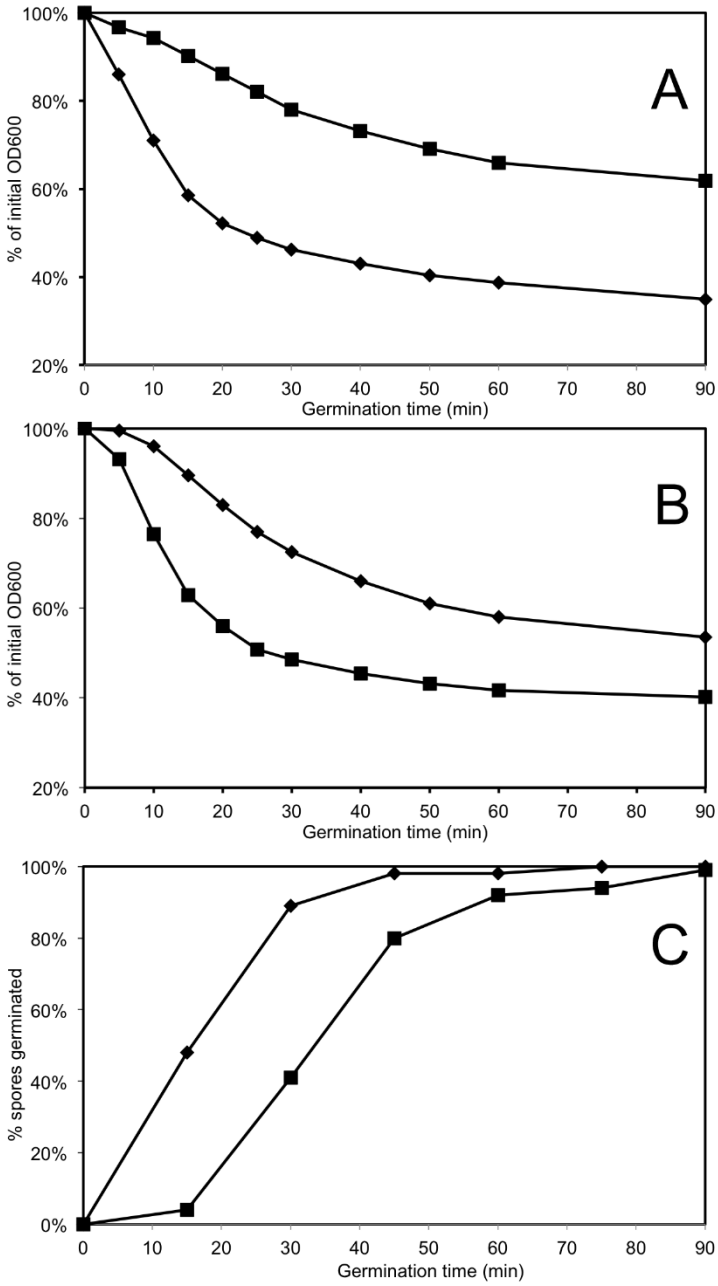

Figure 2.2. Germination of dormant and superdormant spores with nutrient and non-nutrient germinants. Superdormant spores of *B. subtilis* strain PS832 (wild type) were isolated following prolonged germination with 10 mM L-Valine as described in materials and methods. Squares (■) indicate isolated superdormant spores, and diamonds (◆) indicate the initial dormant spores used for isolation. A) Germination with 10 mM L- Valine; B) Germination with AGFK; C) Germination with Ca^{2+}-DPA. Data from one biological replicate of dormant and superdormant spores is shown. Analyses of the other two biological replicates produced very similar results.

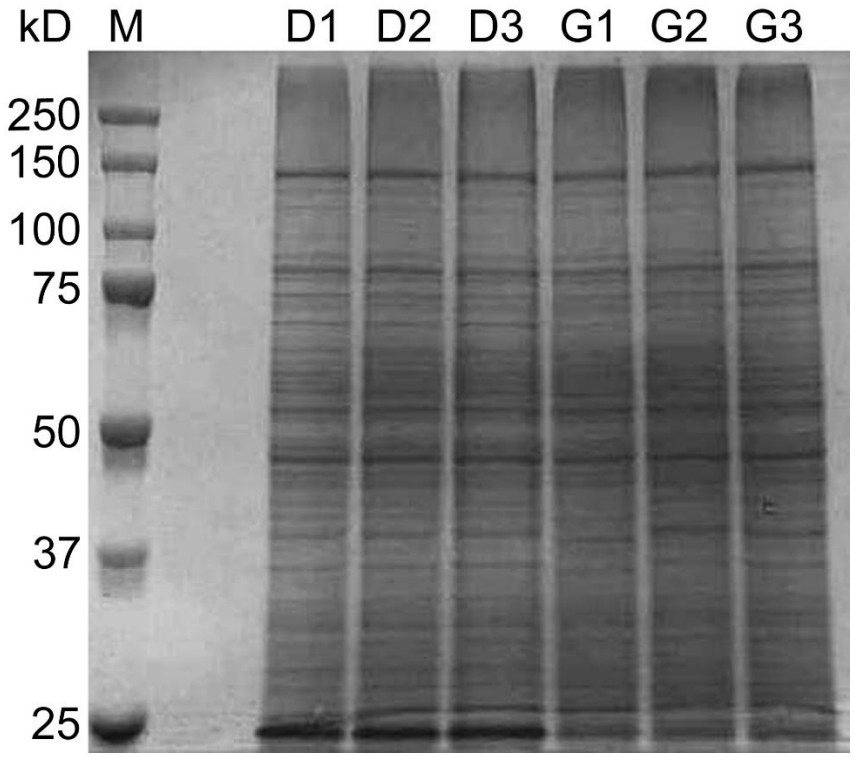

Figure 2.3. Gel electrophoresis of membrane-associated spore proteins. Membrane preparations were obtained from dormant (D) and germinated (G) spores produced from three independent spore preparations (1, 2, and 3). Protein concentrations in membrane preparations were determined by quantitative amino acid analyses, and identical protein amounts were loaded onto a 9% polyacrylamide gel. Sizes of protein standard markers (M) are indicated on the left. Proteins were stained using Coomassie blue.

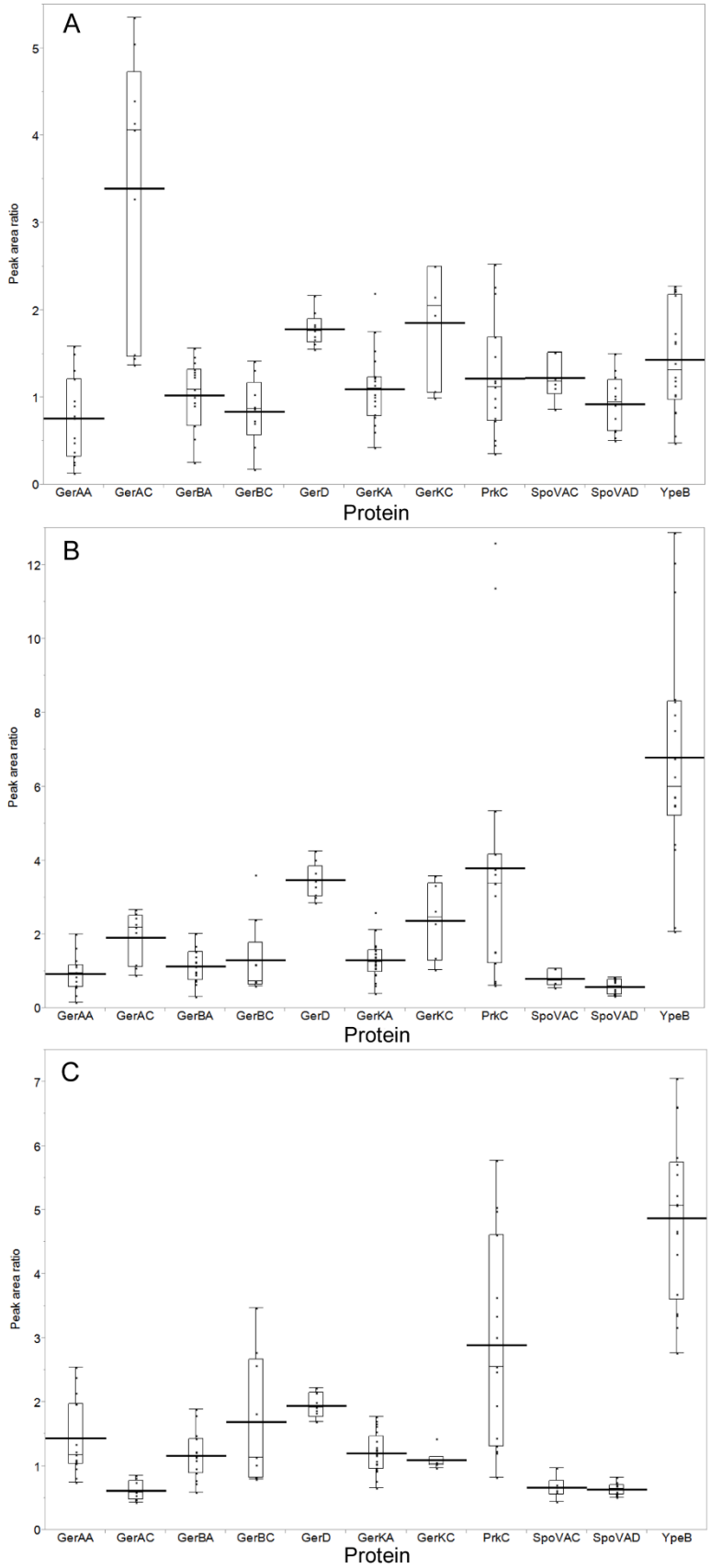

Figure 2.4. Relative quantities of germination proteins in dormant, superdormant, and germinated spores. Proteins were quantified in membrane samples by MRM analyses. The relative abundance of each protein is expressed as the ratio of each particular product ion peak area detected in dormant versus superdormant (A), dormant versus germinated (B), or superdormant versus germinated (C) spore samples derived from the same spore preparation. Ratios determined for samples from three independent spore preparations were then pooled. Each box and whisker plot indicates individual product ion ratio values (dots), 25-75 percentiles (boxes) and full ranges (whiskers), excluding statistically determined outliers. Means are indicated by the short lines traversing the boxes and medians are shown by the lines traversing the boxes.

Table 2.1. Peptide Details for MRM Analysis of the *B. subtilis* germination proteins.

Protein	Proteotypic peptide sequence (position in protein)	Parent ion m/z (charge state)	Fragment ion m/z (ion)	LOQ fmoles (peak area) [c]
GerAA	LDQLDARPVETAK (77-89)	486.2 (+3)	672.0 (y_{12}^{+2})	10 ($3\times E^{+5}$)
		486.2 (+3)	614.5 (y_{11}^{+2})	10 ($3\times E^{+5}$)
	DEETLTLDQVK (64-74)	646.1 (+2)	703.4 (y_6^{+1})	10 ($8\times E^{+4}$)
	VSSALFNGR (233-241)	476.3 (+2)	765.3 (y_7^{+1})	10 ($1\times E^{+4}$)
		476.3 (+2)	374.1 (y_7-NH_3^{+2})	10 ($1\times E^{+4}$)
GerAC	ADVTGLGNEVR (321-331)	565.8 (+2)	744.3 (y_7^{+1})	50 ($1\times E^{+4}$)
		565.8 (+2)	845.5 (y_8^{+1})	100 ($1\times E^{+4}$)
		565.8 (+2)	687.4 (y_6^{+1})	50 ($1\times E^{+4}$)
GerBA	TSDPNLVIK (156-164)	493.9 (+2)	683.2 (y_6^{+1})	10 ($2\times E^{+4}$)
		493.9 (+2)	798.3 (y_7^{+1})	10 ($2\times E^{+4}$)
	SLDEPSSEVVER (124-135)	674.1 (+2)	902.3 (y_8^{+1})	10 ($4\times E^{+4}$)
		674.1 (+2)	316.2 (y_5^{+2})	10 ($3\times E^{+4}$)
	VESSLLEGR (235-243)	495.4 (+2)	761.3 (y_7^{+1})	10 ($1\times E^{+4}$)
GerBC	GILTEDQNPNENSFSK (279-294)	897.3 (+2)	922.4 (y_8^{+1})	50 ($1\times E^{+4}$)
		897.3 (+2)	1036.6 (y_9^{+1})	50 ($1\times E^{+4}$)
	GNAADVFTK (135-143)	461.8 (+2)	609.4 (y_5^{+1})	10 ($1\times E^{+4}$)
		461.8 (+2)	680.3 (y_6^{+1})	50 ($1\times E^{+4}$)
GerKA	ERPVLISPSLAK (31-42)	437.4 (+3)	595.3 (b_5^{+1})	10 ($2\times E^{+4}$)
		437.4 (+3)	515.2 (y_5^{+1})	10 ($2\times E^{+4}$)
		437.4 (+3)	602.1 (y_6^{+1})	50 ($1\times E^{+4}$)
	SIQEPSTQVSFR (159-170)	690.2 (+2)	921.7 (y_8^{+1})	10 ($1\times E^{+4}$)
		690.2 (+2)	329.0 (b_3^{+1})	50 ($1\times E^{+4}$)
		690.2 (+2)	1050.5 (y_9^{+1})	50 ($1\times E^{+4}$)
	EVGSSSDVIIR (50-60)	581.5 (+2)	789.5 (y_7^{+1})	10 ($1\times E^{+4}$)
GerKC	TLDFTEAQYGR (166-176)	651.0 (+2)	330.2 (b_3^{+1})	10 ($1\times E^{+4}$)
		651.0 (+2)	723.5 (y_6^{+1})	50 ($1\times E^{+4}$)

GerD	NIFEDTDFAEGFAK (90-103)	802.5 (+2)	1376.6 (y_{12}^{+1})	100 ($1 \times E^{+4}$)
		802.5 (+2)	422.1 (y_{4}^{+1})	300 ($1 \times E^{+4}$)
		802.5 (+2)	1229.6 (y_{11}^{+1})	300 ($7 \times E^{+5}$)
SpoVAC	SEGLVLGVATNM(ox)FK (109-122)	741.5 (+2)	883.2 (y_{8}^{+1})	50 ($1 \times E^{+4}$)
		741.5 (+2)	996.3 (y_{9}^{+1})	50 ($1 \times E^{+4}$)
	SEGLVLGVATNMFK (109-122)	733.6 (+2)	867.3 (y_{8}^{+1})	300 ($1 \times E^{+4}$)
		733.6 (+2)	980.7 (y_{9}^{+1})	300 ($1 \times E^{+4}$)
SpoVAD	ETIPTIAHGVVFER (320-333)	523.9 (+3)	409.3 (y_{11}^{+3})	50 ($1 \times E^{+4}$)
		523.9 (+3)	613.6 (y_{11}^{+2})	50 ($1 \times E^{+4}$)
	QLMEDAVNVALQK (57-69)	730.2 (+2)	459.3 (y_{4}^{+1})	100 ($1 \times E^{+4}$)
		730.2 (+2)	672.3 (y_{6}^{+1})	100 ($1 \times E^{+4}$)
YpeB	IGVFSYVPVENK (326-337)	676.7 (+2)	586.1 (y_{5}^{+1})	50 ($1 \times E^{+4}$)
		676.7 (+2)	935.3 (y_{8}^{+1})	50 ($1 \times E^{+4}$)
	TIPKPAITEAEAK (372-384)	457.2 (+3)	577.9 (y_{11}^{+2})	10 ($2 \times E^{+5}$)
		457.2 (+3)	929.5 (y_{9}^{+1})	10 ($5 \times E^{+4}$)
	VALDDGEVVGFSAR (349-362)	718.2 (+2)	636.3 (y_{6}^{+1})	100 ($1 \times E^{+5}$)
		718.2 (+2)	537.4 (y_{5}^{+1})	100 ($3 \times E^{+5}$)
PrkC	EAASGYLEDNGLK (508-520)	684.3 (+2)	789.3 (y_{7}^{+1})	10 ($1 \times E^{+4}$)
		684.3 (+2)	1096.5 (y_{10}^{+1})	10 ($1 \times E^{+4}$)
	EAYSDDVPEGQVVK (525-538)	768.7 (+2)	756.3 (y_{7}^{+1})	50 ($1 \times E^{+4}$)
		768.7 (+2)	1085.6 (y_{10}^{+1})	50 ($1 \times E^{+4}$)
	TEIGDVTGQTVDQAK(429-443)	781.8 (+2)	947.6 (y_{9}^{+1})	50 ($1 \times E^{+4}$)
		781.8 (+2)	1218.8 (y_{12}^{+1})	10 ($1 \times E^{+4}$)

[a] LOQ is the limit of quantitation determined for this fragment ion, as described in Materials and Methods.

CHAPTER 3

Membrane Proteomes in *Bacillus anthracis* and *Bacillus subtilis* Dormant and Germinating Spores

Yan Chen, W. Keith Ray, Richard F. Helm, Stephen B. Melville, and David L. Popham

Manuscript in preparation

ATTRIBUTIONS

Conceived and designed the experiments: Yan Chen, W. Keith Ray, Richard F. Helm, Stephen B. Melville, and David L. Popham. Performed the experiments: Yan Chen, and David L. Popham. Analyzed the data: Yan Chen, Richard F. Helm, and David L. Popham. Contributed reagents/materials/analysis tools: Yan Chen, W. Keith Ray, Richard F. Helm, and David L. Popham. Wrote the paper: Yan Chen, W. Keith Ray, Richard F. Helm, Stephen B. Melville, and David L. Popham.

ABSTRACT

Bacterial endospores produced by *Bacillus* and *Clostridium* species can remain dormant and highly resistant to environmental insults for long periods, but can also rapidly germinate in response to a nutrient rich environment. Multiple proteins involved in sensing and responding to nutrient germinants, initiating solute and water transport, and accomplishing spore wall degradation are associated with the membrane surrounding the spore core. To identify protein changes taking place during germination, as well as to identify unknown proteins that might be involved in spore germination, a global proteomics approach was applied to membrane preparations isolated from dormant and germinated spores of *Bacillus anthracis* and *Bacillus subtilis.* Membrane-associated proteins were fractionated by SDS-PAGE, gel slices were trypsin-digested, and isolated peptides were fractionated by liquid chromatography and MALDI-TOF-TOF mass spectrometry. Over 500 proteins were identified from each preparation. Bioinformatic methods were used to characterize proteins with regard to membrane association, cellular function, and conservation across species. Numerous proteins not previously known to be spore associated, 35 in *B. subtilis* and 59 in *B. anthracis*, were identified. A significant number of these proteins are implicated in the transport of metal ions, a process that plays a major role in spore formation and germination. Spectral counting methods indicated that the majority of spore membrane proteins decrease in abundance during the first 20 min of germination.

INTRODUCTION

Bacterial endospores produced by *Bacillus*, *Clostridium*, and related genera can remain dormant for extended periods of time. In addition, these spores are highly resistant to most chemical and physical treatments commonly used to reduce bacterial contamination (13). Upon exposure to conditions conducive to resumption of vegetative growth, generally a nutrient rich environment, these spores can rapidly germinate and resume metabolism (20, 21). These factors allow certain spore-forming species to act as significant human pathogens including potential biological weapons (89), as agents of food poisoning and spoilage (114), and, on a positive note, as effective vehicles for delivery of antigens or metabolic and enzymatic activities of industrial, consumer, or patient benefit (115-117).

Major factors in spore dormancy and resistance properties are the relative dehydration of the spore core (cytoplasm) and high core concentrations of solutes such as calcium dipicolinate (Ca^{2+}-DPA) (13). The dehydrated and metabolically inactive state of the core is maintained by the spore membrane, which exists in a novel non-fluid state (6), and the surrounding spore cortex peptidoglycan cell wall (118). Spore germination proceeds through the rapid release of the core Ca^{2+}-DPA pool, a concomitant uptake of water (20), and the subsequent return of the spore membrane fluidity (6). This is immediately followed by degradation of most of the cortex wall (63), allowing full core rehydration, resumption of metabolic activity, and spore outgrowth. Knowledge of the mechanisms driving spore germination will allow targeting of this process for the improvement of decontamination regimens as well as regulating germination during antigen or activity delivery (119).

Genome sequencing and transcriptome profiling have produced predictions of proteins present within spores (15, 67, 120-122). A number of proteome studies have examined spore fractions in several species (67, 79-85). Most of these studies were biased towards soluble

proteins, as opposed to membrane-associated proteins, although many of the proteins currently known to function in the spore germination process are associated with the spore membrane. These include germinant receptor complexes (28, 112), the SpoVA proteins involved in Ca^{2+}DPA transport (27, 54, 96, 97), the GerD lipoprotein (37, 40), and the YpeB-SleB proteins involved in cortex degradation (64). Some of these germination-associated proteins are known to decrease in amount or in their membrane-associations during germination (37, 64).

The goals of the current study were to catalog the spore membrane proteomes of *Bacillus subtilis* and *Bacillus anthracis* and to examine changes in these proteomes during germination. Over 500 proteins were identified in each proteome, and approximately 100 of these were found to contain amino acid sequences predicted to result in integral or peripheral membrane association. The majority of previously recognized membrane-associated germination proteins were identified, and over 50 proteins were identified for the first time in the membrane proteomes of both species. Spectral counting methods for determining protein abundance changes during germination revealed that the level of a majority of spore membrane proteins decreased significantly during germination.

MATERIALS AND METHODS

Spore sample preparation. Spores of *B. anthracis* Sterne strain 34F2, an attenuated vaccine strain, were prepared in Modified G broth (123). Spores of *B. subtilis* strain PS832, a prototrophic laboratory derivative of strain 168 were prepared in 2xSG broth (102). Spores were harvested after 3-4 days incubation at 37 ℃, washed in water for several days, and purified by centrifugation through a 50% sodium diatrizoate (Sigma) layer as described (103). All spores used in this work were 99% free of vegetative cells and were stored in deionized water at 4 ℃ until analysis.

To prepare germinated spores, a 10-ml suspension of dormant spores at an optical density at 600 nm (OD_{600}) of 20 in water was heat-activated at 70 ℃ for 30 min (*B. anthracis*) or 75 ℃ for 30 min (*B. subtilis*) and cooled on ice for 10 min. The spores were then germinated at 37 ℃ and at an OD_{600} of 2 with 50 mM L-alanine plus 1 mM inosine (*B. anthracis*) or 10 mM L-valine (*B. subtilis*) in 25 mM Tris-HCl buffer (pH 7.4). The germination of spores was terminated after the OD_{600} dropped to 50% of the initial value (within 10 min and 35 min after germinant addition for *B. anthracis* and *B. subtilis*, respectively). Germinated spores were collected by centrifugation at 12,000 *g* for 5 min at 4 ℃, quickly washed with cold deionized water, centrifuged again, and frozen at -80 ℃. Examination by phase-contrast microscopy indicated that >95% of the spores in each preparation had germinated.

Preparation of spore membrane fractions. Spore membrane fractions were prepared by a modification of a previously described method (124). Dormant and germinated spores were lyophilized, and the dry spores (~19 mg for germinated spores and ~24 mg for dormant spores) were pulverized with 100 mg of glass beads in a dental amalgamator (Wig-L-Bug) at 4,600 rpm for pulses of 30 s each, with 30 s pauses on ice between pulses. Spore disruption was monitored by suspending an aliquot of spore material in H_2O and observing under phase-

contrast microscopy. After >80% of spores were disrupted, the dry powder was suspended in 0.5 ml of 4 ℃ extraction buffer (10 mM Tris-HCl [pH 7.4], 1 mM EDTA, 2 mg/ml RNase A, 2 mg/ml DNase I, 1 mM phenylmethylsulfonyl fluoride (PMSF)). The suspension was centrifuged (6,000 X *g*, 10 min, 4 ℃) and the resultant supernatant was centrifuged again (13,000 X *g*, 10 min, 4 ℃) to remove insoluble material. The remaining supernatant was centrifuged at 100,000 X *g* for 60 min at 4 ℃, and the resulting pellet was designated as the crude spore membrane fraction. This membrane fraction was homogenized in 1 ml alkaline buffer (100 mM Na_2CO_3-HCl [pH 11], 10 mM EDTA, 100 mM NaCl, 1 mM PMSF) and was gently shaken for 60 min at 4 ℃. The homogenate was subjected to ultracentrifugation as described above. The resulting pellet was homogenized in 1 ml high salt buffer (20 mM Tris-HCl [pH 7.5], 10 mM EDTA, 1 M NaCl, 1 mM PMSF) and was again subjected to ultracentrifugation. After a final wash with 1 ml TE buffer (10 mM Tris-HCl [pH 7.4], 1 mM EDTA, 1 mM PMSF), the resulting pellet was homogenized in 200 µl TE buffer, flash frozen, and stored at -80 ℃ until analysis. Protein concentrations were determined by acid hydrolysis and amino acid analysis (105) with comparison to a standard set of amino acids (Sigma).

SDS-PAGE, Trypsin digestion, and peptide fractionation. Membrane fractions were dried and re-suspended in SDS-PAGE sample loading buffer (62.5 mM Tris-HCl pH 6.8, 2% SDS, 10% glycerol, 5% β-mercaptoethanol, 0.05% bromophenol blue) to a final protein concentration of 2 µg/µl. SDS-PAGE was used to separate 30 µg protein of each spore membrane sample in both 10% polyacrylamide and 12.5-14% gradient polyacrylamide gels for *B. subtilis* samples, and in a 12.5-14% gradient polyacrylamide gel for *B. anthracis* samples. Gels were stained with ProtoBlue Safe (National Diagnostics). Each gel lane was cut into 10-12 slices, consistently for all samples within each species, in an effort to isolate regions containing many lower abundance proteins away from higher abundance proteins that could dominate MS profiles. Gel slices were ground and de-stained with 50% LC/MS-grade

acetonitrile supplemented with 25 mM NH_4HCO_3. The gel slices were then dehydrated with 100% acetonitrile and vacuum dried. Gel slices were soaked in 25 mM NH_4HCO_3 containing 10 µg/ml trypsin (Sigma), and digestion was carried out at 37 ℃ for at least 16 hours. Tryptic peptides were extracted from gel slices into 50% LC/MS-grade acetonitrile, 0.1% trifluoroacetic acid (TFA) using a sonication bath. Peptides were vacuum dried and re-suspended in 40 µl 2% LC/MS-grade acetonitrile, 0.1% TFA.

An Eksigent nano2D-LC unit, flowing at 0.7 µL/min, was used to inject 10 µl of each peptide sample through a Captrap cartridge (Michrom Bioresources) and a self-packed New Objective Integrafrit 50 X 0.1 mm column, both packed with Magic C18 AQ (200Å, 3 µm)(Michrom Bioresources). Elution was with 5% acetonitrile for 25 minutes, a 5 min linear increase to 14% acetonitrile, and a 95 min linear increase to 34% acetonitrile. An Ekspot plate spotter (Eksigent) was used to spot the eluate onto MALDI target plates at a rate of 10-15 seconds per spot, dependent on the band intensity and the size of a gel slice, and the spots were air-dried. Samples from matching gel slices of biological replicates were spotted at the same rate.

Mass spectrometry and protein identification. Matrix was prepared by suspending approximately 200 mg αCHCA (Aldrich) in 1 ml 100 mM acetic acid and mixing vigorously. Following centrifugation for 2 min at 1000 x g, the supernatant was removed, and the wash procedure was repeated. Two additional washes were performed with 100% acetonitrile, and the αCHCA was vacuum-dried and stored at 4 ℃. Matrix solution was prepared by dissolving 4 mg of washed αCHCA in 1 ml 1:1:0.001(v/v/v) water:acetonitrile:TFA, to which 2 M NH_4Cl was then added to a final concentration of 10 mM. Each dried sample spot on the MALDI plates were overlaid with 1 µl of matrix solution and air-dried.

For calibrating and tuning the MALDI-TOF/TOF 4800 analyzer (AB SCIEX), 200 µl of the matrix solution was added to an aliquot of a mix of six standard peptides (Anaspec,

#60882). This mix was spotted onto all calibration spots when analyzing a sample MALDI plate. For each peptide sample spot, a scan for the m/z range of 800-4,000 was acquired with averaged data from 1,000 laser shots in reflector positive ion mode. The 10 most abundant ions for each spot, above a minimum signal-to-noise ratio (>50), were then automatically selected for subsequent MS/MS analysis. Parent ions chosen for one spot were excluded from analyses in subsequent spots. MS/MS scans were the averages of 3,000 laser shots (1 kV, positive ion mode).

The MS and MS/MS data were analyzed using ProteinPilot™ software version 4.0 (AB SCIEX) and Scaffold version 3.0 software (Proteome Software, Inc.). The parameters used in ProteinPilot™ were: identification as sample type, no cysteine alkylation, trypsin as digestion enzyme, gel-based identification as special factors, biological modifications and amino acid substitutions as ID focus, thorough ID as search effort, and detected protein threshold (unused protein score) > 0.05 (10%) as result quality. The *B. subtilis* 168 protein database (2/10/2012) and *B. anthracis* (BACAN) protein database (12/18/2012) were downloaded from Universal Protein Resources (http://www.uniprot.org/). Based on the ProteinPilot™ false discovery rate for analysis of acquired protein list, 5% false discovery rate (FDR) and a minimum of one peptide at 95% identification confidence were applied to each biological sample protein profile. The raw data is available from the PRIDE database (http://www.ebi.ac.uk/pride/archive/) (In process). Proteins identified in at least two biological replicates were considered a valid identification. For membrane proteins that only produced one peptide with these parameters, confirmation of the identification was performed by manual interpretation of their MS/MS spectra. All proteins in dormant and germinated protein profiles were then annotated according to their accession number using two databases: the National Center for Biological Information (http://www.ncbi.nlm.nih.gov/) and Universal Protein Resources. Other online resources that were used for predicting membrane

associations are: Brinkman Laboratory at Simon Fraser University (http://www.psort.org/psortb/index.html) and PRED-LIPO server at University of Athens (http://bioinformatics.biol.uoa.gr/PRED-LIPO/input.jsp). Protein NCBI Cluster of Orthologous Groups (COG) were predicted using the COMBREX database (http://combrex.bu.edu/).

To acquire preliminary relative protein quantification, the Mascot data files of three biological replicates were merged and onsite Mascot searches were performed for each peptide fragmentation mass spectrum against the *B. subtilis* and *B. anthracis* protein databases. Mascot parameters were: Trypsin specificity with one missed cleavage, carbamidomethylation was a fixed modification, and deamidation, pyro-cmC, and oxidations were considered variable modifications. The peptide mass tolerance and fragment mass tolerance were set to ±500 ppm and ±0.2 Da, respectively. Search results were analyzed using Scaffold^{TM} version 3.4.9. The Scaffold^{TM} parameters were 95% protein threshold and 1 minimum identified peptide at 95% of threshold, and normalization was selected for quantitative analysis. The unique spectrum count of a protein was used to relatively quantify the protein changes between two samples (125).

All identified *B. anthracis* membrane proteins were searched against the whole *B. subtilis* protein database and the proteins identified in *B. subtilis* spore membrane profile using the NCBI protein BLAST tool (126). Only sequences with alignment coverage ≥60% were considered possible orthologs in the two species. If the protein in the full *B. subtilis* protein database that had the highest identity percentage against a *B. anthracis* membrane query protein was also identified in the *B. subtilis* spore membrane profile, these two proteins were considered to be the most likely orthologs. If a protein in *B. subtilis* spore membrane proteome had high similarity to a *B. anthracis* membrane query protein, but it was not the

highest identity match in the full *B. subtilis* protein database, then the two proteins were considered to be likely paralogs.

RESULTS

Proteins identified in dormant spore membrane preparations. Membranes were isolated from three independent preparations of *B. anthracis* and *B. subtilis* dormant spores. Proteins were separated by SDS-PAGE (Figure 3.1) followed by gel slice preparation and processing to provide peptides that were submitted to LC-MALDI separation and analysis. A total of 603 and 592 proteins were identified in *B. subtilis* and in *B. anthracis* samples, respectively. Bioinformatic predictions suggested that 104 (17%) and 87 (15%) of these proteins were membrane-associated proteins in *B. subtilis* and *B. anthracis*, respectively (Table 3.1). Predicted membrane proteins were further categorized based on their mechanism of membrane association and number of predicted membrane-spanning helices (Figure 3.2). The presence of a wide variety of lipoproteins, peripheral (monotopic), and integral polytopic membrane proteins indicates that the method used was successful in recovering a broad membrane proteome. A total of 11 known germination-related membrane proteins were identified in *B. subtilis* samples (Table 3.2). Similarly, a total of 5 known germination related proteins were identified in *B. anthracis* samples (Table 3.2). The remaining identified membrane proteins have predicted functions in 14 COG function categories.

Proteins identified in germinated spore membrane preparations. A portion of each spore preparation was exposed to nutrient germinants until the optical density of the suspension had decreased 50%, which resulted in germination of ≥95% of the spores. The membrane fractions were then isolated, and the proteins were separated by SDS-PAGE (Fig. 3.1). Collection and processing of gel slices provided samples for LC-MALDI separation and analysis. A total of 497 and 508 proteins were identified in *B. subtilis* and *B. anthracis* germinated spore membrane profiles, respectively. In each species, some proteins (82 and 88 proteins in *B. subtilis* and *B. anthracis*, respectively) were identified only in the germinated samples and not in the dormant spore samples, and these were predominantly predicted to be

cytoplasmic proteins. Of the 52 (10.5%) and 38 (7.5%) proteins that were predicted to be membrane-associated in *B. subtilis* and B. *anthracis*, respectively, all but two in *B. subtilis* (P40780 and Q01464) were also present in the dormant spore samples.

Novel membrane proteins identified in spore membrane fractions. The spore membranes are derived from the sporangium cytoplasmic membranes during the engulfment stage of sporulation, so, it was no surprise to find that membrane proteins expected to be in vegetative cells were present in spore membrane fractions. Among the predicted membrane proteins we detected in dormant or germinated spores, 57 out of 104 *B. subtilis* proteins had been identified in previous vegetative proteome studies (Table 3.1). An additional three proteins, YhcM, YodI, and YlaJ were reported in previous proteome studies of *B. subtilis* spores (79), but were not included in vegetative cell proteome studies. The genes that encode these three proteins are transcribed under control of sporulation sigma factors σ^F, σ^K, and σ^G, respectively (79, 121), and are therefore likely spore-specific proteins. GerAC, GerBC, GerKC, GerD, SpoVAD, and YpeB are known germination-active proteins that were previously detected in spores (64, 99). An additional five known germination-active proteins: PrkC, SpoVAC, SpoVAF, YfkR, and YhcN were assumed to be present in spores, but had not been previously detected or had been detected only in a previous vegetative cell proteome study (77). Among the remaining 35 spore membrane proteins identified here, 13 have unknown functions and others have predicted COG functions in inorganic ion transport and metabolism (6); amino acid transport and metabolism (4); posttranslational modification, protein turnover, chaperones (2); lipid biogenesis and metabolism (2); intracellular trafficking, secretion, and vesicular transport (2); cell wall biogenesis (2); general transport (1); signal transduction (1); cell cycle control (1); and energy production and conversion (1).

A similar analysis of the *B. anthracis* samples revealed that 15 predicted membrane proteins were reported previously in a vegetative cell proteome study (78), and 13 proteins

were reported previously in spore proteome studies (82, 83). Among the remaining 59 spore membrane proteins identified here, 16 are presently listed with unknown functions, 5 are known germination-active proteins (Table 3.2), and the rest sort into 12 different COG categories.

Membrane proteins under control of sporulation-specific sigma factors. Predicted membrane-associated proteins identified in *B. subtilis* samples were searched against the relatively well-characterized sporulation transcriptomes of that species (15, 79, 122, 127). Of the 104 predicted membrane-associated proteins, 29 have been shown to be controlled at the transcriptional level by the sporulation-specific sigma factors σ^E, σ^F, σ^G, and σ^K (Table 3.1). Only a small number of membrane proteins were identified from the mother cell-specific σ^E and σ^K regulons, 4 and 2 proteins, respectively. The remaining membrane proteins for which transcriptome data is available were in the forespore-specific σ^F (4 proteins) and σ^G (19 proteins) regulons, though the similarity between these two sigma factors results in some overlap of their regulons (15). The genes of 10 known germination-active proteins identified are all within the σ^G regulon. Eight σ^G-dependent proteins had not been previously detected in spore proteomes. Among these, YutC, YhcC, YrbG, and YqfX have unknown functions, while YveA, YwjE, YitG, and YthA were categorized into amino acid transport and metabolism, lipid biogenesis and metabolism, general transporter, and energy production and conversion, respectively.

Similarities between the spore membrane proteomes in the two *Bacillus* species. Searches using the BLAST program were done to compare the predicted membrane proteins identified in samples from each species. Fifty-one *B. anthracis* spore membrane proteins showed high similarity to 48 spore membrane proteins identified in *B. subtilis* (Table 3.3). Forty-five of these proteins were considered to be orthologous, based on A) a high level of amino acid sequence identity (>23%) and similarity (>42%) across an alignment of >62% of

the protein sequences and B) synteny. Among these, GerD, MisCA, SpoVAC, SpoVAD, SpoVAF, YetF, YpeB, YthA, and YutC have been previously identified in spores under more defined studies and/or were expressed in the forespore-specific σ^F and σ^G regulons. Several of these are known germination-active proteins. MisCA (SpoIIIJ) is required for activation of σ^G after engulfment of the forespore is completed (128). YthA was suggested to compensate for the loss of cytochrome aa_3, which is critical for sporulation as one of two heme copper terminal oxidases in *B. subtilis* (129). There is no known function reported for YutC and YetF. This leaves eight proteins that were detected in both species and had not been previously identified in spore proteomes or sporulation-specific regulons. ArtP, MetQ, and AdcA are components of ABC transporters involved in amino acid or inorganic ion transport. YpmQ is involved in assembly of a copper center in cytochrome *c* oxidase, which has an important function in energy conversion and metabolism (130). YyxA was predicted to be a serine protease due to its sequence similarity to the S1B peptidase family. YndM, YugS and YkrK are proteins of unknown function.

Three *B. subtilis* membrane proteins, YhcC, YveA, and YitG, that are expressed in the σ^G regulon (15, 127) and do not have similar proteins in the *B. anthracis* protein database, were detected. Three other σ^G regulon proteins, YhbJ, YrbG, and YwjE (127), have highly similar proteins in *B. anthracis* (BAS4465, BAS4309, and BAS5195, respectively) but were only detected in *B. subtilis*.

Membrane protein changes during spore germination. Spectral counting methods (125, 131) were applied to determine protein abundance information before and after spore germination. To test the validity of this method, we compared the ratio changes of proteins in this data to more precise, previously published quantification data for several germination proteins (124) (Table 3.4). The trends in terms of proteins increasing, decreasing, or not changing in membrane association during germination were generally consistent in the two

data sets with only one protein, SpoVAC, exhibiting an inverse trend in the two studies. The decreased abundance of *B. anthracis* proteins BAS2560, BAS1302, and BAS4323 after spore germination was also consistent with a previous whole spore quantitative proteomic study (83). On the other hand, our results showed that BAS0812 and BAS3922 decreased 5.9- and 3.7-fold respectively, and BAS0405 increased 2-fold after spore germination, but these proteins showed no change in quantity in the previous study (83). Preliminary protein quantity changes during germination were determined for 99 *B. subtilis* and 83 *B. anthracis* spore membrane proteins. Strikingly, most of the membrane proteins (>70%) in both species were either not detected (Table 3.5) or greatly reduced in quantity after spore germination (73 *B. subtilis* proteins and 65 *B. anthracis* proteins) (Table 3.6). In *B. subtilis* samples, two membrane proteins, YtxH and MinD, were present in germinated spore samples that were not detected in the dormant spore samples.

DISCUSSION

Proteins associated with the membranes separating the mother cell and forespore play crucial roles in communication between the cells during sporulation, allowing the two cells to coordinate the timing of gene expression changes and morphological development. Membrane proteins localized at the inner spore membrane have been demonstrated to play key roles in multiple stages of spore germination. In addition, germination processes such as ion efflux and water influx are likely to involve membrane proteins, yet few proteins involved in these processes have been identified. The goal of this study was to compare and contrast spore membrane-associated proteins present in two *Bacillus* species in an effort to further our understanding of cell differentiation processes at the molecular level and to identify new germination-active proteins. A gel-based approach was used to provide a set of integral membrane proteins, lipoproteins, and peripheral membrane proteins. This study identified 65 membrane-associated spore proteins that had not been previously reported in any *B. subtilis* or *B. anthracis* vegetative or spore proteomic study. The percentages of proteins identified that are predicted to be membrane associated were high, 15-17% of all proteins identified, which is a significant improvement over previous spore proteomic studies (<5%) (79, 82, 83). Identification of these proteins provides potential novel pathways to better understand the role of membrane proteins during sporulation and germination.

The functions of identified spore membrane proteins in both *Bacillus* species spread into almost all membrane protein functional categories. Aside from those proteins known to function in sporulation or germination, the top three functional categories for identified spore membrane proteins were transport (carbohydrate, amino acid, and inorganic ions), protein fate determination (posttranslational modification, trafficking, and turnover) and energy production and conversion.

Cations such as Ca^{2+}, Mn^{2+}, and Zn^{2+} accumulate in spores the during the sporulation of *Bacillus* species (132). Divalent metal ions, predominantly Ca^{2+}, conjugated with DPA contribute to spore resistance to heat (50, 133) and ionizing radiation (134). The rapid release of cations is a distinct early germination step (135). Nine newly-identified spore membrane proteins have predicted functions involved in inorganic ion transport and metabolism. These proteins may play roles in accumulation of ions during sporulation and/or the rapid release of ions during germination. Zn^{2+} ions are accumulated during sporulation and are released very early during germination (136). AdcA was suggested to be important for zinc transport in *B. subtilis* vegetative cells (137), and this protein and its apparent *B. anthracis* ortholog were present in the spore membranes. YfkE was previously demonstrated to be a Ca^{2+}/H^{+} antiporter expressed under the control of forespore-specific σ^{G} (138) and was detected in the spore membrane. This protein could be involved in Ca^{2+} accumulation during sporulation and/or Ca^{2+} release during germination. YcnL, YflS, and YjbQ were present in the *B. subtilis* spore membrane, and may be involved in copper, malate, potassium, and sodium transport (139, 140). BAS4953, BAS0564 and BAS0368 are three novel *B. anthracis* spore membrane proteins that are predicted to be involved in iron and other heavy metal cation transport. *B. subtilis* YugS and the homologous *B. anthracis* protein BAS0575 belong to the uncharacterized protein family 0053 (UPF0053). Several proteins from other bacterial species in this family have been suggested to function in the transport of magnesium and cobalt ions (141). Further characterization of these proteins is needed to determine their functions and potential roles during sporulation and germination.

Several proteins involved in amino acid transport were identified in the spore membranes. YveA was previously characterized to be the primary L-aspartate transporter in *B. subtilis* vegetative cells (142), and transcriptome analysis showed that this gene was expressed under control of the forespore-specific σ^{G} (15). MetQ and ArtP were previously

characterized in *B. subtilis* vegetative cells as involved in methionine and arginine transport, respectively (143, 144). These proteins, as well as their apparent *B. anthracis* orthologs, were present in the spore membranes. The roles of these amino acid transporters in either sporulation or germination processes are unknown at present.

Several proteins detected in spore membranes are involved in protein degradation. *B. subtilis* HtrC (YyxA, YycK), a predicted Htr-type serine protease, was suggested to be transcribed from its own σ^G promoter (145). Loss of HtrC produced no obvious phenotypic change in *B. subtilis* vegetative cells (145, 146), however, the presence of HtrC, and its apparent *B. anthracis* ortholog, which is also expressed during sporulation (67), in the spore membrane suggests that it may play a role in spore formation or germination. *B. subtilis* HtpX and *B. anthracis* RasP are two predicted zinc proteases detected in the spore membranes. Their functions have not been characterized, but may be involved in membrane protein quality control based on the function of the well-known homolog FtsH (147). Further characterization of the roles these proteases play in the spore may shed light on the observed decrease in membrane proteins during spore germination.

In both *Bacillus* species, one quarter of the identified spore membrane proteins have no assigned COG functional category and most have no significant sequence similarity to known genes or functional domains. More interestingly, most of these proteins were not identified in vegetative cell membranes previously, and some were present in both *Bacillus* spores, suggesting that these proteins are likely expressed for particular purposes in spores. Further characterization of these proteins may reveal roles in the sporulation, germination, or outgrowth processes. For example, *B. subtilis* YetF and YutC were previously characterized to be expressed under control of spore-specific σ^F and σ^G, respectively (127), and their apparent *B. anthracis* orthologs were also identified in this study. Five other *B. subtilis* proteins together with YetF are grouped in an uncharacterized protein family (UPF0702), in

which a σ^G-regulated protein YrbG (127) was also identified in *B. subtilis* spore membrane. Homologs of these proteins with no known function are not found in other bacteria, indicating that they might be very specific for *Bacillus* species. Considering their expression is under the control of forespore sigma factors, these proteins may play key roles in either spore formation, stabilization, and/or germination processes.

To provide preliminary information about the fate of spore membrane proteins during germination, relative quantities were derived using label-free spectral counting methods. This strategy is based on the empirical observation that the amount of unique MS/MS spectrum counts of a protein has strong linear correlation with relative protein abundance (125, 131). Although this method is not as accurate as targeted MRM-based methods, it has higher dynamic range than other mass spectrometry quantification methods (148) and therefore is a popular method to detect global protein changes between experiments groups. Note that this relative quantification method was established using data generated by electrospray ionization mass spectrometry. The limitations of applying this method on data generated by MALDI mass spectrometry have not been previously examined. However, the relative quantity values for multiple proteins acquired in this work were consistent to those acquired by our previous MRM study (124) and a previous stable isotope labeled quantitative study (83), suggesting that this method is applicable to MALDI-generated data. Results published while this work was in progress indicate that membrane fractions produced by methods such as those used here recover only a portion of the spore membrane proteins, and extensive chemical extraction is required to recover the full amount of several spore membrane proteins (109). However, such a chemical extraction precludes the separation of membrane and soluble proteins. In the absence of a spore membrane extraction process that provides high recovery, protein quantitation will have to be done using whole spore extracts or will require evidence that the partial membrane extract is representative of the entire membrane.

A notable trend in our study is that the number of identified membrane proteins is greatly reduced after spore germination. Several membrane proteins, mostly lipoproteins, have been previously suggested to dissociate from the membrane during spore germination (37, 83, 124). Spectral counting showed similar results with most lipoproteins diminished or undetectable following germination. The decreased recovery of lipoproteins may be due to proteolysis or may indicate a change in ability to maintain membrane association during fractionation, which in turn could be associated with the membrane reorganization processes. Surprisingly, over half of the membrane proteins that decreased to below detectable levels during germination of both *Bacillus* species spores were integral membrane proteins. Although previous efforts to quantify spore integral membrane proteins are rare, decreased levels of BAS1302 after spore germination was consistent with previous work (83). Since the membrane proteins identified that were observed to decrease are involved in multiple COG function categories, this decrease appears to be a general spore germination phenomenon. The shift from a relatively nonfluid impermeable membrane to a fluid membrane with solute transfer may require a rather complex rearrangement of the membrane and membrane-associated proteome. Targeted knockout studies involving these proteins and their associated germination phenotypes may lend insight into this rearrangement process.

ACKNOWLEDGEMENTS

Research reported in this publication was supported by the National Institute of Allergy and Infectious Disease of the National Institutes of Health under award number R21AI088298. The mass spectrometry resources used in this work are maintained in part through funding by the Fralin Life Science Institute at Virginia Tech and the Agricultural Experiment Station Hatch Program at Virginia Tech (CRIS Project Number: VA-135981)

Table 3.1. *B. subtilis* and *B. anthracis* spore membrane-associated proteins identified by mass spectrometry.

Gene[a]	COG Functional category	*B. subtilis* Uniprot number	*B. anthracis* Uniprot number	Membrane prediction[b]	Previous ID[c]	Regulon[d]
adcA/BAS188	Ion transport & metab.	O34966	Q81RK9	Lipoprotein		
ahpF	Posttranslational	P42974	Q81ZC5	Peripheral	Y2	
artP/BAS0353	Amino acid transport &	P54535	Q6I447	Lipoprotein		
atpD	Energy production	P37809	Q81JZ5	Peripheral	Y1/Y4	
atpF	Energy production	P37814	Q81JZ1	Integral	Y1	
atpG	Energy production	P37810	Q81JZ4	Peripheral	Y1	
bdbD	Posttranslational	O32218	Q81YT8	Integral	Y1	σ^E
era	Unknown	P42182	Q81LT7	Peripheral	Y6	
fhuD/BAS0336	Ion transport & metab.	P37580	Q81ZB8	Integral	Y1/Y5	
ftsH	Posttranslational	P37476	Q81VX5	Integral	Y1/Y5	
gerD	Germination	P16450	Q81VP4	Lipoprotein		σ^G
lytR	Transcription	Q02115	Q81K33	Integral	Y1	
metQ/BAS485	Amino acid transport &	O32167	Q81XL5	Lipoprotein		
misCA/*yidC2*	Intracellular trafficking	Q01625	Q81JH1	Integral		
msmX/PotA	Amino acid transport &	P94360	Q81TH8	Peripheral	Y2/Y5	
oppA/BAS062	Amino acid transport &	P24141	Q81V45	Lipoprotein	Y1/Y5	
oppB/BAS110	General Transporter	P24138	Q81TS3	Integral	Y2/Y5	
oppC/BAS110	General Transporter	P24139	Q81TS2	Integral	Y2	
oppD/BAS110	General Transporter	P24136	Q81TS1	Peripheral	Y2/Y5	
oppF/BAS110	Amino acid transport &	P24137	Q81TS0	Peripheral	Y2	
pbpF/BAS136	Cell wall biogenesis	P38050	Q81T17	Integral	Y2/Y5	
plsY/*plsY3*	Lipid metabolism	Q45064	Q81Y92	Integral		
ponA/BAS218	Cell wall biogenesis	P39793	Q6HYZ2	Integral	Y1	
prsA/*prsA1*	Posttranslational	P24327	Q81U45	Lipoprotein	Y1	

ptsG/*ptsG*	Carbohydrate transp. &	P20166	Q81MH9	Integral	Y1	
qcrA	Energy production	P46911	Q81SV1	Integral	Y2	
qcrB	Energy production	P46912	Q81SV0	Integral	Y2	
qoxA/*ctaC*	Energy production	P34957	Q81MT9	Integral	Y1	
resA	Posttranslational	P35160	Q81SZ9	Integral	Y2	
secDF	Intracellular trafficking	O32047	Q81LH8	Integral	Y1/Y5	
secY/*secY1*	Intracellular trafficking	P16336	Q81VR0	Integral	Y1	
spoVAC	DPA transport	P40868	Q81X68	Integral		σ^G
spoVAD	DPA transport	P40869	Q81X67	Peripheral		σ^G
spoVAF	DPA transport	P31845	Q81MG2	Integral		σ^G
tcyA/	Amino acid transport &	P42199	Q81UL3	Lipoprotein	Y6	
yetF/BAS4999	Unknown	O31533	Q81X64	Integral		σ^F
yfmC/BAS442	Ion transport & metab.	O34348	Q81L65	Lipoprotein	Y1/Y5	
ykrK/BAS2651	Unknown	O31656	Q81PG5	Peripheral		
ylaJ/BAS2560	Unknown	O07634	Q81PQ5	Lipoprotein	Y3/Y6	σ^G
yndM/BAS290	Unknown	O31816	Q6HWX1*	Integral		*Same
ypeB	Germination	P38490	Q81PQ4	Integral		σ^G
ypmQ/BAS209	Energy production	P54178	Q81R11	Lipoprotein		
yqfX/BAS1302	Unknown	P54481	Q81T77	Integral	Y6	σ^G
ythA/*cydA3*	Energy production	C0SP90	Q81WZ0	Integral		σ^G
yugS/BAS0575	Unknown	O05241	Q81V91	Integral		
yutC/BAS4834	Unknown	O32128	Q81XN4	Lipoprotein		σ^G
yyxA/BAS5314	Posttranslational	P39668	Q81JJ5	Integral		
artQ	Amino acid transport &	P54536		Integral		
atpB	Energy production	P37813		Integral	Y1	
dacA	Cell wall biogenesis	P08750		Integral	Y1	
dltD	Cell wall biogenesis	P39578		Integral	Y1	
ezrA	Cell cycle control	O34894		Integral	Y2	
fruA	Carbohydrate transp. &	P71012		Integral	Y1	

ftsY	Intracellular trafficking	P51835		Peripheral	Y2	σ^K
gerAC	Germinations	P07870		Lipoprotein		σ^G
gerBC	Germination	P39571		Lipoprotein		σ^G
gerKC	Germination	P49941		Lipoprotein		σ^G
htpX	Posttranslational	O31657		Integral		
lgt	Posttranslational	O34752		Integral	Y2	
murG	Cell wall biogenesis	P37585		Peripheral		σ^E
opuAB	Amino acid transport &	P46921		Integral	Y2	
opuAC	Amino acid transport &	P46922		Lipoprotein	Y1	
pbuG	General transporter	O34987		Integral	Y1	
phoR	Signal transduction	P23545		Integral		σ^E
prkC	Germination	O34507		Integral	Y2	
rbsA	Carbohydrate transp. &	P36947		Peripheral	Y1	
sipS	Intracellular trafficking	P28628		Integral	Y2	σ^E
sipT	Intracellular trafficking	P71013		Integral	Y2	
sppA	Intracellular trafficking	O34525		Integral	Y2	
tagG	Cell wall biogenesis	P42953		Integral	Y2	
yacD	Posttranslational	P37566		Integral	Y1	
yckB	Amino acid transport &	P42400		Lipoprotein	Y1	
ycnL	Ion transport & metab.	P94434		Integral		
yerB	Unknown	O34968		Lipoprotein		
yerH	Unknown	O34629		Lipoprotein	Y1	
yfkE	Ion transport & metab.	O34840		Integral		
yfkR	Germination	O35028		Lipoprotein		σ^G
yflS	Ion transport & metab.	O34726		Integral		
yhbJ	Defense mechanisms	O31593		Integral	Y2	σ^G
yhcC	Unknown	P54587		Integral		σ^G
yhcM	Unknown	P54597		Integral	Y3	σ^F
yhcN	Germination	P54598		Lipoprotein	Y2	σ^F & σ^G

yheB	Unknown	O07543		Integral	Y1	
yhfQ	Ion transport & metab.	C0SP94		Lipoprotein	Y1	
yitG	General transporter	Q796Q1		Integral		σ^G
yjbQ	Ion transport & metab.	O31615		Integral		
ylbC	Unknown	O34586		Integral	Y2	σ^F
ylbL	Signal transduction	O34470		Integral	Y1	
yodI	Unknown	O34654		Integral	Y3	σ^K
yqaR	Unknown	P45914		Integral		
yqfA	Unknown	P54466		Integral	Y1	
yqgF	Cell wall biogenesis	P54488		Integral		
yrbF	Intracellular trafficking	O32052		Integral		
yrbG	Unknown	O32050		Integral		σ^G
yrvD	Unknown	O32045		Integral	Y2	
ysdB	Transcription	P94520		Integral	Y2	
ytxG	Unknown	P40779		Integral	Y2	
ytxH	Unknown	P40780		Integral	Y2	
yuaB	Colony structure	P71014		Integral		
yuaG	Unknown	O32076		Integral	Y2	
yugP	Posttranslational	O05248		Integral	Y2	
yvcA	Colony structure	O06965		Lipoprotein	Y2	
yveA	Amino acid transport &	O07002		Integral		σ^G
ywjE	Lipid metabolism	P45865		Integral		σ^G
BAS0191	Unknown		Q81VK7	Lipoprotein	Y6	
BAS0350	Energy production		Q81ZA6	Peripheral		
BAS0360	Unknown		Q81Z98	Integral		
BAS0368	Ion transport & metab.		Q81Z90	Lipoprotein		
BAS0405	Unknown		Q81Z55	Peripheral	Y6	
BAS0564	Ion transport & metab.		Q81VA3	Integral		
BAS0569	Unknown		Q6I3I4	Lipoprotein		

BAS0581	Ion transport & metab.		Q81V85	Lipoprotein	Y5	
BAS1412	Unknown		Q81SX1	Integral		
BAS2689	Unknown		Q81PC7	Lipoprotein		
BAS2733	Unknown		Q81P74	Lipoprotein	Y6	
BAS2751	Unknown		Q81P56	Integral		
BAS2834	Defense mechanisms		Q81NX4	Peripheral	Y5	
BAS2910	Unknown		Q81NQ0	Peripheral	Y4	
BAS3134	Energy production		Q81N37	Peripheral		
BAS3468	Unknown		Q81Y17	Integral		
BAS3643	Unknown		Q81WP4	Lipoprotein		
BAS3922	Carbohydrate transp. &		Q81ML8	Lipoprotein	Y6	
BAS3998	Unknown		Q81MD9	Lipoprotein		
BAS4323	Unknown		Q6HSW8	Lipoprotein	Y6	
BAS4406	Unknown		Q81L82	Lipoprotein		
BAS4700	Unknown		Q81KD9	Peripheral	Y4	
BAS4796	Energy production		Q81XS1	Peripheral		
BAS4797	Posttranslational		Q81XS0	Peripheral		
BAS4808	Energy production		Q81XR0	Peripheral		
BAS4865	Unknown		Q81XK0	Lipoprotein		
BAS4935	Energy production		Q81XC7	Peripheral		
BAS4953	Ion transport & metab.		Q6HR45	Lipoprotein		
BAS4994	Unknown		Q6HR05	Lipoprotein		
BAS5287	Cell wall biogenesis		Q81JM0	Integral		
cccA	Energy production		Q81LU6	Integral		
ecsA	Defense mechanisms		Q81U40	Peripheral		
fabF	Lipid metabolism		Q81JF9	Peripheral		
ffh	Intracellular trafficking		Q81WJ2	Peripheral		
ftsY	Intracellular trafficking		Q81WJ0	Peripheral		
potD	Amino acid transport &		Q81TH5	Lipoprotein		

proV2	Amino acid transport &		Q81PL6	Peripheral		
psd	Lipid metabolism		Q81LP7	Peripheral		
rasP	Cell wall/membrane		Q81WL5	Integral		
typA	Signal transduction		Q81MS8	Peripheral		

[a] If a protein doesn't have an annotated gene name, the ordered locus name is listed.

[b] Mechanism of membrane association predicted as described in Materials and Methods.

[c] Previous identification of the protein in a proteomic analysis: Y1, *B. subtilis* vegetative cell proteome (76); Y2: *B. subtilis* vegetative cell proteome (77); Y3: *B. subtilis* spore proteome (79); Y4: *B. anthracis* spore proteome (82); Y5: *B. anthracis* vegetative cell proteome (78); Y6: *B. anthracis* spore proteome (83).

[d] Sigma factor dependence was drawn from references: (15, 79, 122, 127).

Table 3.2. Known *B. anthracis* and *B. subtilis* spore germination proteins that were identified.

Gene	Function	*B. subtilis* Uniprot number	*B. anthracis* Uniprot number	Membrane prediction[a]
gerAC	Germinant receptor	P07870		Lipoprotein
gerBC	Germinant receptor	P39571		Lipoprotein
gerD	Germinant response	P16450	Q81VP4	Lipoprotein
gerKC	Germinant receptor	P49941		Lipoprotein
prkC	Peptidoglycan receptor	O34507		Integral
spoVAC	DPA transport	P40868	Q81X68	Integral
spoVAD	DPA transport	P40869	Q81X67	Peripheral
spoVAF	DPA transport	P31845	Q81MG2	Integral
yfkR	Germinant receptor	O35028		Lipoprotein
yhcN	Outgrowth	P54598		Lipoprotein
ypeB	Cortex degradation	P38490	Q81PQ4	Integral

[a] Mechanism of membrane association predicted as described in Materials and Methods.

Table 3.3. Proteins detected in both *Bacillus* species spore membrane proteomes

B. subtilis **Uniprot number**	***B. anthracis*** **Uniprot number**	**Protein function**	**Sequence identity**[1] (%)	**Sequence similarity** [1] (%)	**Alignment length**[2] (%)
C0SP90	Q81WZ0	Cytochrome bd menaquinol oxidase	53	71	98
O05241	Q81V91	Unknown	59	75	100
O07634	Q81PQ5	Unknown , lipoprotein	47	67	100
O31533	Q81X64	Unknown	35	59	63
O31656	Q81PG5	Unknown	37	59	94
O31816	Q81P56	Unknown	27	47	92
O31816	Q6HWX1	Unknown	35	50	88
O32047	Q81LH8	Protein translocase, SecDF	60	76	97
O32128	Q81XN4	Unknown, lipoprotein	35	58	72
O32167	Q81XL5	Methionine-binding lipoprotein, MetQ	57	76	100
O32218	Q81YT8	Disulfide bond formation	42	64	85
O34348	Q6HR45[3]	Unknown	25	46	93
O34348	Q81V85[3]	Unknown	34	49	99
O34348	Q81L65	Fe-citrate-binding, YfmC	33	53	96
O34966	Q81RK9	Zinc uptake, ZnuA	37	55	97
P16336	Q81VR0	Protein translocase, SecY	72	82	100
P16450	Q81VP4	Germination, GerD	43	69	89
P20166	Q81MH9	PTS system	61	79	100
P24136	Q81TS1	Oligopeptide transport, OppD	73	85	97
P24137	Q81TS0	Oligopeptide transport, OppF	80	89	97
P24138	Q81TS3	Oligopeptide transport, OppB	50	70	100
P24139	Q81TS2	Oligopeptide transport, OppC	46	66	98

P24141	Q81V45	Oligopeptide transport, OppA	28	45	92
P24327	Q81U45	Foldase, PrsA	47	66	96
P31845	Q81MG2	DPA transport SpoVAF	63	80	96
P34957	Q81MT9[3]	Quinol oxidase	36	56	62
P35160	Q81SZ9	Thiol-disulfide oxidoreductase, ResA	52	69	99
P36947	Q81U40[3]	Ribose import, RbsA	28	49	84
P37476	Q81VX5	Zinc metalloprotease, FtsH	80	89	100
P37580	Q81ZB8	Iron-hydroxamate-binding, FhuD	38	61	93
P37809	Q81JZ5	ATP synthase	86	92	99
P37810	Q81JZ4	ATP synthase	68	84	100
P37814	Q81JZ1	ATP synthase	57	76	98
P38050	Q81T17	Penicillin-binding protein 1F	42	61	89
P38490	Q81PQ4	Cortex degradation, YpeB	57	77	99
P39668	Q81JJ5	Serine protease, YyxA	50	68	97
P39793	Q6HYZ2	Penicillin-binding protein 1	46	65	89
P40868	Q81X68	DPA transport, SpoVAC	60	78	89
P40869	Q81X67	DPA transport, SpoVAD	50	65	98
P42182	Q81LT7	GTPase Era	75	89	100
P42199	Q81UL3	L-cystine-binding protein TcyA	53	69	98
P42974	Q81ZC5	NADH dehydrogenase	84	91	100
P46911	Q81SV1	Menaquinol-cytochrome c reductase	70	80	95
P46912	Q81SV0	Menaquinol-cytochrome c reductase	95	97	100
P54178	Q81R11	SCO1 protein homolog	49	70	96
P54481	Q81T77	Unknown	33	48	92
P54535	Q6I447	Arginine-transport, ArtP	37	55	95
P94360	Q81TH8[3]	Maltodextrin import, MsmX	51	71	76

Q01625	Q81JH1	Membrane protein insertase, MisCA	68	81	100
Q02115	Q81K33	Transcriptional regulator, LytR	50	72	93
Q45064	Q81Y92	Glycerol-3-PO_4 acyltransferase	63	75	94

[1] Sequences were aligned using BlastP (126).

[2] The percent of the *B. subtilis* protein sequence that was aligned with the *B. anthracis* sequence.

[3] A more similar protein than that detected in the spore proteome was present in the full *B. subtilis* genome: (*B. anthracis* gene:Most similar *B. subtilis* gene) (Q6HR45:P94421) (Q81V85:O31567) (Q81MT9:P24011) (Q81U40:P55339) (Q81TH8:O32151)

Table 3.4. Validation of membrane protein quantification.

B. subtilis **protein**	**Dormant/Germinated spore ratio by spectral counting**	**Dormant/Germinated spore ratio by MRM[a]**
GerAC	1.7	1.9
GerBC	0.8	1.5
GerKC	1.5	2.4
GerD	3.0	3.5
PrkC	1.9	3.3
SpoVAC	3.3	0.8
SpoVAD	0.5	0.6
YpeB	4.2	6.8

[a] MRM data are from reference (124).

Table 3.5. Spore membrane proteins that were no longer detected following germination.

Gene	*B. subtilis* Uniprot number	*B. anthracis* Uniprot number
artQ	P54536	
atpB	P37813	
bdbD	O32218	Q81YT8
clsB	P45865	
dltD	P39578	
ezrA	O34894	
htpX	O31657	
lgt	O34752	
lytR	Q02115	Q81K33
misCA	Q01625	
msmX/*potA*	P94360	Q81TH8
oppB/BAS11	P24138	Q81TS3
opuAC	P46922	
pbpF/BAS13	P38050	Q81T17
pbuG	O34987	
phoR	P23545	
plsY/*plsY3*	Q45064	Q81Y92
ponA/BAS21	P39793	Q6HYZ2
qcrA	P46911	
rbsB	P36949	
resA	P35160	Q81SZ9
secY	P16336	Q81VR0
sipS	P28628	
sipT	P71013	
sppA	O34525	
tagG	P42953	
yacD	P37566	
ybC	O34586	
yckB	P42400	
ycnL	P94434	
yerB	O34968	
yerH	O34629	
yfkE	O34840	
yfkR	O35028	
yhbJ	O31593	
yhcC	P54587	
yjbQ	O31615	
ylbL	O34470	
yndM	O31816	

yqaR	P45914	
yqgF	P54488	
yrbG	O32050	
ysdB	P94520	
ytxG	P40779	
yuaB	P71014	
yuaG	O32076	
yutC	O32128	
yvcA	O06965	
BAS0336		Q81ZB8
BAS0353		Q6I447
BAS0360		Q81Z98
BAS0368		Q81Z90
BAS0564		Q81VA3
BAS1103		Q81TS2
BAS1104		Q81TS1
BAS1889		Q81RK9
BAS2093		Q81R11
BAS2560		Q81PQ5
BAS2651		Q81PG5
BAS2689		Q81PC7
BAS2733		Q81P74
BAS2909		Q6HWX1
BAS3998		Q81MD9
BAS4406		Q81L82
BAS4424		Q81L65
BAS4700		Q81KD9
BAS4808		Q81XR0
BAS4834		Q81XN4
BAS4853		Q81XL5
BAS4865		Q81XK0
BAS4953		Q6HR45
BAS4994		Q6HR05
BAS5314		Q81JJ5
ctaC		Q81MT9
ecsA		Q81U40
ffH		Q81WJ2
gerD		Q81VP4
ptsG		Q81MH9
qcrB		Q81SV0
rasP		Q81WL5
secDF		Q81LH8
spoVAC		Q81X68
spoVAF		Q81MG2
ypeB		Q81PQ4

Table 3.6. Changes in *Bacillus* spore membrane protein detection following germination.

Gene	*B. subtilis* Uniprot number	*B. anthracis* Uniprot number	Membrane prediction	Fold change in unique spectra (D/G)
fruA	P71012		Integral	5.4
qcrB	P46912		Integral	4.5
ypeB	P38490		Integral	4.2[e]
yheB	O07543		Integral	3.9
znuA	O34966		Lipoprotein	3.6
ylaJ	O07634		Lipoprotein	3.3
oppC	P24139		Integral	3.3
atpF	P37814		Integral	3.3
spoVAC	P40868		Integral	3.3[a]
fhuD	P37580		Lipoprotein	3.1
yugS	O05241	Q81V91	Integral	3.0 / 3.3
gerD	P16450		Lipoprotein	3.0[e]
ythA	C0SP90		Integral	2.9
secDF	O32047		Integral	2.9
ypmQ	P54178		Lipoprotein	2.8
yitG	Q796Q1		Integral	2.7
yqfX	P54481	Q81T77	Integral	2.6 / INF[b, c]
oppA	P24141	Q81V45	Lipoprotein	2.6 / 3.8
qoxA	P34957		Integral	2.2
rbsA	P36947		Peripheral	2.2
yfmC	O34348		Lipoprotein	2.1
yhcN	P54598		Lipoprotein	2.0
yugP	O05248		Integral	2.0
spoVAD	P40869	Q81X67	Peripheral	0.5[e] / 1.4
atpG	P37810	Q81JZ4	Peripheral	0.5 / 3.9
BAS4323		Q6HSW8	Lipoprotein	8.9[b]
BAS2751		Q81P56	Integral	7.0
prsA1		Q81U45	Lipoprotein	6.3
BAS0812		Q81UL3	Lipoprotein	5.9[c]
BAS0581		Q81V85	Lipoprotein	4.8
BAS2834		Q81NX4	Peripheral	4.1
BAS5287		Q81JM0	Integral	3.9
BAS3922		Q81ML8	Lipoprotein	3.7[d]
cccA		Q81LU6	Integral	3.3
psd		Q81LP7	Peripheral	3.3
BAS1105		Q81TS0	Peripheral	3.0
BAS1412		Q81SX1	Integral	2.2
BAS3643		Q81WP4	Lipoprotein	13

BAS0405		Q81Z55	Peripheral	0.5[d]

[a] Result is not consistent that of (124).

[b] Result is consistent with that of (83).

[c] This protein was detected in *B. anthracis* dormant spores but not in germinated spores.

[d] Result is not consistent with that of (83).

[e] Result is consistent that of (124).

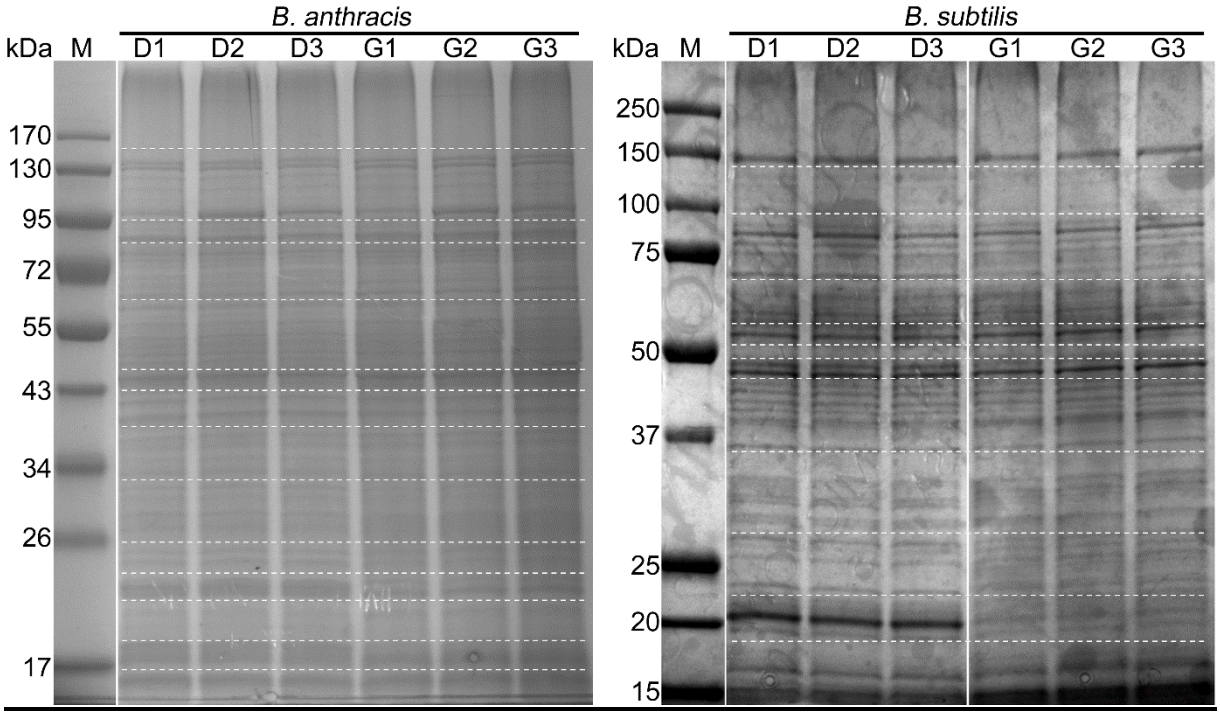

Figure 3.1. SDS-PAGE separation of *B. anthracis* and *B. subtilis* spore membrane preparations. Samples from three independent dormant (D1, D2, D3) and germinated (G1, G2, G3) spore preparations were prepared and broken, and membrane fractions were purified as described in Materials and Methods. Protein concentrations were determined by amino acid analysis, and equal amounts of protein from each preparation were loaded on gels. Gels were stained with Coomassie blue. The approximate positions at which each lane was cut into slices are indicated by dashed lines. The masses of standard protein markers (M) are shown to the left of each gel.

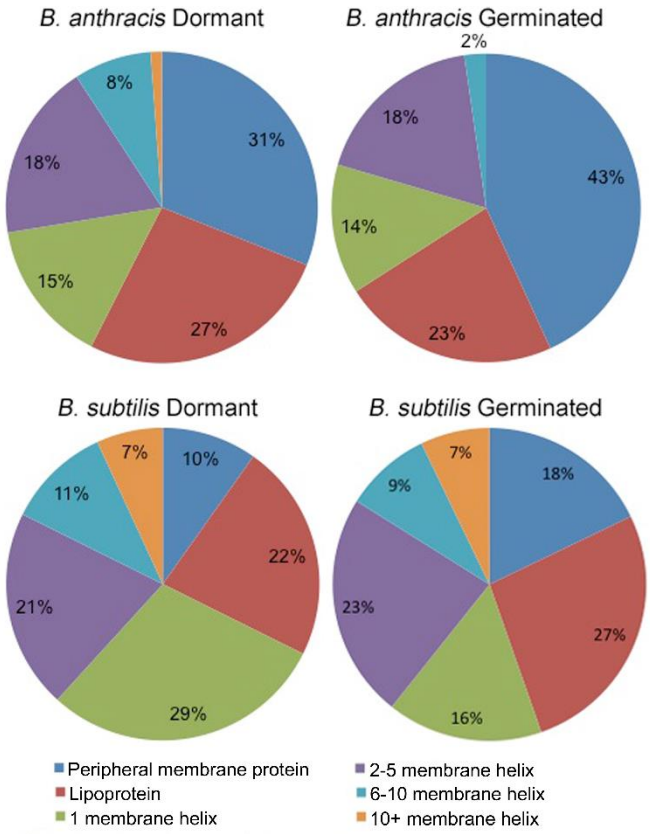

Figure 3.2. Predicted membrane-spanning domains of *B. anthracis* and *B. subtilis* spore membrane proteins. Predictions of membrane association mechanisms were made for proteins identified in membrane fractions as described in materials and methods. Proteins were further classified based upon their predicted number of membrane spanning helices.

CHAPTER 4

HtrC is involved in proteolysis of YpeB during germination of *Bacillus anthracis* and *Bacillus subtilis* spores

Casey B. Bernhards*, Yan Chen*, Hannah Toutkoushian, and David L. Popham

Manuscript in preparation

Attributions

Yan Chen and Casey B. Bernhards contributed equally to the research, experimentation, and data analysis of the material presented herein. Yan is responsible for the work presented in Table 4.3 and Figures 4.5, 4.6, 4.7, 4.8. Casey is responsible for the work presented in Figures 4.1, 4.2, 4.3, 4.4, and 4.9. Hannah K. Toutkoushian performed germination rate assays involving *htrC* mutants and provided laboratory assistance. David L. Popham was the principle investigator. Casey, Yan, and David all contributed to the writing of the manuscript.

ABSTRACT

Bacterial endospores can remain dormant for decades, yet can respond to nutrients, germinate, and resume growth within minutes. An essential step in the germination process is degradation of the spore cortex peptidoglycan wall, and the SleB protein in *Bacillus* species plays a key role in this process. Stable incorporation of SleB into the spore requires the YpeB protein, and some evidence suggests that these two proteins interact within the dormant spore. Early during germination, YpeB is proteolytically processed to a stable fragment. In this work, the primary sites of YpeB cleavage were identified in *B. anthracis*, and it was shown that the stable products are comprised of the C-terminal domain of YpeB. Modification of the predominant YpeB cleavage sites reduced proteolysis, but cleavage at other sites still resulted in loss of full-length YpeB. A *B. anthracis* strain lacking the HtrC protease did not generate the same stable YpeB products. In *B. anthracis* and *B. subtilis htrC* mutants, YpeB was partially stabilized during germination but was still degraded at a reduced rate by other unidentified proteases. Purified HtrC cleaved YpeB to a fragment similar to that observed *in vivo*, and this cleavage was stimulated by Mn^{2+} or Ca^{2+} ions. A lack of HtrC did not stabilize YpeB or SleB during spore formation in the absence of the partner protein, indicating other proteases are involved in their degradation during sporulation.

INTRODUCTION

Endospores produced by Gram-positive genera such as *Bacillus* and *Clostridium* possess extreme resistance properties and can remain in a fully dormant state for years. The dormant state and resistance properties are dependent on the maintenance of the spore core (cytoplasm) in a relatively dehydrated state, and this in turn depends on the intact state of the inner spore membrane and the cortex peptidoglycan (PG) wall surrounding that membrane (13). Upon exposure to nutrient germinants, spores begin to release low molecular weight solutes, including a large depot of Ca^{2+}-dipicolinic acid (Ca^{2+}-DPA), and take up water (149). Degradation of the cortex PG by germination-specific lytic enzymes (GSLEs) is required for full expansion of the membrane, full hydration of the core, and resumption of metabolism (98, 150-152). As GSLEs hydrolyze the cortex PG before new protein synthesis can occur, they must be produced during spore formation and held stable and inactive in the dormant spore until germination is triggered (63).

Bacillus species possess two major, partially redundant GSLEs: CwlJ and SleB (63). CwlJ is produced in the mother cell of the developing sporangium (71), is associated with the spore coats on the outer surface of the cortex (64, 72, 73, 153), and becomes active when exposed to a high concentration of Ca^{2+}-DPA normally when that solute is released from the germinating spore (65, 73, 154). SleB is produced within the developing forespore (68, 70) and is located interior to the cortex in the dormant spore, most likely in close association with the inner spore membrane (64, 112). The mechanisms by which SleB is held inactive during spore dormancy and released to become active during germination are unclear.

A potential factor in regulation of SleB activity is YpeB, which is encoded in an operon with *sleB* and possesses a transmembrane anchor sequence that should also localize it to the outer surface of the inner spore membrane (61, 69, 70). SleB and YpeB exhibit a co-

dependence for their stable incorporation into the dormant spore (64, 69, 155). In the absence of their partner protein, both SleB and YpeB are produced and rapidly degraded during spore formation (69). It has also been observed that YpeB is proteolytically processed during spore germination (64), and it has been suggested that this processing could be involved in the initiation of SleB activity during germination (155).

The current study examined the cleavage sites generating the stable YpeB products during germination and identified HtrC as the protease responsible for these cleavage events. The resulting cleavage products were shown to contain the C-terminus and PepSY domains of YpeB. Strains lacking HtrC or with mutations at the YpeB cleavage sites were constructed to evaluate the role of YpeB processing in SleB activation. In the absence of HtrC, YpeB was degraded in a more non-specific manner during germination, and activity of SleB was not significantly affected.

MATERIALS AND METHODS

Strains, culture conditions, and spore preparation. *Escherichia coli* strains used for plasmid propagation were grown at 37°C in LB medium with 500 μg/ml erythromycin or 20 μg/ml kanamycin. Strains used for protein overexpression were grown in LB with 30 μg/ml chloramphenicol and 50 μg/ml ampicillin. *Bacillus anthracis* strains were derived from the Sterne strain 34F2 and were grown on brain heart infusion (BHI; Difco) agar plates with 5 μg/ml erythromycin or 20 μg/ml kanamycin, where appropriate. *B. anthracis* strains maintaining pBKJ236-derivatives extrachromosomally were grown at 25 ℃, while those in which the plasmid was integrated into the chromosome were grown at 37 ℃. *Bacillus subtilis* strains were derived from PS832, a prototrophic laboratory derivative of strain 168, and were grown on 2xSG medium (102) with 0.5 μg/ml erythromycin and 12.5 μg/ml lincomycin (MLS resistance), and/or 10 μg/ml tetracycline, when appropriate. Spores were prepared in Modified G (123) broth for *B. anthracis*, or 2xSG (102) broth for *B. subtilis* with appropriate antibiotics. After 72 h incubation at 37 ℃, spores were harvested, washed in deionized water for several days, and any remaining vegetative cells were heat killed at 65°C for 25 min. *B. anthracis* spores were further purified by centrifugation through a 50% sodium diatrizoate (Sigma) layer as described (103). Where indicated, *B. anthracis* spores were decoated as previously detailed (69, 98). All spores used in this work were 99% free of vegetative cells and were stored in deionized water at 4 ℃ until analysis.

Mutant strain construction. All strains and plasmids used are listed in Table 4.1, and the primer sequences used for plasmid construction are listed in Table 4.2. Construction of DPBa127, a *B. anthracis* strain expressing YpeB-His_6, was published previously (69). In this strain, the plasmid pDPV424 encoding YpeB-His_6 was integrated into the Δ*ypeB* chromosome. Strains in which the YpeB T202-S203 or A168-S169 cleavage sites were

changed to E202-L203 or E168-L169 were created by site-directed mutagenesis of *ypeB* using overlap extension PCR (156). The PCR products were subsequently cloned into pDPV424 through restriction-free cloning (157), generating plasmids encoding YpeB$^{T202E/S203L}$-His$_6$ (pDPV447) and YpeB$^{A168E/S169L}$-His$_6$ (pDPV454). To construct a strain in which both cleavage sites had been mutated, pDPV447 was used as template for overlap extension PCR, and the PCR product was cloned into pDPV447, producing pDPV455. Plasmids pDPV447, pDPV454, and pDPV455 were screened for the gain or loss of a restriction site in *ypeB* that was designed as part of the mutagenic primers, and were also verified by DNA sequencing. Plasmids were introduced into the Δ*ypeB* strain of *B. anthracis* (69) by conjugation, as in the initial steps of the markerless gene replacement procedure (158), and chromosomal integrants were selected by shifting the temperature to 42°C. PCR amplification and sequencing verified plasmid integration within the 500-bp homologous region downstream of Δ*ypeB* in the chromosome and confirmed the presence of the desired cleavage site mutations.

To create a *B. anthracis* Δ*htrC* strain, *htrC* and approximately 500-bp flanking each side of the gene were PCR amplified from chromosomal DNA. The PCR product was inserted into the vector pBKJ236 (158) by digesting with the restriction enzymes BamHI and PstI and ligating the DNA to create pDPV459. Inverse PCR of the plasmid using primers with BglII restriction sites at the 3′ ends resulted in a linear PCR product with the majority of *htrC* deleted, leaving only the first five and last two codons of the gene. Subsequent BglII digestion and ligation of the PCR product produced pDPV460. This plasmid containing the *htrC* deletion was introduced into *B. anthracis* using the markerless gene replacement strategy as previously described (158), except plasmid pSS4332 (159) was used for I-SceI expression in place of pBKJ223. Gene deletion was verified by PCR amplification and sequencing. Complementation of the Δ*htrC* mutation was achieved by introduction and

chromosomal integration of pDPV459. To create Δ*sleB* Δ*htrC* and Δ*ypeB* Δ*htrC* double deletion strains, pDPV460 was used to introduce the *htrC* deletion into Δ*sleB* (DPBa38, (61)) and Δ*ypeB* (DPBa89, (69)) strains of *B. anthracis* using the markerless gene replacement strategy (158) with pSS4332 (159). Gene deletions were verified by PCR amplification and sequencing.

To create a *B. subtilis* Δ*htrC* strain, approximately 1000-bp flanking each side of the gene were PCR amplified from chromosomal DNA and linked to the *ermC* Macrolide-Lincosamide-Streptogramin (MLS) antibiotic resistance gene cassette by long-flanking homology PCR (160). The PCR product was transformed into *B. subtilis* PS832 with selection for MLS resistance to produce DPVB668, in which all but the first 7 and last 8 codons of the *htrC* coding sequence were deleted and replaced by the MLS cassette. Chromosomal DNA from FB111 (73) was transformed into *B. subtilis* DPVB668 with selection for tetracycline resistance to produce DPVB669.

Spore germination assays. The rate of germination and outgrowth of spores in liquid BHI (*B. anthracis*) or 2xYT (*B. subtilis*) was assessed by monitoring the change in optical density at 600 nm (OD) as described previously (69). For germination efficiency assays, spores at an OD of 0.2 were heat activated at 70°C for 20 min and quenched on ice. Heat activated spores were serially diluted in deionized water, plated on BHI or 2xSG medium without antibiotics, and incubated at 37°C overnight. Colonies were counted to determine CFU/OD unit values. Statistical analyses of spore germination rates were performed using unpaired, two-tailed Student's *t*-tests with unequal variance.

Preparation and analysis of spore fractions. Sporangia samples were collected at hours 2 through 6 of sporulation from strains grown in modified G broth, as described previously (69). To prepare germinated spores for western blot analysis, a suspension of dormant spores at a concentration of 5 OD units per ml in 10 mM Tris-HCl pH 7.0 were heat

activated at 70 ℃ for 30 min (*B. anthracis*) or 75 ℃ for 30 min (*B. subtilis*) and cooled on ice for 10 min. Chloramphenicol was added to a final concentration of 10 μg/ml to inhibit protein synthesis and 7.5 OD units of spores were removed for the dormant spore sample. The spore suspension was briefly prewarmed before spores were germinated at 37 ℃ with shaking at 250 rpm by the addition of 10 or 100 mM L-alanine with 1 mM inosine (*B. anthracis*) or 10 mM L-valine (*B. subtilis*). Samples equivalent to 7.5 OD units based on the starting OD were collected at various times after the addition of germinants and centrifuged at 15,800 x *g* for 2 min. The resulting pellets were flash frozen in liquid N_2 and lyophilized.

Dried spores or sporangia were pulverized with 100 mg of 0.1 mm glass beads in a dental amalgamator (Wig-L-Bug) at 4,200 rpm for 20 pulses of 30 s each. Samples were put on ice for at least 30 s between pulses. Proteins were extracted from the mixture with 75 μl (dormant and germinated spores) or 100 μl (sporangia) of 1X sample loading buffer (62.5 mM Tris-HCl pH 6.8, 2% SDS, 10% glycerol, 5% β-mercaptoethanol, 0.05% bromophenol blue). Following heating at 100°C for 5 min, extracts were centrifuged at 15,800 x *g* for 1 min, and supernatants were analyzed by western blotting. In some cases, proteins were extracted in sample loading buffer without bromophenol blue and quantified using amino acid analyses (105).

To extract and purify His_6-tagged YpeB cleavage products for N-terminal sequencing, 250 OD units of DPBa127 or DPBa157 spores in a final volume of 100 ml 10 mM Tris-HCl pH 7.0 were heat activated and germinated with 100 mM L-alanine and 1 mM inosine as described above. Spores were germinated for approximately 1 h, or until ≥ 90% of spores had germinated, as determined by phase contrast microscopy. The germinated spores were collected by centrifugation at 10,000 x *g* for 10 min at 4°C and washed with 5 ml Buffer A (50 mM NaCl, 50 mM Tris-HCl pH 7.5, 5% glycerol, 30 mM imidazole). Following another

centrifugation, the pellet was resuspended in 5 ml Buffer A, split between 4 microcentrifuge tubes, and centrifuged at 15,800 x *g* for 2 min. The pellets were frozen at -80°C, lyophilized, and broken with glass beads as described above. Proteins were extracted by resuspending and combining samples in a total of 5 ml Buffer B (500 mM NaCl, 50 mM Tris-HCl pH 7.5, 30 mM imidazole, 8M urea) and incubating at 4°C with slow rocking for at least 2 h. The sample was centrifuged at 6,800 x *g* for 10 min at 4°C, and the supernatant containing soluble extracted proteins was filtered and loaded on a 1-ml Ni-Sepharose HisTrap HP affinity column (GE Healthcare) equilibrated with Buffer B. YpeB cleavage products were eluted with Buffer C (500 mM NaCl, 50 mM Tris-HCl pH 7.5, 500 mM imidazole, 8M urea). To precipitate the affinity-purified cleavage products, deoxycholate and TCA (0.05% and 20% final concentrations, respectively) were added to the pooled elution fractions, which were then incubated on ice overnight. The mixture was centrifuged at 15,000 x *g* for 10 min at 4°C, and the pellet was washed 3 times with 1 ml ice-cold 100% acetone. The pellet was dried and mixed with 25 µl 1X sample loading buffer, and additional 0.5 M Tris-HCl pH 6.8 was added until the sample was blue again.

The entire precipitated sample was run on a SDS-PAGE gel that had first been incubated overnight in 1X Tris-Glycine SDS Running Buffer with 0.1 mM sodium thioglycolate. Sodium thioglycolate scavenges free radicals, thereby protecting the N-termini of proteins from modification. The proteins were transferred to Immobilon-PSQ PVDF membrane (Millipore) in CAPS transfer buffer (10 mM CAPS pH 11.0, 10% methanol), and the membrane was briefly washed with deionized water before being stained with 0.1% Coomassie Brilliant Blue R-250 (Jersey Lab Supply) for 30 s. The membrane was destained repeatedly with 50% methanol until bands were visible. Bands corresponding to YpeB cleavage products were cut from the membrane, washed with deionized water, dried, and stored at -80 ℃. N-terminal sequencing via automated Edman degradation was performed on

extracted bands using an ABI 494 Protein Sequencer (Tufts University Analytical Core Facility).

Western blot analysis. Polyclonal antibodies raised in rabbits against *B. anthracis* SleB and YpeB (69), and monoclonal mouse anti-His (C-term) antibodies (Invitrogen) were used for detection of SleB, YpeB, and derivatives in western blots. Anti-SleB and anti-YpeB antibodies were used at 1:1,000 and 1:3,000 dilutions, respectively, while anti-His antibodies were used at a 1:5,000 dilution. Secondary goat anti-rabbit-HRP antibodies (Bio-Rad) were used at a 1:5,000 (cat. #166-2408) or 1:200,000 (cat. #170-6515) dilution, while goat-anti-mouse-HRP antibodies (PerkinElmer) were used at a 1:5,000 dilution. Western blots utilized Amersham Hybond-P (PVDF) membranes (GE Healthcare), and antibody detection was carried out using colorimetric (BM Blue POD Substrate, Precipitating; Roche) or chemiluminescent (Amersham ECL Prime Western Blotting Detection Reagent; GE Healthcare) substrates.

HtrC and YpeB purification and assay. The *B. anthracis htrC* coding sequence, lacking the first 44 codons containing the predicted transmembrane anchor, was PCR-amplified and introduced into the entry vector pDonR201 (Invitrogen) and then the destination vector pDEST-HisMBP-T (a modified version of pDEST-HisMBP (161) containing a tobacco etch virus (TEV) cleavage site). The resulting plasmid, pDPV458, encoding an N-terminal His_6-tagged maltose binding protein (MBP) fused to a TEV cleavage site and HtrC lacking its signal sequence/membrane anchor, was verified by DNA sequencing. Overexpression strain DPVE501 was cultured at 37 ℃ until the OD reached ~0.8, at which point isopropyl-β-D-thiogalactopyranoside was added to a final concentration of 0.7 mM, the culture temperature was reduced to 12 ℃, and incubation was continued for 16 h.

Cells were harvested by centrifugation, resuspended in Buffer D (50 mM NaCl, 50 mM Tris-HCl pH 7.5, 5% glycerol, 25 mM imidazole) and lysed using sonication. Soluble and insoluble protein fractions were separated by centrifugation at 117,000 x *g* for 1 h. Soluble His_6-MBP-$HtrC_{45-391}$ was purified using a Ni-Sepharose HisTrap HP affinity column equilibrated with Buffer D. Protein was eluted with a step gradient of Buffer D containing 100 mM increasing concentrations of imidazole and fractions were dialyzed in Buffer D. His_6-MBP-$HtrC_{45-391}$ at a concentration of ~1.5 mg/ml was incubated with 0.5 mg/ml His_6-tagged TEV (S219V) protease (162) at 15 ℃ for 16 h. Cleavage was verified by SDS-PAGE analysis. $HtrC_{45-391}$ was separated from His_6-TEV, His_6-MBP, and undigested protein using a Ni-Sepharose HisTrap HP affinity column. Fractions containing $HtrC_{45-391}$ were dialyzed in Buffer D, flash frozen, and stored at -80 ℃. $YpeB_{21-446}$ overexpression and purification was performed as described previously (69).

Protease activity of HtrC was assayed in 50 mM Tris-HCl pH 8.0 with 1 μM $HtrC_{45-391}$ and 6 μM $YpeB_{21-446}$ at 37 ℃ for 4 h, unless indicated otherwise. The reaction was terminated by adding 2X SDS-PAGE sample loading buffer to a final concentration of 1X and incubating at 100 ℃ for 5 min. Proteins were separated using SDS-PAGE and were stained with Coomassie Brilliant Blue.

RESULTS

***B. anthracis* YpeB is proteolytically processed during spore germination.** A previous study indicated that YpeB of *B. subtilis* is proteolytically cleaved during spore germination (64). A *B. anthracis ypeB* deletion mutant was previously complemented with a gene expressing YpeB with a C-terminal His_6 tag (69). This His_6-tagged protein accumulated in spores to an abundance equivalent to that of the wild-type, complemented fully for stabilization of SleB in the dormant spore, and allowed a wild-type germination rate (69). Spores of this *B. anthracis* YpeB-His_6 strain (DPBa127) were germinated and extracted at various times for western blotting to examine YpeB processing. By the 45 min time point, spores had lost at least 50% of their initial OD, and examination by phase-contrast microscopy indicated that > 95% of the spores in each preparation had germinated. Full-length 51 kDa YpeB-His_6 diminished during germination, with the appearance of an abundant stable product at ~28 kDa product and a minor ~32 kDa product (Fig. 4.1, upper panel). The same banding pattern was observed during germination of wild-type *B. anthracis* spores (not shown). Western blotting of the same YpeB-His_6 germinating spore fragments using anti-His_6 antibodies indicated that the 28 and 32 kDa YpeB fragments possessed the His_6 tag (Fig. 4.1, lower panel), and were therefore C-terminal portions of YpeB. The abundant 28 kDa YpeB-His_6 fragment was purified from germinated spores using metal-affinity chromatography, and the N-terminal sequence was determined to be SAQKN. The sequence indicated cleavage between residues T202 and S203 of YpeB (Fig. 4.2). In an effort to block this specific cleavage event, the *ypeB*-His_6 allele was mutagenized to change residues T202-S203 to E202-L203. The altered YpeB-$^{T202E/S203L}$-His_6 protein accumulated to levels equivalent to YpeB-His_6 in the spore and complemented for SleB stabilization and for germination rate (Figs. 4.3A and 4.4). YpeB-$^{T202E/S203L}$-His_6 protein was not cleaved to the 28 kDa fragment during germination, indicating that the mutation at the cleavage site succeeded

in blocking proteolysis, but the stability of full-length YpeB during germination was not increased; rather, the abundance of the 32 kDa product increased (Fig. 4.3A and C). In addition, a small amount of a new ~29 kDa cleavage product, slightly larger than the original 28 kDa fragment, was observed (Fig. 4.3A and C). The 32 kDa product was purified from germinated YpeB-$^{T202E/S203L}$-His_6 spores and the N-terminal sequence was determined to be SNRDP, indicating processing between residues A168 and S169 (Fig. 4.2). Once again, the amino acids flanking this cleavage site were changed by site-specific mutagenesis, allowing the expression of YpeB-$^{A168E/S169L}$-His_6 and YpeB-$^{A168E/S169L, T202E/S203L}$-$His_6$. Both of these proteins accumulated to normal levels in the spore (Fig. 4.3B) and both allowed normal spore germination (Fig. 4.4). Western blotting of germinating spore samples indicate that the A168E/S169L change prevented proteolysis at that site (Fig. 4.3B and C). YpeB-$^{A168E/S169L}$-His_6 was instead processed to the dominant 28 kDa fragment (Fig. 4.3B and C). Stable cleavage products were not as strongly detected during germination of YpeB-$^{A168E/S169L, T202E/S203L}$-$His_6$ spores, but the full-length protein still diminished during germination (Fig. 4.3B and C). Two less stable products of ~29 and ~33 kDa were produced (Fig. 4.3B and C).

Identification of candidate *B. anthracis* proteases that might cleave YpeB. A variety of data sources were used to identify a protease, herein called HtrC, as a candidate to be involved in YpeB cleavage. Recent studies of *B. anthracis* and *B. subtilis* spore membrane proteomes indicated that this protease might be associated with the membrane that YpeB is embedded in (Chen, Y. and D.L. Popham, unpublished). A transcriptome study had indicated that *htrC* (BAS5314) was expressed during the latter stages of *B. anthracis* sporulation (120). In *B. subtilis*, the apparent ortholog (*yycK/htrC*) is expressed during sporulation under the control of σ^G, which would place it in the forespore compartment (145) along with *sleB-ypeB* expression (68). Studies of HtrC and paralogs in other species have indicated that these proteases cross and remain associated with the outer surface of the cytoplasmic membrane

due to an uncleaved signal sequence/membrane anchor (147). HtrC expressed in the developing spore would therefore be expected to remain on the outer surface of the inner spore membrane, in the same location as YpeB. While multiple proteases in each species possess some properties consistent with a role in YpeB processing, the HtrC proteins of *B. anthracis* and *B. subtilis* were considered the strongest candidates.

Strains lacking HtrC are altered in YpeB proteolysis. *B. anthracis* and *B. subtilis* strains carrying null mutations in *htrC* were constructed, and YpeB cleavage was examined by western blotting using antisera against *B. anthracis* YpeB (69). The *B. anthracis* Δ*htrC* mutant lost full-length YpeB during germination more slowly than the wild-type and did not accumulate the specific 27 and 31 kDa cleavage products (Fig. 4.5A) (These cleavage products are slightly smaller than those in Fig. 4.1 because they lack the His_6 tag). In some cases, western blots exhibited a heavier background in the 30-50 kDa range for germinating Δ*htrC* spores (Fig. 4.5A), suggesting that YpeB might be degraded to non-specific products, but this has not been further confirmed. While the antibodies did not recognize the cleavage products of *B. subtilis* YpeB, the *htrC* mutant maintained increased amounts of full-length YpeB during germination relative to the wild-type strain (Fig. 4.5B).

The germination of *htrC* mutant spores was examined to determine if slowed degradation of YpeB resulted in decreased SleB activity. This was done in *B. anthracis* decoated spores and in a *B. subtilis* Δ*cwlJ* background in order to render the function of SleB more easily observed (65, 163). In both *Bacillus* species, the germination rates of Δ*htrC* spores were not significantly different from those of the wild-type spores (Fig. 4.6A and B). In both species, the colony-forming efficiency of Δ*htrC* spores lacking CwlJ activity was also not different from the corresponding wild-type spores (Table 4.3).

***In vitro* cleavage of YpeB by HtrC.** *B. anthracis* HtrC, lacking its signal sequence/membrane anchor, was expressed in *E. coli* as a His_6-MBP fusion protein and was

purified by metal-affinity chromatography. Following purification of His_6-MBP-$HtrC_{45-391}$, the His_6-MBP domain was removed using TEV protease, and $HtrC_{45-391}$ was purified (Fig. 4.7). The pure protease exhibited little activity against a generic substrate (fluorescently-labeled casein, data not shown) and, initially, very little activity against purified *B. anthracis* YpeB (Fig. 4.8, lanes 8, 10, and 15-16). Assay attempts using a wide variety of conditions revealed that HtrC-catalyzed cleavage of YpeB to produce an ~27 kDa fragment, as observed *in vivo*, was greatly stimulated by the presence of Mn^{2+} (Fig. 4.8, lanes 10-13) and, to a lesser degree, by Ca^{2+} (Fig. 4.8, lanes 16-19), but not by Mg^{2+}, Zn^{2+}, Na^{+}, or K^{+} (Fig. 4.8, lanes 1-10). Relatively high concentrations of Mn^{2+} or Ca^{2+} were required to achieve maximum HtrC activity (Fig. 4.8, lanes 10-13 and 16-19). Metal-stimulated HtrC activity was inhibited by EDTA, a chelator of divalent cations (Fig. 4.8, lanes 16, 18, and 20). The presence of an equimolar concentration of DPA, another strong chelator, blocked the positive effect of Ca^{2+} on HtrC (Fig. 4.8, lanes 22-26). HtrC action on YpeB was found to be maximal at pH 7-9 (data not shown).

HtrC is not an important factor in SleB or YpeB degradation during spore formation. To determine if HtrC is involved in degradation of SleB and/or YpeB in the absence of the partner protein during spore formation, Δ*sleB* Δ*htrC* and Δ*ypeB* Δ*htrC* double mutants were constructed in *B. anthracis*. As demonstrated previously (69), in a Δ*sleB* mutant, YpeB failed to accumulate during spore formation, and in a Δ*ypeB* mutant, SleB did not accumulate (Fig. 4.9A and B). The additional deletion of *htrC* from these strains still resulted in the degradation of YpeB or SleB, respectively, during sporulation (Fig. 4.9), indicating that other proteases are likely active in their degradation during spore formation. Additionally, the production of YpeB during Δ*sleB* Δ*htrC* spore formation coincided with the appearance of YpeB-specific degradation products (Fig. 4.9C), similar to those seen during sporulation of the Δ*sleB* strain (69) and to specific cleavage products seen during spore

germination. This finding indicates that, at least during sporulation, other proteases are capable of producing similar cleavage products.

DISCUSSION

B. anthracis YpeB is processed to a relatively stable fragment during germination, as in *B. subtilis* (64). The ultimate N-termini of the stable YpeB fragments were determined to be in a region between an undefined N-terminal YpeB domain and the C-terminal region containing three putative PepSY domains. This C-terminal fragment persists well into the germination process. The N-terminal cleavage product was observed neither in western blots of germinating spore extracts nor in *in vitro* reactions using purified proteins. While this might be due to poor recognition of this domain by the antiserum and/or poor staining of the domain, it raises the possibility that this domain is subject to more rapid degradation to smaller fragments. Interestingly, the YpeB N-terminal domain was recently shown to exert an inhibitory effect on SleB activity *in vitro* (155). Processing of YpeB could play a role in the activation of SleB during germination.

Deletion of *htrC* was found to result in the disappearance of specific YpeB degradation products in both species, though the amount of full-length YpeB still decreased during germination. This indicates that multiple proteases are active in this region of the spore during germination. The degradation of YpeB during germination may be a multistep process, carried out by multiple proteases, with the ultimate stable products being produced by HtrC. However, initial cleavage of YpeB by another protease is apparently not a requirement for HtrC action, as the action of HtrC was reproducible *in vitro* using purified proteins.

The inability to fully block YpeB degradation during germination precludes demonstration of a role of YpeB instability in SleB activation during germination. Even when YpeB degradation was slowed by the loss of HtrC, the spore germination rate was not significantly affected. Under the experimental conditions tested, germination was dependent

on SleB activity (61, 73). A previous study indicated that a 30% decrease in SleB abundance resulted in an observable germination defect (69), so the delay in YpeB degradation observed here must not have inhibited SleB to this degree. This may indicate that YpeB degradation is not required for SleB activation and that YpeB degradation is merely the natural disposal of this protein following the breakage of spore dormancy. Alternatively, the slowed kinetics of YpeB degradation may not have been sufficient to affect the outward assays of germination progression. Unfortunately, strains in which N-terminal regions of YpeB were deleted, including the identified HtrC cleavage sites and potential upstream cleavage sites, did not retain stable SleB in the dormant spore (69), and thus could not be used to determine what effect a non-cleavable YpeB has on SleB activity during germination.

Alteration of the dominant HtrC cleavage sites in YpeB resulted in the appearance of alternative dominant *in vivo* cleavage sites in the same region of the protein. Several pieces of evidence suggest that the C-terminal domain of YpeB is relatively protease resistant, while the N-terminal domain is more sensitive, and the region linking the domains may be especially sensitive. The N-terminal domain was not observed in either *in vivo* or *in vitro* experiments where the C-terminal domain could be detected. In the absence of SleB, YpeB is degraded during spore formation, producing dominant cleavage products similar in size to those produced during germination (69). Similar YpeB cleavage products were produced during sporulation of a Δ*sleB* Δ*htrC* mutant, indicating that another protease(s) targets this same region between the YpeB domains. These experiments also revealed that proteases other than HtrC must be involved in the degradation of both YpeB and SleB when produced in the absence of SleB or YpeB, respectively, during spore formation. The use of multiple protease-deficient strains to block SleB and YpeB degradation during sporulation, and potentially during germination, is challenging, as multiple proteases present in the

intermembrane space of the developing spore are necessary for proper spore formation (164, 165).

B. anthracis HtrC, expressed and purified from *E. coli*, cleaved YpeB *in vitro* but with relatively poor kinetics. A four-hour digestion was required to achieve catalysis of approximately three YpeB molecules per HtrC molecule. This activity was dependent on the presence of relatively high concentrations of Mn^{2+} or Ca^{2+} ions. The high ion concentrations required suggests that their function is not directly in catalysis, which is consistent with the absence of a metal role in catalysis by this class of serine protease (166). Interestingly, HtrC action on YpeB coincides closely with the release of a large amount of Ca^{2+}-DPA from the spore core during germination. The local Ca^{2+}-DPA concentration is apparently quite high at this time, as it can activate CwlJ activity, a process that requires > 20 mM Ca^{2+}-DPA (19). While most of the Ca^{2+} released during germination is likely bound to DPA, and our findings indicate that the Ca^{2+}-DPA complex is ineffective in promoting HtrC activity, it is possible that enough free Ca^{2+} is present to increase HtrC activity during germination. Spores also contain significant amounts of Mn^{2+} (134, 167), which is likely complexed with DPA and released during germination, and could thus play a role in stimulating HtrC.

Chemicals that function as protease inhibitors have been shown to block spore germination at different stages, suggesting that protease activity is critical during germination (168-171). While it has not been shown that this activity is actually due to inhibition of a protease rather than another protein function or what specific germination processes are affected, these results raise the possibility that initiation of cortex hydrolysis could require a protease activity. Proteolytic processing of a Clostridial GSLE, SleC, is required for induction of activity during germination, but this GSLE is unrelated to *Bacillus* GSLEs. Further study of the roles of proteases in spore germination, and of their potential direct effect

on activation of cortex hydrolysis, may allow the improvement of spore decontamination or application methods.

ACKNOWLEDGEMENTS

Research reported in this publication was supported by the National Institute of Allergy and Infectious Disease of the National Institutes of Health under award number R21AI088298. The content is solely the responsibility of the authors and does not necessarily represent the official views of the National Institutes of Health. We thank Roger Plaut and Scott Stibitz for the gift of plasmid pSS4332. Dr. Florian Schubot contributed reagents and Jessica Blackwood provided laboratory assistance.

Table 4.1. Bacterial strains and plasmid.

Strain or plasmid	Relevant genotype/phenotype [a]	Construction [b]	Source
E. coli			
DPVE13	BL21 (λDE3) pLysS (Cm^r)		Novagen
DPVE501	pDPV458 (His_6-MBP-$HtrC_{45-391}$ Amp^r) Cm^r	pDPV458→DPVE13	This study
B. anthracis			
Sterne 34F2	$pXO1^+$ $pXO2^-$		P. Hanna
DPBa38	Δ*sleB*		(61)
DPBa89	Δ*ypeB*		(69)
DPBa113	Δ*ypeB*::pDPV416 (*ypeB*$^+$ Er^r)		(69)
DPBa127	Δ*ypeB*::pDPV424 (YpeB-His_6 Er^r)		(69)
DPBa157	Δ*ypeB*::pDPV447 ($YpeB^{T202E/S203L}$-His_6 Er^r)	pDPV447→DPBa89	This study
DPBa167	Δ*ypeB*::pDPV454 ($YpeB^{A168E/S169L}$-His_6 Er^r)	pDPV454→DPBa89	This study
DPBa168	Δ*ypeB*::pDPV455 ($YpeB^{A168E/S169L, T202E/S203L}$-$His_6$ Er^r)	pDPV455→DPBa89	This study
DPBa178	Δ*htrC*	pDPV460→34F2	This study
DPBa182	Δ*htrC*::pDPV459 (*htrC*$^+$ Er^r)	pDPV459→DPBa178	This study
DPBa187	Δ*sleB* Δ*htrC*	pDPV460→DPBa38	This study
DPBa188	Δ*ypeB* Δ*htrC*	pDPV460→DPBa89	This study
B. subtilis			
PS832	Prototrophic derivative of strain 168		P. Setlow
FB111	Δ*cwlJ*::Tet^r		(73)
DPVB668	Δ*htrC*::MLS^r	PCR→PS832	This study
DPVB669	Δ*cwlJ*::Tet^r Δ*htrC*::MLS^r	FB111→DPVB668	This study

Plasmids			
pBKJ236	Er^r *ori*(Ts)		(158)
pSS4332	Kan^r, I-SceI, AmCyan		(159)
pDEST-HisMBP-T	His_6-MBP, Amp^r Cm^r		F. Schubot
pDPV416	*ypeB*$^+$		(69)
pDPV424	YpeB-His_6		(69)
pDPV447	YpeB$^{T202E/S203L}$-His_6	pBKJ236::Δ*sleB* *ypeB*$^{T202E/S203L}$-His_6	This study
pDPV454	YpeB$^{A168E/S169L}$-His_6	pBKJ236::Δ*sleB* *ypeB*$^{A168E/S169L}$-His_6	This study
pDPV455	YpeB$^{A168E/S169L,\ T202E/S203L}$-$His_6$	pBKJ236::Δ*sleB* *ypeB*$^{A168E/S169L,\ T202E/S203L}$-$His_6$	This study
pDPV458	His_6-MBP-HtrC$_{45-391}$	pDEST-HisMBP-T::*htrC*$_{45-391}$	This study
pDPV459	*htrC*$^+$	pBKJ236::*htrC*	This study
pDPV460	Δ*htrC*	pBKJ236::Δ*htrC*	This study

[a] Cm^r, chloramphenicol resistance; Amp^r, ampicillin resistance; Er^r, erythromycin resistance; Tet^r, tetracycline resistance; MLS^r, macrolide-lincosamide-streptogramin B resistance; *ori*(Ts), temperature-sensitive origin of replication; Kan^r, kanamycin resistance.

[b] Strains were constructed by conjugation or electroporation for *B. anthracis*, or transformation for *B. subtilis*. The designation preceding the arrow is the plasmid or source of donor DNA, while the designation following the arrow is the recipient strain

Table 4.2. Primer sequences.

Plasmid/Strain constructed	Primer name	Sequence 5′ to 3′ [a]
pDPV447	593	CTTCGGACCTACCTTTGAATTAGCACAAAAAAATAAAAAAGGTGG
	594	CCACCTTTTTTATTTTTTTGTGCTAATTCAAAGGTAGGTCCGAAG
	603	GTCTTCTTTACATAAAAGCGAGCCTTTTACAAAACATAACC
	604	GCTTTACGTTCTTCCATAACTTTCACATCTGGATTG
pDPV454	605	GTTGAGATGGCACTCGAGTTAAATCGTGATCCTGCCG
	606	CGGCAGGATCACGATTTAACTCGAGTGCCATCTCAAC
	603, 604	
pDPV455	603, 604, 605, 606	
pDPV458	612	***GTGGAGAACCTGTACTTCCAGGGT***TCAAATGATACGGGCGC
	613	*CCACTTTGTACAAGAAAGTTGCATT*TTAATACTTTTGAATGCCTAGTTTAAC
pDPV459	614	CGCGGATCCGATATTGAGGTCGAGTCATTTG
	615	CGCCTGCAGCAATGACATGCGTATCATCAG
pDPV460	616	CGCAGATCTAAAGGACATATTTGTTCACCTATC
	617	CGCAGATCTAAGTATTAAAAACAGGAGGGCCTAC
DPVB668	607	ACAAGTACGCAGGTGCTGGC
	608	CGATTATGTCTTTTGCGCAGTCGGCCCTCACGTTCGTAATCCACC
	609	GAGGGTTGCCAGAGTTAAAGGATCCCTCCGCAGACCAATTAGGC
	610	GATACACCGATTGACGTACG

[a] Restriction sites are underlined, TEV cleavage site regions of pDEST-HisMBP-T are italicized and in bold, and *att*R2.1 regions of pDEST-HisMBP-T are italicized and underlined.

Table 4.3. Germination efficiencies of Δ*htrC B. anthracis* and *B. subtilis* spores.

Species	Strain	Genotype	CFU/OD/ml [a]
B. anthracis	DPBa2	WT	6.7×10^7
	DPBa178	Δ*htrC*	6.0×10^7
	DPBa182	*htrC*$^+$	6.3×10^7
B. subtilis	PS832	WT	1.7×10^8
	FB111	Δ*cwlJ*	3.0×10^8
	DPVB668	Δ*htrC*	1.9×10^8
	DPVB669	Δ*cwlJ* Δ*htrC*	2.0×10^8

[a] Decoated spores were used for *B. anthracis* studies. Values are averages of three independent spore preparations. Among the strains for each species, no statistical difference in colony forming efficiency was present.

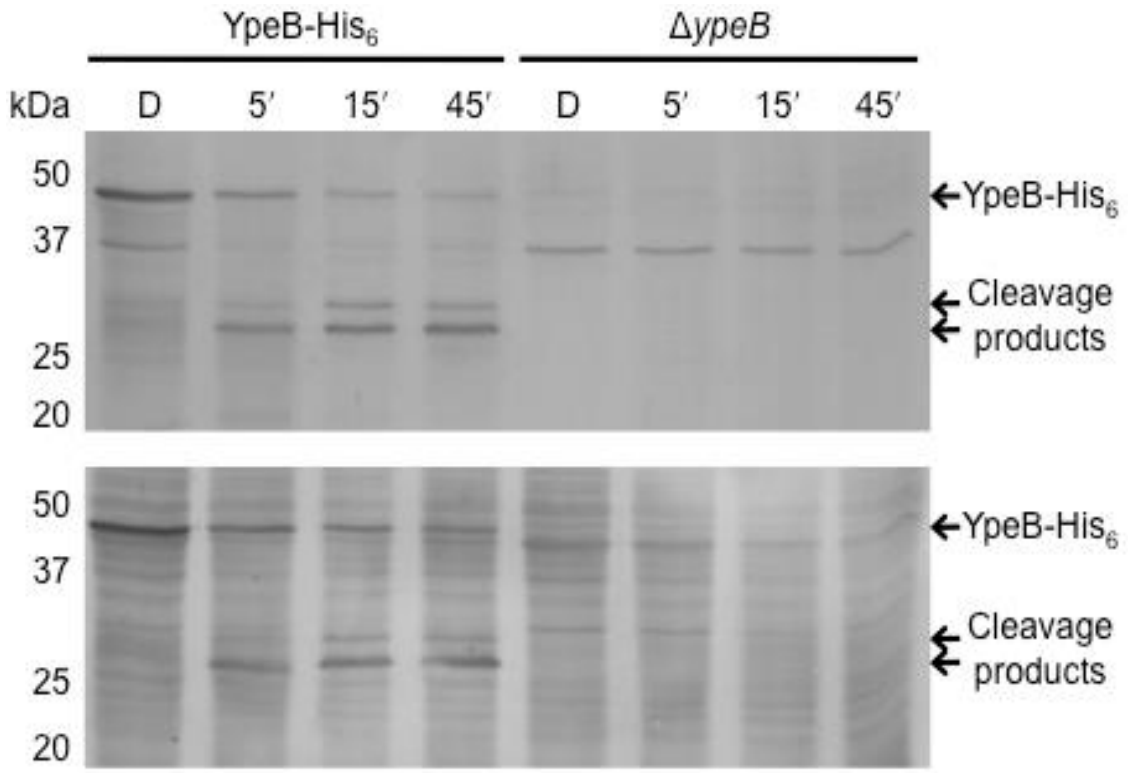

Figure 4.1. YpeB is cleaved during germination of *B. anthracis* spores. Dormant (D) DPBa127 (YpeB-His_6) and DPBa89 (Δ*ypeB*) spores were germinated with 100 mM L-alanine and 1 mM inosine at 37°C, and samples were collected at 5 (5′), 15 (15′), and 45 (45′) min. Extracted proteins were probed with anti-YpeB (top panel) and anti-His_6 (bottom panel) antibodies. The predicted molecular weight of YpeB-His_6 is 51 kDa. The positions of the molecular weight marker proteins (not shown) are indicated on the left.

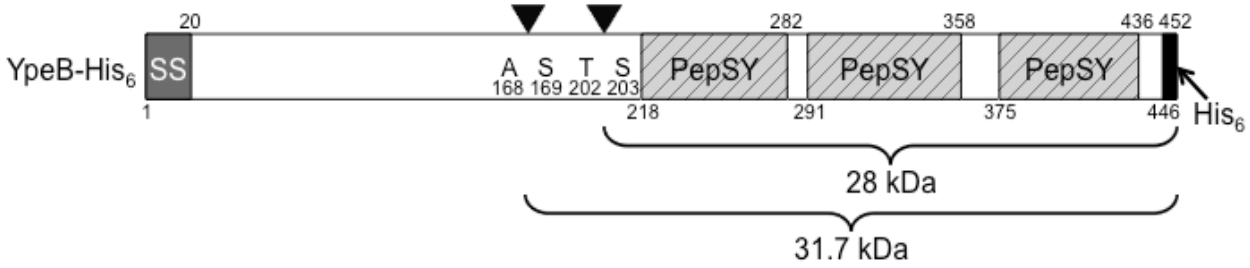

Figure 4.2. Locations of major *B. anthracis* YpeB cleavage sites. Scale drawing of the domain architecture of YpeB showing the N-terminal signal sequence (SS), C-terminal PepSY domains, and YpeB cleavage sites (▼) with predicted molecular weights of C-terminal cleavage products. Residue numbers designate amino acid positions of domain boundaries and positions of YpeB cleavage during spore germination.

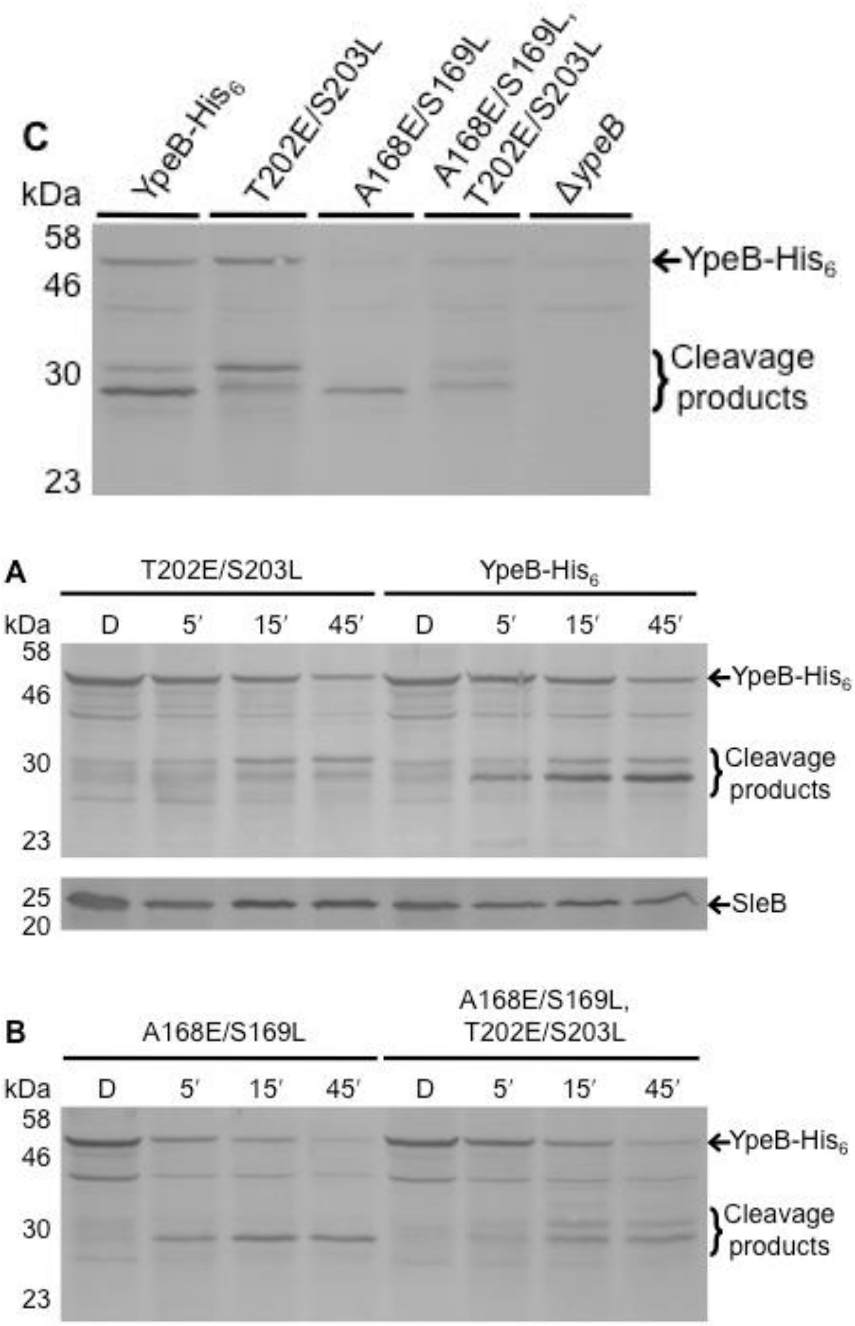

Figure 4.3. YpeB cleavage during germination of *B. anthracis* mutant spores. Dormant (D) spores were germinated with 100 mM L-alanine and 1 mM inosine at 37°C, and samples were collected at 5 (5′), 15 (15′), and 45 (45′) min. (A) DPBa157 (T202E/S203L) and DPBa127 (YpeB-His_6) sample extracts probed with anti-YpeB (top panel) and anti-SleB (bottom panel) antibodies. (B) DPBa167 (A168E/S169L) and DPBa168 (A168E/S169L, T202E/S203L) sample extracts were probed with anti-YpeB antibodies. (C) Extracts from 45 min-germinated spores from each strain were probed with anti-YpeB antibodies. The predicted molecular weight of YpeB-His_6 and derivatives is approximately 51 kDa. The positions of the molecular weight marker proteins (not shown) are indicated on the left.

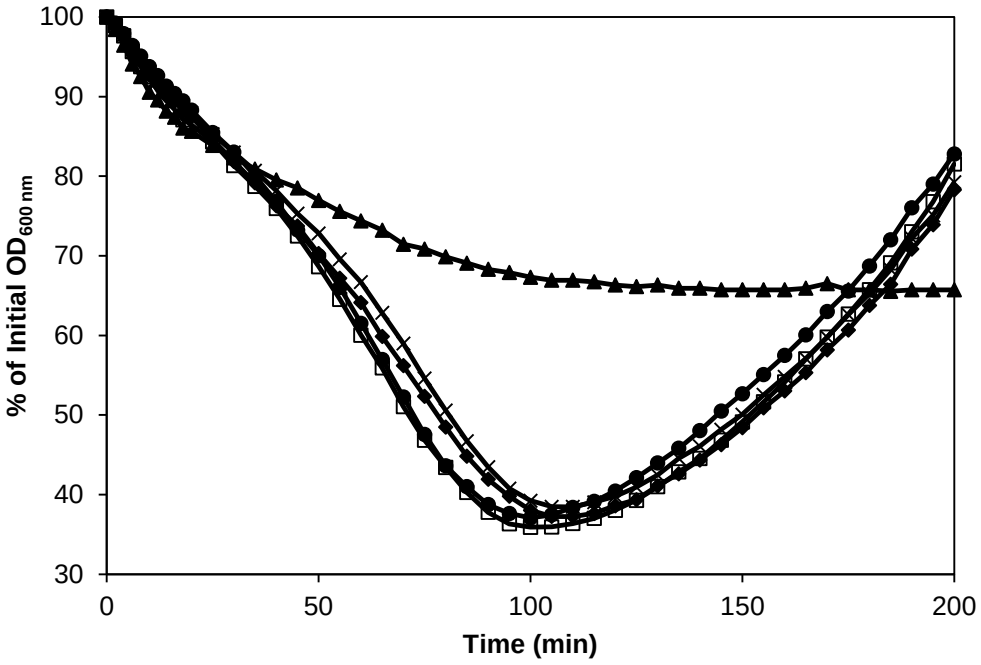

Figure 4.4. Altered YpeB proteolysis does not slow spore germination and outgrowth. Decoated Δ*ypeB* (▲), YpeB$^{T202E/S203L}$-His$_6$ (□), YpeB$^{A168E/S169L}$-His$_6$ (◆), YpeB$^{A168E/S169L, T202E/S203L}$-His$_6$ (×), and YpeB-His$_6$ (●) *B. anthracis* spores were heat activated and germinated in BHI medium at 37°C; germination and outgrowth was tracked as changes in OD. Data shown are averages of results from three independent spore preparations; error bars are omitted for clarity. Germination of YpeB$^{T202E/S203L}$-His$_6$, YpeB$^{A168E/S169L}$-His$_6$, and YpeB$^{A168E/S169L, T202E/S203L}$-His$_6$ spores is not significantly different ($P > 0.06$) at any time point. Likewise, germination of YpeB-His$_6$ and YpeB$^{T202E/S203L}$-His$_6$ spores is not significantly different ($P > 0.07$) at any time point. Focusing on stage two of germination, from 45 to 95 min (69), YpeB$^{A168E/S169L}$-His$_6$ and YpeB-His$_6$ spores do not significantly differ ($P > 0.07$), whereas YpeB$^{A168E/S169L, T202E/S203L}$-His$_6$ and YpeB-His$_6$ spores are not significantly different ($P > 0.05$), except from 75 to 80 min ($P < 0.05$).

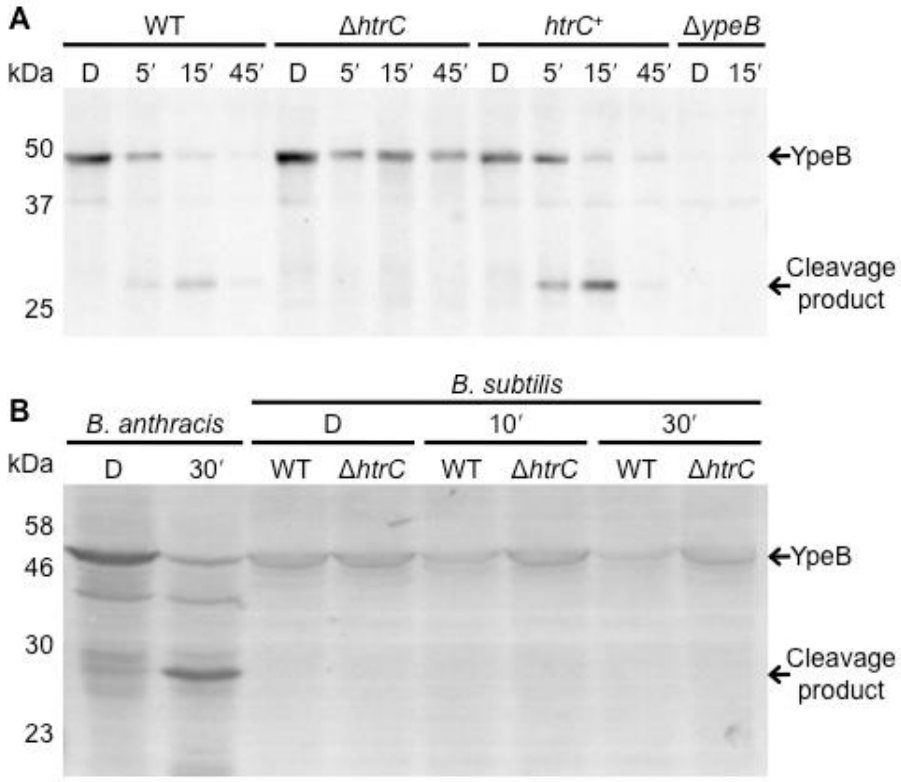

Figure 4.5. HtrC cleaves YpeB during germination of *B. anthracis* and *B. subtilis* spores. Spores were prepared, germinated, and analyzed by western blot with *B. anthracis* anti-YpeB antibodies as described in materials and methods. (A) *B. anthracis* spores were dormant (D) or collected 5 (5′), 15 (15′), and 45 (45′) min after addition of germinants. Strains were DPBa2 (WT), DPBa178 (Δ*htrC*), DPBa182 (*htrC*$^{+}$), and DPBa89 (Δ*ypeB*). (B) *B. anthracis and B. subtilis* spores were dormant (D) or collected 10 (10′) and 30 (30′) min after addition of germinants. Strains were DPBa2 (*B. anthracis* WT), PS832 (*B. subtilis* WT), and DPVB668 (*B. subtilis* Δ*htrC*). The predicted molecular weights of YpeB from *B. anthracis* and *B. subtilis* are 50 and 51 kDa, respectively. The positions of the molecular weight marker proteins (not shown) are indicated on the left.

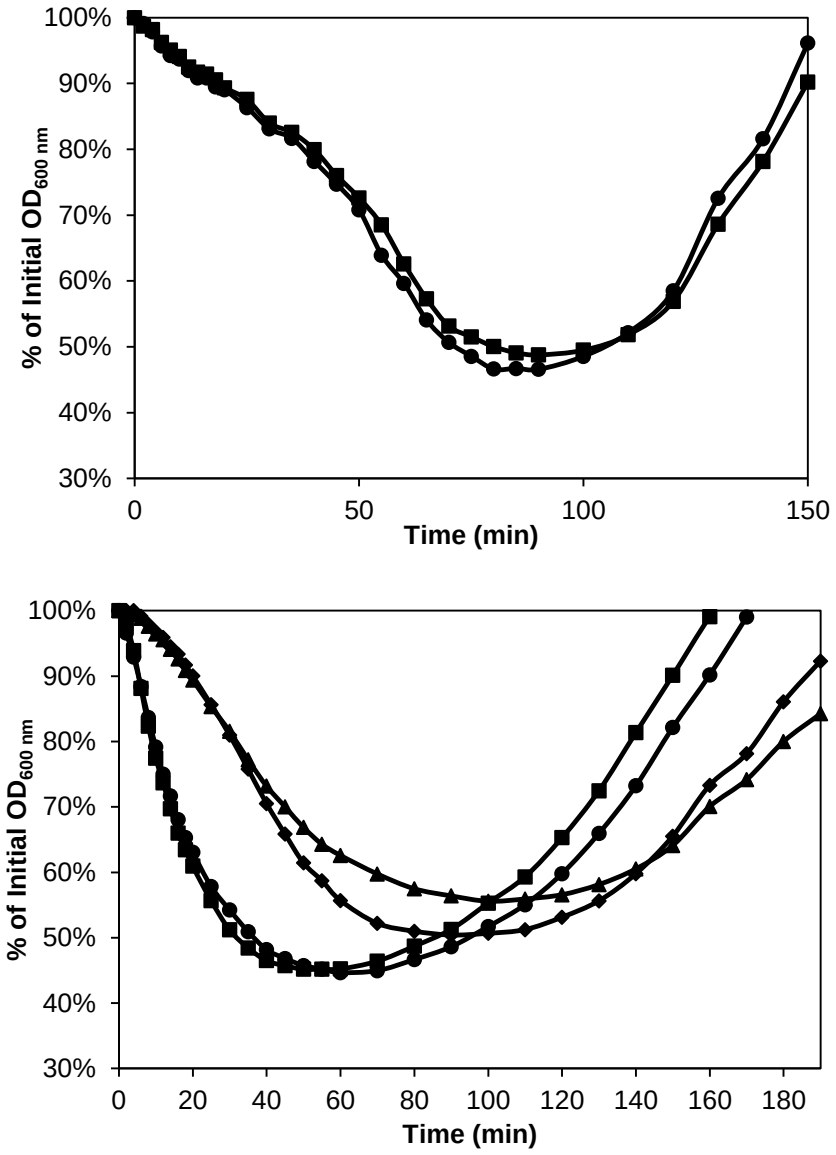

Figure 4.6. Loss of HtrC does not alter the germination rates of *B. anthracis* and *B. subtilis* spores. Spores were heat activated and germinated in rich medium as described in materials and methods; germination and outgrowth were tracked as changes in OD_{600}. Data shown are averages of results from three (*B. anthracis*) or two (*B. subtilis*, preliminary results) independent spore preparations; error bars are omitted for clarity. (A) *B. anthracis* wild-type (DPBa2, ■) and Δ*htrC* (DPBa178, ●) spores were decoated and germinated in BHI broth. The two strains were not statistically different from one another ($P > 0.3$) at any time point. (B) *B. subtilis* wild-type (PS832, ■), Δ*cwlJ* (FB111, ◆), Δ*htrC* (DPVB668, ●), and Δ*cwlJ* Δ*htrC* (DPVB669, ▲) spores were germinated in 2xYT broth. The wild-type and Δ*htrC* strains were not significantly different, and Δ*cwlJ* and Δ*cwlJ* Δ*htrC* strains were not significantly different ($P > 0.2$) at any time point. The wild-type and Δ*cwlJ* strains were significantly different from 30-60 min and the Δ*htrC* and Δ*cwlJ* Δ*htrC* strains were significantly different from 12-50 min ($P < 0.05$).

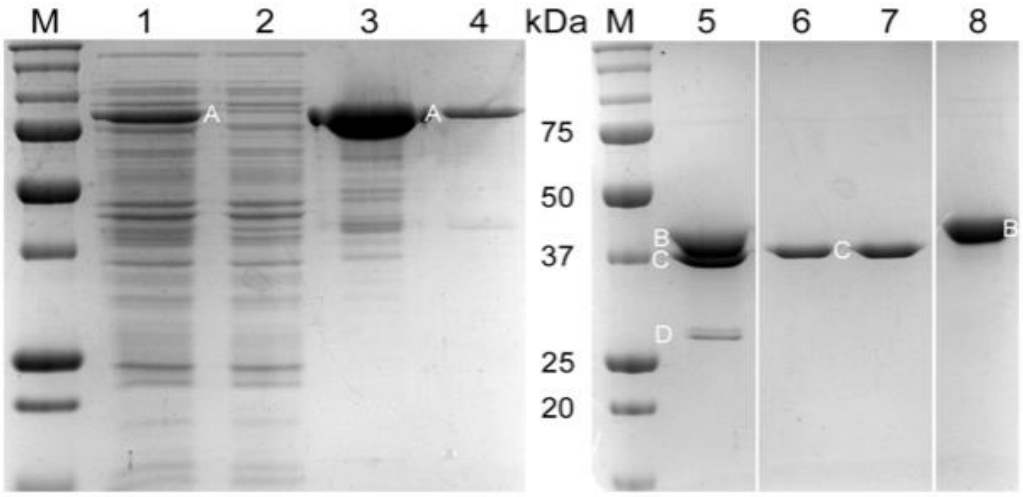

Figure 4.7. Purification of *B. anthracis* HtrC. A His_6-MBP-$HtrC_{45-391}$ fusion protein was overexpressed in *E. coli*, purified by metal-affinity chromatography, cleaved with TEV protease, and separated from the His_6-MBP tag and His_6-TEV using a second metal-affinity column. Samples were soluble protein extracts of induced (lane 1) and uninduced cells (lane 2), eluate fractions from the metal-affinity column containing His_6-MBP-$HtrC_{45-391}$ (A)(lanes 3 and 4), His_6-MBP-$HtrC_{45-391}$ digested with His_6-TEV protease (D)(lane 5), flow-through fractions from the second metal-affinity column containing $HtrC_{45-391}$ (C)(lanes 6 and 7), and eluate from the second metal-affinity column containing His_6-MBP (B)(lane 8). Lanes 1-4 and 5-8 are from two different gels; intervening lanes between 5-6 and 7-8 were removed for clarity. Masses of standard proteins (M) are indicated in the center.

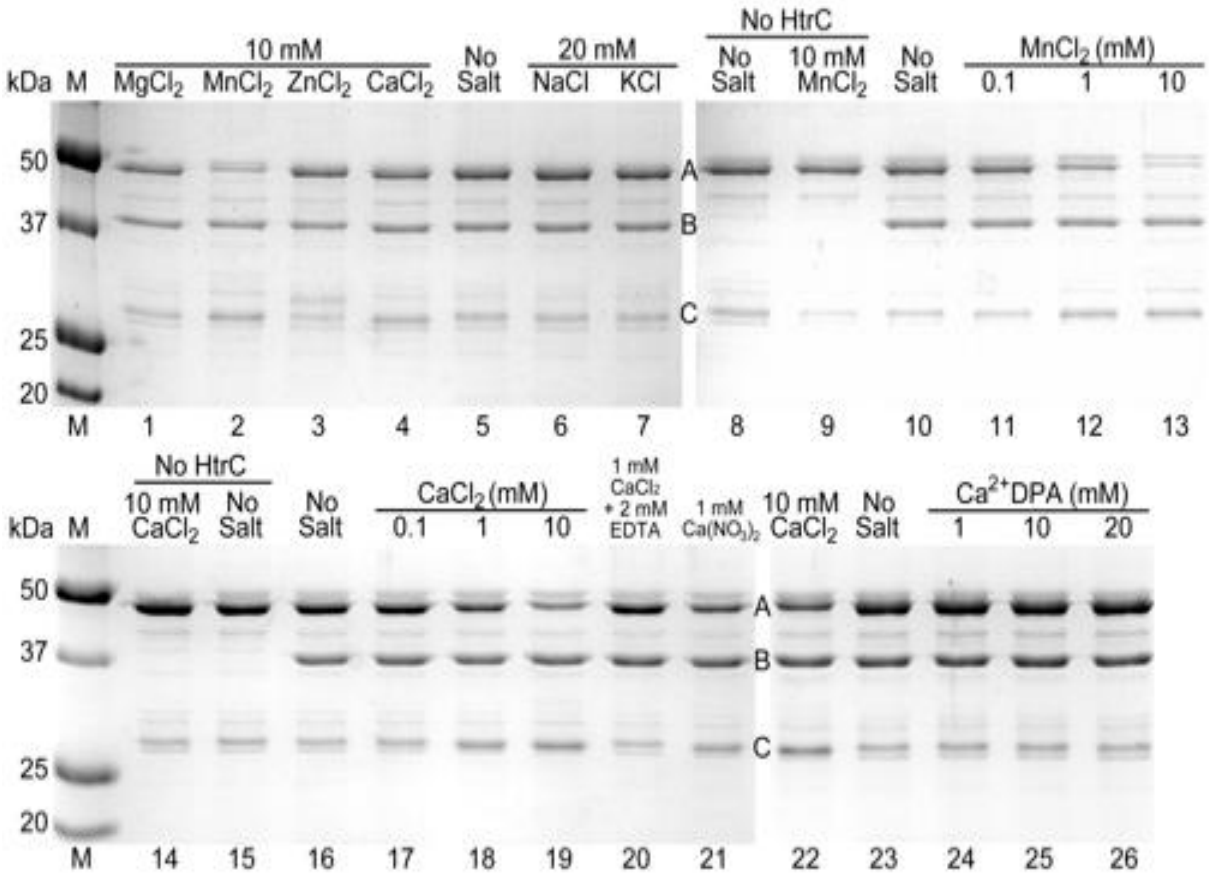

Figure 4.8. *In vitro* cleavage of YpeB by HtrC. Purified $YpeB_{21\text{-}446}$ (A) (6 μM) was incubated for 4 hours with purified $HtrC_{45\text{-}391}$ (B) (1 μM), unless otherwise indicated, with the indicated small molecule additions. Reactions were terminated using SDS and heat. Samples were separated by SDS-PAGE and proteins, including the YpeB cleavage product (C), were detected by staining with Coomassie Brilliant Blue. Protein concentrations were 12 μM $YpeB_{21\text{-}446}$ and 2 μM $HtrC_{45\text{-}391}$ in lanes 22-26. Lanes 1-7, 8-13, 14-21, and 22-26 are from four different gels. Masses of standard proteins (M) are indicated on the left.

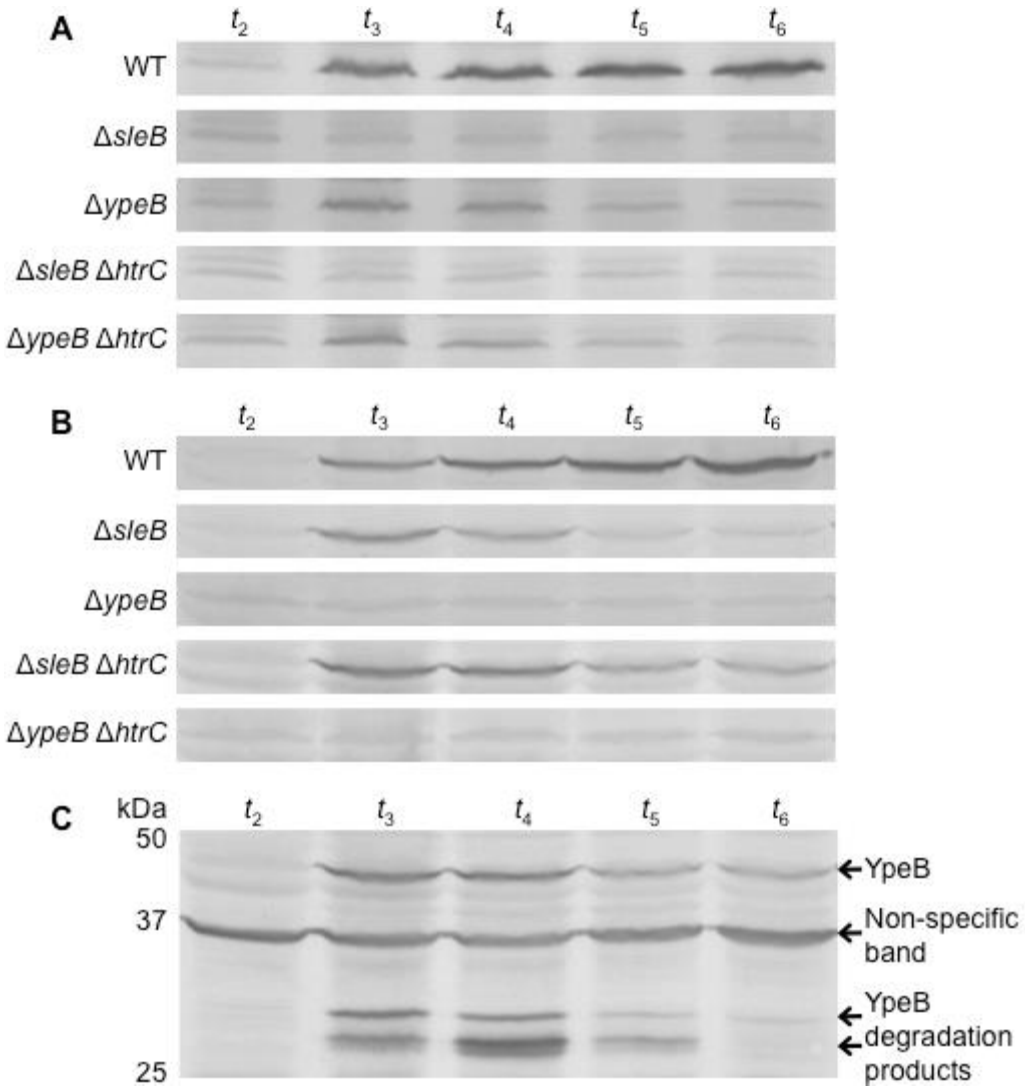

Figure 4.9. SleB and YpeB production during sporulation. Wild-type (WT), Δ*sleB*, Δ*ypeB*, Δ*sleB* Δ*htrC*, and Δ*ypeB* Δ*htrC* strains of *B. anthracis* were grown in modified G broth at 37°C, and sporangia collected during sporulation were subjected to western blot analysis. Labels t_2 through t_6 designate hours since the initiation of sporulation. (A) Sporangia probed with anti-SleB antibodies. (B) Sporangia probed with anti-YpeB antibodies. (C) Sporangia from the Δ*sleB* Δ*htrC* strain probed with anti-YpeB antibodies. The positions of the molecular weight marker proteins (not shown) are indicated on the left.

CHAPTER 5

Final Discussion

The germination of *B. subtilis* spores has been intensively studied for decades. Many germination-related proteins have been shown to be involved in four distinct germination stages. While the significance of several individual proteins in the germination process has been characterized, the mechanisms of how these proteins perform their functions and the network connecting these proteins in the complete germination process are still a mystery. A substantial number of proteins that are expressed under the control of sporulation specific sigma factors have no significant sequence similarity to known genes or functional domains. Characterization of these unknown proteins may provide key insights into the germination network. For example, when and how does a large quantity of water penetrate the spore inner membrane in a short time in the conditions that the inner membrane lipids are immobile? If peptidoglycan degradation is triggered by exogenous Ca^{2+}-DPA, how is the timing of this process related to spore core Ca^{2+}-DPA release? How is the germination signal transmitted from germinant receptors to DPA channel proteins? This work is focused on generating a comprehensive protein identity list for the spore membrane fraction and investigating candidate proteins for their roles in the spore germination process.

In Chapter 2, we characterized a superdormant spore population that drastically differs from that described in a previous publication. A quantitative MRM-MS assay was performed to analyze the relative abundance of 11 germination-related proteins in dormant, germinating, and superdormant spores. Our findings showed that superdormancy was not due to a low abundance of germinant receptor proteins. We found that germination of the superdormant spores was delayed at a germination stage where the GerD lipoprotein is involved. This evidence suggested that there is more than one pathway that can result in spore superdormancy.

Previous studies have shown that germinant receptor proteins, SpoVA proteins, and GerD interact with each other at the membrane (110, 111). The interaction is most likely

involved in germination signal transmission from recognition of the germinant to initiation of Ca^{2+}-DPA release. The mechanism of these interactions remains to be elucidated. Our results showed that the abundance of germinant receptor C-subunit proteins significantly decreased after incubating spores with nutrient germinant. A recent study also showed that altering the level of germinant receptor C-subunit proteins or influencing their lipidation had negative effects on both spore formation and germination (172). This evidence suggests that the decreased level of germinant receptor C-subunit proteins might be a critical step in the germination process. However, it is difficult to elucidate the function of each germinant receptor subunit *in vivo* because the function of germinant receptors relies on the complete heterocomplex of three subunits (27). Expression and purification of individual subunits or intact receptor complexes could be the future direction to a comprehensive biochemical analysis of Ger receptor proteins.

The interaction between germinant receptor proteins and the GerD lipoprotein is another key element to be elucidated in the future. Previous evidence suggested that the germination signal passed from multiple germinant receptors converge at GerD lipoprotein (26). The co-localization of GerD with germinant receptor proteins might facilitate the signal transduction. Previous studies also showed that the level of GerD is greatly reduced in germinating spores (38, 124). However, whether the loss of GerD has direct or indirect connection to the loss of germinant receptor C-subunit proteins is unclear. A recent crystallographic study demonstrated that GerD protein (PDB ID: 4O8W) forms a triple-stranded rope structure that is essential for its role on nutrient germination (173). It is likely, as suggested in the publication, that GerD trimers self-associate to form a large mechanically rigid structure to facilitate the interaction of various germination related proteins. If this is the case, then what proteins receive the signal from GerD and how do they transmit it to SpoVA proteins? Considering a significant loss of GerD from the membrane after germination, it is also

possible that this structure is disrupted following the release of germinant receptor C-subunit proteins. The disruption of the GerD protein complex might be the signal to release Ca^{2+}-DPA through SpoVA proteins. Although the nature GerD signal transduction is unknown, its resolved crystal structure will speed up the process of understanding its role in germinant receptor dependent germination.

Another question that needs to be addressed in the future is the function of PrkC. Our study showed that the quantity of this protein decreased significantly after spore germination. PrkC was previously characterized as a germinant receptor that responds to vegetative peptidoglycan fragments (48). What function, if any, it plays during nutrient germination remains to be determined.

To further explore the full map of protein content on the spore membrane, we carried out the shot-gun proteomic study in chapter 3. We chose SDS-PAGE-based MS approach because it gave the best coverage of membrane proteins in a previous study (104). A total of 104 and 87 proteins were identified as membrane-associated in *B. subtilis* and *B. anthracis*, respectively. The percentages of membrane proteins among the total proteins identified achieved 15-17%. This study identified 65 membrane-associated spore proteins that had not been previously reported in any *B. subtilis* or *B. anthracis* vegetative or spore proteomic studies. The functions of identified spore membrane proteins spread into almost all membrane protein function categories, including transport, protein fate determination, and energy production and conversion. Novel membrane-associated spore proteins that were expressed under the control of forespore-specific σ^G are highly interesting targets to be further investigated. Some of these proteins have amino acid sequence homologies to known inorganic ion transporters, amino acid transporters, and proteases. Proteins with these functions may play major roles in spore formation and germination, therefore further characterization of these proteins is needed. A quarter of these membrane-associated spore

proteins have no known function or significant sequence similarities to known proteins. Further characterization of these proteins may reveal missing pieces in understanding the sporulation, germination, and/or outgrowth processes.

Quantitative analysis of proteins in both *Bacillus* species revealed a notable trend that the number of identified membrane proteins is greatly reduced in germinating spores. These reduced membrane proteins are in multiple COG function categories, which suggested that the protein abundance decrease is a general spore germination phenomenon. The reason behind this phenomenon is unclear. Evidence showed that the area of the IFM experienced significant decrease late in sporulation and dramatic increase after spore cortex is degraded (6). Perhaps the change of membrane-associated proteome is due to the rearrangement of membrane during spore germination.

HtrC, a membrane-associated serine protease homolog identified in both *Bacillus* spore membrane proteomes, was characterized in Chapter 4 to examine its role in determining YpeB protein fate during spore germination. We demonstrated that YpeB was proteolytically processed during germination and a stable C-terminal fragment was produced. The primary cleavage site was identified in *B. anthracis*, but other cleavage sites are accessible when the primary site is blocked. The *in vivo* and *in vitro* evidence accumulated in this study proved that HtrC is responsible for proteolytically cleaving YpeB and producing the stable fragment during germination. However, without HtrC presenting in the spore, other proteases appear to degrade YpeB at a reduced rate. This may explain why there was no significant germination defect in *htrC* deletion spores. We also demonstrated that YpeB and SleB, in the absence of their partner protein, were degraded by unknown proteases other than HtrC during spore formation. The unknown proteases cleave YpeB at a site close to the HtrC cleavage site, and therefore they may not be the proteases that cleave YpeB during germination when HtrC is absent. Identification and characterization of these unknown proteases would be a future

direction for revealing the roles of proteases in spore germination. Further study of the proteases identified in spore membrane proteomes could be a good start point.

In vitro characterization of HtrC showed a relatively low protease activity with a requirement for a relatively high concentration of Mn^{2+} or Ca^{2+} ions. We suspect that the ions may not be directly involved in HtrC catalytic function for the following reasons: 1) HtrC belongs to a class of serine protease that requires no metal ion in catalysis (166); 2) Most Mn^{2+} and Ca^{2+} released during germination is likely bound to DPA, and we have demonstrated that at least Ca^{2+}-DPA is ineffective in promoting HtrC activity; 3) The concentration requirement of metal ions as cofactor for a protease activity is at least 1,000-fold less than that is required for HtrC activation (174, 175). The reason why a high concentration of Mn^{2+} or Ca^{2+} ions promotes HtrC activity *in vitro* is still unclear. Perhaps like other HtrA family proteases, the PDZ domain of HtrC is critical for fully activating its protease activity (176, 177), and the high concentration of metal ions may drive the PDZ domain towards the active configuration. It is also possible that other proteins associated with HtrC or other native materials released from spore core could be the native cofactors for HtrC protease activity. Further characterization of this protease, and possibly study of its crystal structure, would help achieve a full understand its role in the YpeB degradation process.

We hope that the studies presented here will promote an understainding of the nutrient-mediated germination signal pathway in which many spore membrane proteins may be involved. Our long-term purpose is to drive the development of more effective decontamination methods utilizing knowledge of the spore germination pathway to germinate spores prematurely and synchronously. These efforts will alleviate the public health burden caused by spore contamination and will prevent disease transmission.

REFERENCES

1. Waites WM (1984) Antimicrobial Agents Acting on Bacterial-Spores. *Journal of Applied Bacteriology* 57(3):R6-R6.
2. Russell AD (1990) Bacterial spores and chemical sporicidal agents. *Clin Microbiol Rev* 3(2):99-119.
3. Foster SJ & Johnstone K (1990) Pulling the trigger: the mechanism of bacterial spore germination. *Mol Microbiol* 4(1):137-141.
4. Setlow P (2007) I will survive: DNA protection in bacterial spores. *Trends Microbiol* 15(4):172-180.
5. Raju D, Waters M, Setlow P, & Sarker MR (2006) Investigating the role of small, acid-soluble spore proteins (SASPs) in the resistance of Clostridium perfringens spores to heat. *BMC Microbiol* 6:50.
6. Cowan AE, *et al.* (2004) Lipids in the inner membrane of dormant spores of *Bacillus* species are largely immobile. *Proc Natl Acad Sci U S A* 101(20):7733-7738.
7. Ramamurthi KS, Clapham KR, & Losick R (2006) Peptide anchoring spore coat assembly to the outer forespore membrane in *Bacillus subtilis*. *Mol Microbiol* 62(6):1547-1557.
8. Atrih A, Zollner P, Allmaier G, Williamson MP, & Foster SJ (1998) Peptidoglycan structural dynamics during germination of *Bacillus subtilis* 168 endospores. *J Bacteriol* 180(17):4603-4612.
9. Meador-Parton J & Popham DL (2000) Structural analysis of *Bacillus subtilis* spore peptidoglycan during sporulation. *J Bacteriol* 182(16):4491-4499.
10. Driks A (1999) *Bacillus subtilis* spore coat. *Microbiol Mol Biol Rev* 63(1):1-20.
11. Driks A (2002) Maximum shields: the assembly and function of the bacterial spore coat. *Trends Microbiol* 10(6):251-254.
12. Nicholson WL, Munakata N, Horneck G, Melosh HJ, & Setlow P (2000) Resistance of *Bacillus* endospores to extreme terrestrial and extraterrestrial environments. *Microbiol Mol Biol Rev* 64(3):548-572.
13. Setlow P (2006) Spores of Bacillus subtilis: their resistance to and killing by radiation, heat and chemicals. *J Appl Microbiol* 101(3):514-525.
14. Henriques AO & Moran CP, Jr. (2007) Structure, assembly, and function of the spore surface layers. *Annu Rev Microbiol* 61:555-588.
15. Wang ST, *et al.* (2006) The forespore line of gene expression in *Bacillus subtilis*. *J Mol Biol* 358(1):16-37.
16. Stragier P & Losick R (1996) Molecular genetics of sporulation in *Bacillus subtilis*. *Annu Rev Genet* 30:297-241.
17. Errington J (2003) Regulation of endospore formation in *Bacillus subtilis*. *Nat Rev Microbiol* 1(2):117-126.
18. Phillips ZE & Strauch MA (2002) *Bacillus subtilis* sporulation and stationary phase gene expression. *Cell Mol Life Sci* 59(3):392-402.
19. Paidhungat M & Setlow P (2000) Role of ger proteins in nutrient and nonnutrient triggering of spore germination in *Bacillus subtilis*. *J Bacteriol* 182(9):2513-2519.
20. Setlow P (2003) Spore germination. *Curr Opin Microbiol* 6(6):550-556.
21. Moir A (2006) How do spores germinate? *Journal of Applied Microbiology* 101(3):526-530.
22. Ghosh S & Setlow P (2009) Isolation and characterization of superdormant spores of *Bacillus* species. *J Bacteriol* 191(6):1787-1797.
23. Ghosh S & Setlow P (2009) The preparation, germination properties and stability of superdormant spores of *Bacillus cereus*. *J Appl Microbiol*.
24. Ghosh S, Scotland M, & Setlow P (2012) Levels of germination proteins in dormant and superdormant spores of *Bacillus subtilis*. *J Bacteriol* 194(9):2221-2227.
25. Wang G, Yi X, Li YQ, & Setlow P (2011) Germination of individual *Bacillus subtilis* spores with alterations in the GerD and SpoVA proteins, which are important in spore germination. *J Bacteriol* 193(9):2301-2311.
26. Pelczar PL, Igarashi T, Setlow B, & Setlow P (2007) Role of GerD in germination of *Bacillus subtilis* spores. *J Bacteriol* 189(3):1090-1098.
27. Vepachedu VR & Setlow P (2005) Localization of SpoVAD to the inner membrane of spores of *Bacillus subtilis*. *J Bacteriol* 187(16):5677-5682.
28. Paidhungat M & Setlow P (2001) Localization of a germinant receptor protein (GerBA) to the inner membrane of *Bacillus subtilis* spores. *J Bacteriol* 183(13):3982-3990.
29. Masayama A, *et al.* (2006) Subcellular localization of a germiantion-specific cortex-lytic enzyme, SleB, of Bacilli during sporulation. *Genes Genet Syst* 81(3):163-169.

30. Moir A, Lafferty E, & Smith DA (1979) Genetic-Analysis of Spore Germination Mutants of *Bacillus-Subtilis* 168 - Correlation of Phenotype with Map Location. *Journal of General Microbiology* 111(Mar):165-180.
31. Sammons RL, Moir A, & Smith DA (1981) Isolation and Properties of Spore Germination Mutants of *Bacillus-Subtilis*-168 Deficient in the Initiation of Germination. *Journal of General Microbiology* 124(Jun):229-241.
32. Corfe BM, Sammons RL, Smith DA, & Mauel C (1994) The *gerB* region of the *Bacillus subtilis* 168 chromosome encodes a homologue of the gerA spore germination operon. *Microbiology* 140 (Pt 3):471-478.
33. Irie R, Fujita Y, & Kobayashi M (1996) Nucleotide sequence and gene organization of the *gerK* spore germination locus of *Bacillus subtilis* 168. *Journal of General and Applied Microbiology* 42(2):141-153.
34. Moir A, Corfe BM, & Behravan J (2002) Spore germination. *Cell Mol Life Sci* 59(3):403-409.
35. Kunst F, *et al.* (1997) The complete genome sequence of the gram-positive bacterium *Bacillus subtilis*. *Nature* 390(6657):249-256.
36. Kemp EH, Sammons RL, Moir A, Sun D, & Setlow P (1991) Analysis of transcriptional control of the *gerD* spore germination gene of *Bacillus subtilis* 168. *J Bacteriol* 173(15):4646-4652.
37. Pelczar PL & Setlow P (2008) Localization of the germination protein GerD to the inner membrane in *Bacillus subtilis* spores. *J Bacteriol* 190(16):5635-5641.
38. Mongkolthanaruk W, Robinson C, & Moir A (2009) Localization of the GerD spore germination protein in the *Bacillus subtilis* spore. *Microbiology* 155(Pt 4):1146-1151.
39. Robinson C, Rivolta C, Karamata D, & Moir A (1998) The product of the *yvoC* (*gerF*) gene of *Bacillus subtilis* is required for spore germination. *Microbiology* 144 (Pt 11):3105-3109.
40. Igarashi T, Setlow B, Paidhungat M, & Setlow P (2004) Effects of a *gerF* (*lgt*) mutation on the germination of spores of *Bacillus subtilis*. *J Bacteriol* 186(10):2984-2991.
41. Sankaran K & Wu HC (1994) Lipid modification of bacterial prolipoprotein. Transfer of diacylglyceryl moiety from phosphatidylglycerol. *J Biol Chem* 269(31):19701-19706.
42. Fisher N & Hanna P (2005) Characterization of *Bacillus anthracis* germinant receptors in vitro. *J Bacteriol* 187(23):8055-8062.
43. Ireland JA & Hanna PC (2002) Amino acid- and purine ribonucleoside-induced germination of *Bacillus anthracis* DeltaSterne endospores: *gerS* mediates responses to aromatic ring structures. *J Bacteriol* 184(5):1296-1303.
44. Weiner MA, Read TD, & Hanna PC (2003) Identification and characterization of the *gerH* operon of *Bacillus anthracis* endospores: a differential role for purine nucleosides in germination. *J Bacteriol* 185(4):1462-1464.
45. Read TD, *et al.* (2003) The genome sequence of Bacillus anthracis Ames and comparison to closely related bacteria. *Nature* 423(6935):81-86.
46. Guidi-Rontani C, *et al.* (1999) Identification and characterization of a germination operon on the virulence plasmid pXO1 of *Bacillus anthracis*. *Mol Microbiol* 33(2):407-414.
47. Sirard JC, Guidi-Rontani C, Fouet A, & Mock M (2000) Characterization of a plasmid region involved in *Bacillus anthracis* toxin production and pathogenesis. *Int J Med Microbiol* 290(4-5):313-316.
48. Shah IM, Laaberki MH, Popham DL, & Dworkin J (2008) A eukaryotic-like Ser/Thr kinase signals bacteria to exit dormancy in response to peptidoglycan fragments. *Cell* 135(3):486-496.
49. Sorg JA & Sonenshein AL (2008) Bile salts and glycine as cogerminants for *Clostridium difficile* spores. *J Bacteriol* 190(7):2505-2512.
50. Paidhungat M, Setlow B, Driks A, & Setlow P (2000) Characterization of spores of *Bacillus subtilis* which lack dipicolinic acid. *J Bacteriol* 182(19):5505-5512.
51. Magge A, *et al.* (2008) Role of dipicolinic acid in the germination, stability, and viability of spores of *Bacillus subtilis*. *J Bacteriol* 190(14):4798-4807.
52. Daniel RA & Errington J (1993) Cloning, DNA sequence, functional analysis and transcriptional regulation of the genes encoding dipicolinic acid synthetase required for sporulation in *Bacillus subtilis*. *J Mol Biol* 232(2):468-483.
53. Driks A (2002) Overview: Development in bacteria: spore formation in *Bacillus subtilis*. *Cell Mol Life Sci* 59(3):389-391.
54. Tovar-Rojo F, Chander M, Setlow B, & Setlow P (2002) The products of the *spoVA* operon are involved in dipicolinic acid uptake into developing spores of *Bacillus subtilis*. *J Bacteriol* 184(2):584-587.
55. Vepachedu VR & Setlow P (2004) Analysis of the germination of spores of *Bacillus subtilis* with temperature sensitive spo mutations in the *spoVA* operon. *FEMS Microbiol Lett* 239(1):71-77.

56. Kong L, Zhang P, Setlow P, & Li YQ (2010) Characterization of Bacterial Spore Germination Using Integrated Phase Contrast Microscopy, Raman Spectroscopy, and Optical Tweezers. *Anal Chem*.
57. Zhang P, Setlow P, & Li Y (2009) Characterization of single heat-activated *Bacillus* spores using laser tweezers Raman spectroscopy. *Opt Express* 17(19):16480-16491.
58. Zhang P, *et al.* (2010) Factors affecting variability in time between addition of nutrient germinants and rapid dipicolinic acid release during germination of spores of Bacillus species. *J Bacteriol* 192(14):3608-3619.
59. Zhang P, Kong L, Setlow P, & Li YQ (2010) Characterization of wet-heat inactivation of single spores of *bacillus* species by dual-trap Raman spectroscopy and elastic light scattering. *Appl Environ Microbiol* 76(6):1796-1805.
60. Thackray PD, Behravan J, Southworth TW, & Moir A (2001) GerN, an antiporter homologue important in germination of *Bacillus cereus* endospores. *J Bacteriol* 183(2):476-482.
61. Heffron JD, Orsburn B, & Popham DL (2009) Roles of germination-specific lytic enzymes CwlJ and SleB in *Bacillus anthracis*. *J Bacteriol* 191(7):2237-2247.
62. Lambert EA & Popham DL (2008) The *Bacillus anthracis* SleL (YaaH) protein is an N-acetylglucosaminidase involved in spore cortex depolymerization. *J Bacteriol* 190(23):7601-7607.
63. Popham DL, Heffron JD, & Lambert EA (2012) Degradation of Spore Peptidoglycan During Germination. *Bacterial Spores: Current Research and Applications*:121-142.
64. Chirakkal H, O'Rourke M, Atrih A, Foster SJ, & Moir A (2002) Analysis of spore cortex lytic enzymes and related proteins in *Bacillus subtilis* endospore germination. *Microbiology* 148(Pt 8):2383-2392.
65. Heffron JD, Lambert EA, Sherry N, & Popham DL (2010) Contributions of four cortex lytic enzymes to germination of *Bacillus anthracis* spores. *J Bacteriol* 192(3):763-770.
66. Moriyama R, *et al.* (1996) A germination-specific spore cortex-lytic enzyme from *Bacillus cereus* spores: cloning and sequencing of the gene and molecular characterization of the enzyme. *J Bacteriol* 178(17):5330-5332.
67. Liu H, *et al.* (2004) Formation and composition of the *Bacillus anthracis* endospore. *J Bacteriol* 186(1):164-178.
68. Moriyama R, *et al.* (1999) Expression of a germination-specific amidase, SleB, of Bacilli in the forespore compartment of sporulating cells and its localization on the exterior side of the cortex in dormant spores. *J Bacteriol* 181(8):2373-2378.
69. Bernhards CB & Popham DL (2014) The role of YpeB in cortex hydrolysis during germination of *Bacillus anthracis spores*. *J Bacteriol*.
70. Boland FM, Atrih A, Chirakkal H, Foster SJ, & Moir A (2000) Complete spore-cortex hydrolysis during germination of *Bacillus subtilis* 168 requires SleB and YpeB. *Microbiology* 146 (Pt 1):57-64.
71. Ishikawa S, Yamane K, & Sekiguchi J (1998) Regulation and characterization of a newly deduced cell wall hydrolase gene (*cwlJ*) which affects germination of *Bacillus subtilis* spores. *J Bacteriol* 180(6):1375-1380.
72. Bagyan I & Setlow P (2002) Localization of the cortex lytic enzyme CwlJ in spores of *Bacillus subtilis*. *J Bacteriol* 184(4):1219-1224.
73. Paidhungat M, Ragkousi K, & Setlow P (2001) Genetic requirements for induction of germination of spores of *Bacillus subtilis* by Ca(2+)-dipicolinate. *J Bacteriol* 183(16):4886-4893.
74. Atrih A & Foster SJ (2001) In vivo roles of the germination-specific lytic enzymes of *Bacillus subtilis* 168. *Microbiology* 147(Pt 11):2925-2932.
75. Chen Y, Fukuoka S, & Makino S (2000) A novel spore peptidoglycan hydrolase of *Bacillus cereus*: biochemical characterization and nucleotide sequence of the corresponding gene, sleL. *J Bacteriol* 182(6):1499-1506.
76. Eymann C, *et al.* (2004) A comprehensive proteome map of growing *Bacillus subtilis* cells. *Proteomics* 4(10):2849-2876.
77. Dreisbach A, *et al.* (2008) Monitoring of changes in the membrane proteome during stationary phase adaptation of *Bacillus subtilis* using in vivo labeling techniques. *Proteomics* 8(10):2062-2076.
78. Francis AW, *et al.* (2005) Proteomic analysis of *Bacillus anthracis* Sterne vegetative cells. *Biochim Biophys Acta* 1748(2):191-200.
79. Kuwana R, *et al.* (2002) Proteomics characterization of novel spore proteins of *Bacillus subtilis*. *Microbiology* 148(Pt 12):3971-3982.
80. Mao L, *et al.* (2011) Protein profile of *Bacillus subtilis* spore. *Curr Microbiol* 63(2):198-205.
81. Huang CM, *et al.* (2004) Identification of *Bacillus anthracis* proteins associated with germination and early outgrowth by proteomic profiling of anthrax spores. *Proteomics* 4(9):2653-2661.
82. Delvecchio VG, *et al.* (2006) Proteomic profiling and identification of immunodominant spore antigens of *Bacillus anthracis*, *Bacillus cereus*, and *Bacillus thuringiensis*. *Appl Environ Microbiol* 72(9):6355-6363.

83. Jagtap P, *et al.* (2006) Early events of *Bacillus anthracis* germination identified by time-course quantitative proteomics. *Proteomics* 6(19):5199-5211.
84. Lai EM, *et al.* (2003) Proteomic analysis of the spore coats of *Bacillus subtilis* and *Bacillus anthracis*. *J Bacteriol* 185(4):1443-1454.
85. Abhyankar W, *et al.* (2011) Gel-free proteomic identification of the *Bacillus subtilis* insoluble spore coat protein fraction. *Proteomics* 11(23):4541-4550.
86. Abhyankar W, *et al.* (2013) In pursuit of protein targets: proteomic characterization of bacterial spore outer layers. *J Proteome Res* 12(10):4507-4521.
87. Leggett MJ, McDonnell G, Denyer SP, Setlow P, & Maillard JY (2012) Bacterial spore structures and their protective role in biocide resistance. *J Appl Microbiol* 113(3):485-498.
88. Riesenman PJ & Nicholson WL (2000) Role of the spore coat layers in *Bacillus subtilis* spore resistance to hydrogen peroxide, artificial UV-C, UV-B, and solar UV radiation. *Appl Environ Microbiol* 66(2):620-626.
89. Mallozzi M, Viswanathan VK, & Vedantam G (2010) Spore-forming Bacilli and Clostridia in human disease. *Future Microbiol* 5(7):1109-1123.
90. Wang G, *et al.* (2011) Analysis of the germination of individual *Clostridium perfringens* spores and its heterogeneity. *J Appl Microbiol* 111(5):1212-1223.
91. Zhang P, *et al.* (2012) Analysis of the slow germination of multiple individual superdormant *Bacillus subtilis* spores using multifocus Raman microspectroscopy and differential interference contrast microscopy. *J Appl Microbiol* 112(3):526-536.
92. Zuberi AR, Feavers IM, & Moir A (1985) Identification of three complementation units in the *gerA* spore germination locus of *Bacillus subtilis*. *J Bacteriol* 162(2):756-762.
93. Moir A, Kemp EH, Robinson C, & Corfe BM (1994) The genetic analysis of bacterial spore germination. *J Appl Bacteriol* 77(3):9S-16S.
94. Ramirez-Peralta A, *et al.* (2013) Identification of New Proteins That Modulate the Germination of Spores of *Bacillus* Species. *Journal of Bacteriology* 195(13):3009-3021.
95. Atluri S, Ragkousi K, Cortezzo DE, & Setlow P (2006) Cooperativity between different nutrient receptors in germination of spores of *Bacillus subtilis* and reduction of this cooperativity by alterations in the GerB receptor. *Journal of Bacteriology* 188(1):28-36.
96. Vepachedu VR & Setlow P (2007) Role of SpoVA proteins in release of dipicolinic acid during germination of *Bacillus subtilis* spores triggered by dodecylamine or lysozyme. *J Bacteriol* 189(5):1565-1572.
97. Fort P & Errington J (1985) Nucleotide sequence and complementation analysis of a polycistronic sporulation operon, *spoVA*, in *Bacillus subtilis*. *J Gen Microbiol* 131(5):1091-1105.
98. Popham DL, Helin J, Costello CE, & Setlow P (1996) Muramic lactam in peptidoglycan of *Bacillus subtilis* spores is required for spore outgrowth but not for spore dehydration or heat resistance. *Proc Natl Acad Sci U S A* 93(26):15405-15410.
99. Stewart KA, Yi X, Ghosh S, & Setlow P (2012) Germination protein levels and rates of germination of spores of *Bacillus subtilis* with overexpressed or deleted genes encoding germination proteins. *J Bacteriol* 194(12):3156-3164.
100. Cabrera-Martinez RM, Tovar-Rojo F, Vepachedu VR, & Setlow P (2003) Effects of overexpression of nutrient receptors on germination of spores of *Bacillus subtilis*. *Journal of Bacteriology* 185(8):2457-2464.
101. Picotti P, *et al.* (2010) High-throughput generation of selected reaction-monitoring assays for proteins and proteomes. *Nat Methods* 7(1):43-46.
102. Leighton TJ & Doi RH (1971) The stability of messenger ribonucleic acid during sporulation in *Bacillus subtilis*. *J Biol Chem* 246(10):3189-3195.
103. Nicholson WL & Setlow P (1990) Sporulation, germination, and outgrowth. *Molecular biological methods for Bacillus.*, eds Harwood CR & Cutting SM (John Wiley & Sons Ltd., Chichester, England.), pp 391-450.
104. Hahne H, Wolff S, Hecker M, & Becher D (2008) From complementarity to comprehensiveness--targeting the membrane proteome of growing *Bacillus subtilis* by divergent approaches. *Proteomics* 8(19):4123-4136.
105. González-Castro MJ, López-Hernández J, Simal-Lozano J, & Oruña-Concha MJ (1997) Determination of amino acids in green beans by derivitization with phenylisothiocyanate and high-performance liquid chromatography with ultraviolet detection. *J. Chrom. Sci.* 35:181-185.
106. Fusaro VA, Mani DR, Mesirov JP, & Carr SA (2009) Prediction of high-responding peptides for targeted protein assays by mass spectrometry. *Nat Biotechnol* 27(2):190-198.
107. Paredes-Sabja D, Setlow B, Setlow P, & Sarker MR (2008) Characterization of *Clostridium perfringens* spores that lack SpoVA proteins and dipicolinic acid. *J Bacteriol* 190(13):4648-4659.

108. Forouhar F, *et al.* (2010) Crystal structure of Stage V sporulation protein AD (SpoVAD) from *Bacillus subtilis*, Northeast Structural Genomics Consortium Target SR525. *PDB id: 3LM6*.
109. Stewart KA & Setlow P (2013) Numbers of individual nutrient germinant receptors and other germination proteins in spores of *Bacillus subtilis*. *J Bacteriol* 195(16):3575-3582.
110. Griffiths KK, Zhang J, Cowan AE, Yu J, & Setlow P (2011) Germination proteins in the inner membrane of dormant *Bacillus subtilis* spores colocalize in a discrete cluster. *Mol Microbiol* 81(4):1061-1077.
111. Vepachedu VR & Setlow P (2007) Analysis of interactions between nutrient germinant receptors and SpoVA proteins of *Bacillus subtilis* spores. *FEMS Microbiol Lett* 274(1):42-47.
112. Korza G & Setlow P (2013) Topology and accessibility of germination proteins in the *Bacillus subtilis* spore inner membrane. *J Bacteriol* 195(7):1484-1491.
113. Li Y, *et al.* (2012) Role of a SpoVA protein in dipicolinic acid uptake into developing spores of *Bacillus subtilis*. *J Bacteriol* 194(8):1875-1884.
114. Setlow P & Johnson EA (2007) Spores and Their Significance. *Food Microbiology: Fundamentals and Frontiers, Third Edition*:35-67.
115. Amuguni H & Tzipori S (2012) *Bacillus subtilis*: a temperature resistant and needle free delivery system of immunogens. *Hum Vaccin Immunother* 8(7):979-986.
116. Cutting SM, Hong HA, Baccigalupi L, & Ricca E (2009) Oral vaccine delivery by recombinant spore probiotics. *International reviews of immunology* 28(6):487-505.
117. Knecht LD, Pasini P, & Daunert S (2011) Bacterial spores as platforms for bioanalytical and biomedical applications. *Anal Bioanal Chem* 400(4):977-989.
118. Koshikawa T, *et al.* (1984) Resistance, germination, and permeability correlates of *Bacillus megaterium* spores successively divested of integument layers. *J Bacteriol* 159(2):624-632.
119. Indest KJ, Buchholz WG, Faeder JR, & Setlow P (2009) Workshop report: modeling the molecular mechanism of bacterial spore germination and elucidating reasons for germination heterogeneity. *J Food Sci* 74(6):R73-78.
120. Bergman NH, *et al.* (2006) Transcriptional profiling of the *Bacillus anthracis* life cycle in vitro and an implied model for regulation of spore formation. *J Bacteriol* 188(17):6092-6100.
121. Eichenberger P, *et al.* (2004) The program of gene transcription for a single differentiating cell type during sporulation in *Bacillus subtilis*. *PLoS Biol* 2(10):e328.
122. Eichenberger P, *et al.* (2003) The sigma(Epsilon) regulon and the identification of additional sporulation genes in *Bacillus subtilis*. *Journal of Molecular Biology* 327(5):945-972.
123. Kim HU & Goepfert JM (1974) A sporulation medium for *Bacillus anthracis*. *J Appl Bacteriol* 37(2):265-267.
124. Chen Y, Ray WK, Helm RF, Melville SB, & Popham DL (2014) Levels of germination proteins in *Bacillus subtilis* dormant, superdormant, and germinating spores. *PLoS One* 9(4):e95781.
125. Liu H, Sadygov RG, & Yates JR, 3rd (2004) A model for random sampling and estimation of relative protein abundance in shotgun proteomics. *Anal Chem* 76(14):4193-4201.
126. Altschul SF, Gish W, Miller W, Myers EW, & Lipman DJ (1990) Basic local alignment search tool. *J Mol Biol* 215(3):403-410.
127. Steil L, Serrano M, Henriques AO, & Volker U (2005) Genome-wide analysis of temporally regulated and compartment-specific gene expression in sporulating cells of *Bacillus subtilis*. *Microbiology* 151(Pt 2):399-420.
128. Serrano M, Corte L, Opdyke J, Moran CP, Jr., & Henriques AO (2003) Expression of *spoIIIJ* in the prespore is sufficient for activation of sigma G and for sporulation in *Bacillus subtilis*. *J Bacteriol* 185(13):3905-3917.
129. Winstedt L & von Wachenfeldt C (2000) Terminal oxidases of *Bacillus subtilis* strain 168: one quinol oxidase, cytochrome aa(3) or cytochrome bd, is required for aerobic growth. *J Bacteriol* 182(23):6557-6564.
130. Mattatall NR, Jazairi J, & Hill BC (2000) Characterization of YpmQ, an accessory protein required for the expression of cytochrome c oxidase in *Bacillus subtilis*. *J Biol Chem* 275(37):28802-28809.
131. Gilchrist A, *et al.* (2006) Quantitative proteomics analysis of the secretory pathway. *Cell* 127(6):1265-1281.
132. Charney J, Fisher WP, & Hegarty CP (1951) Managanese as an essential element for sporulation in the genus *Bacillus*. *J Bacteriol* 62(2):145-148.
133. Gerhardt P & Marquis RE (1989) Spore thermoresistance mechanisms. *Regulation of Prokaryotic Development*, eds Smith I, Slepecky RA, & Setlow P (American Society for Microbiology, Washington, D.C.), pp 43-63.

134. Granger AC, Gaidamakova EK, Matrosova VY, Daly MJ, & Setlow P (2011) Effects of Mn and Fe levels on *Bacillus subtilis* spore resistance and effects of Mn^{2+}, other divalent cations, orthophosphate, and dipicolinic acid on protein resistance to ionizing radiation. *Appl Environ Microbiol* 77(1):32-40.
135. Swerdlow BM, Setlow B, & Setlow P (1981) Levels of H+ and other monovalent cations in dormant and germinating spores of *Bacillus megaterium*. *J Bacteriol* 148(1):20-29.
136. Foster SJ & Johnstone K (1986) The Use of Inhibitors to Identify Early Events during *Bacillus-Megaterium* Km Spore Germination. *Biochemical Journal* 237(3):865-870.
137. Gaballa A & Helmann JD (1998) Identification of a zinc-specific metalloregulatory protein, Zur, controlling zinc transport operons in *Bacillus subtilis*. *J Bacteriol* 180(22):5815-5821.
138. Fujisawa M, Wada Y, Tsuchiya T, & Ito M (2009) Characterization of *Bacillus subtilis* YfkE (ChaA): a calcium-specific Ca^{2+}/H^{+} antiporter of the CaCA family. *Arch Microbiol* 191(8):649-657.
139. Tanaka K, Kobayashi K, & Ogasawara N (2003) The *Bacillus subtilis* YufLM two-component system regulates the expression of the malate transporters MaeN (YufR) and YflS, and is essential for utilization of malate in minimal medium. *Microbiology* 149(Pt 9):2317-2329.
140. Chillappagari S, Miethke M, Trip H, Kuipers OP, & Marahiel MA (2009) Copper acquisition is mediated by YcnJ and regulated by YcnK and CsoR in *Bacillus subtilis*. *J Bacteriol* 191(7):2362-2370.
141. Gibson MM, Bagga DA, Miller CG, & Maguire ME (1991) Magnesium transport in Salmonella typhimurium: the influence of new mutations conferring Co^{2+} resistance on the CorA Mg^{2+} transport system. *Mol Microbiol* 5(11):2753-2762.
142. Lorca G, Winnen B, & Saier MH, Jr. (2003) Identification of the L-aspartate transporter in *Bacillus subtilis*. *J Bacteriol* 185(10):3218-3222.
143. Sekowska A, Robin S, Daudin JJ, Henaut A, & Danchin A (2001) Extracting biological information from DNA arrays: an unexpected link between arginine and methionine metabolism in *Bacillus subtilis*. *Genome Biol* 2(6):RESEARCH0019.
144. Hullo MF, Auger S, Dassa E, Danchin A, & Martin-Verstraete I (2004) The metNPQ operon of *Bacillus subtilis* encodes an ABC permease transporting methionine sulfoxide, D- and L-methionine. *Res Microbiol* 155(2):80-86.
145. Fabret C & Hoch JA (1998) A two-component signal transduction system essential for growth of *Bacillus subtilis*: implications for anti-infective therapy. *J Bacteriol* 180(23):6375-6383.
146. Fukuchi K, *et al.* (2000) The essential two-component regulatory system encoded by *yycF* and *yycG* modulates expression of the *ftsAZ* operon in *Bacillus subtilis*. *Microbiology* 146 (Pt 7):1573-1583.
147. Dalbey RE, Wang P, & van Dijl JM (2012) Membrane proteases in the bacterial protein secretion and quality control pathway. *Microbiol Mol Biol Rev* 76(2):311-330.
148. Patel VJ, *et al.* (2009) A comparison of labeling and label-free mass spectrometry-based proteomics approaches. *J Proteome Res* 8(7):3752-3759.
149. Setlow P (2014) Germination of spores of *Bacillus* species: what we know and do not know. *J Bacteriol* 196(7):1297-1305.
150. Atrih A, Zollner P, Allmaier G, & Foster SJ (1996) Structural analysis of *Bacillus subtilis* 168 endospore peptidoglycan and its role during differentiation. *J Bacteriol* 178(21):6173-6183.
151. Sekiguchi J, *et al.* (1995) Nucleotide sequence and regulation of a new putative cell wall hydrolase gene, cwlD, which affects germination in *Bacillus subtilis*. *J Bacteriol* 177(19):5582-5589.
152. Setlow B, Melly E, & Setlow P (2001) Properties of spores of *Bacillus subtilis* blocked at an intermediate stage in spore germination. *J Bacteriol* 183(16):4894-4899.
153. Ragkousi K, Eichenberger P, van Ooij C, & Setlow P (2003) Identification of a new gene essential for germination of *Bacillus subtilis* spores with Ca^{2+}-dipicolinate. *J Bacteriol* 185(7):2315-2329.
154. Setlow B, *et al.* (2009) Characterization of the germination of *Bacillus megaterium* spores lacking enzymes that degrade the spore cortex. *J Appl Microbiol* 107(1):318-328.
155. Li Y, *et al.* (2013) Activity and regulation of various forms of CwlJ, SleB, and YpeB proteins in degrading cortex peptidoglycan of spores of Bacillus species in vitro and during spore germination. *J Bacteriol* 195(11):2530-2540.
156. Ho SN, Hunt HD, Horton RM, Pullen JK, & Pease LR (1989) Site-directed mutagenesis by overlap extension using the polymerase chain reaction. *Gene* 77(1):51-59.
157. van den Ent F & Lowe J (2006) RF cloning: A restriction-free method for inserting target genes into plasmids. *J Biochem Bioph Meth* 67(1):67-74.
158. Janes BK & Stibitz S (2006) Routine markerless gene replacement in *Bacillus anthracis*. *Infect Immun* 74(3):1949-1953.
159. Bishop-Lilly KA, *et al.* (2012) Whole genome sequencing of phage resistant *Bacillus anthracis* mutants reveals an essential role for cell surface anchoring protein CsaB in phage AP50c adsorption. *Virol J* 9:246.

160. Wach A (1996) PCR-synthesis of marker cassettes with long flanking homology regions for gene disruptions in *S. cerevisiae*. *Yeast* 12(3):259-265.
161. Austin BP, Nallamsetty S, & Waugh DS (2009) Hexahistidine-tagged maltose-binding protein as a fusion partner for the production of soluble recombinant proteins in *Escherichia coli*. *Methods Mol Biol* 498:157-172.
162. Kapust RB, *et al.* (2001) Tobacco etch virus protease: mechanism of autolysis and rational design of stable mutants with wild-type catalytic proficiency. *Protein Eng* 14(12):993-1000.
163. Giebel JD, Carr KA, Anderson EC, & Hanna PC (2009) The germination-specific lytic enzymes SleB, CwlJ1, and CwlJ2 each contribute to *Bacillus anthracis* spore germination and virulence. *J Bacteriol* 191(18):5569-5576.
164. Campo N & Rudner DZ (2007) SpoIVB and CtpB are both forespore signals in the activation of the sporulation transcription factor sigma K in *Bacillus subtilis*. *J Bacteriol* 189(16):6021-6027.
165. Mastny M, *et al.* (2013) CtpB assembles a gated protease tunnel regulating cell-cell signaling during spore formation in *Bacillus subtilis*. *Cell* 155(3):647-658.
166. Clausen T, Southan C, & Ehrmann M (2002) The HtrA family of proteases: implications for protein composition and cell fate. *Mol Cell* 10(3):443-455.
167. Slepecky R & Foster JW (1959) Alterations in metal content of spores of *Bacillus megaterium* and the effect on some spore properties. *J Bacteriol* 78(1):117-123.
168. Boschwitz H, Gofshtein-Gandman L, Halvorson HO, Keynan A, & Milner Y (1991) The possible involvement of trypsin-like enzymes in germination of spores of *Bacillus cereus* T and *Bacillus subtilis* 168. *J Gen Microbiol* 137(5):1145-1153.
169. Boschwitz H, Halvorson HO, Keynan A, & Milner Y (1985) Trypsinlike enzymes from dormant and germinated spores of *Bacillus cereus* T and their possible involvement in germination. *J Bacteriol* 164(1):302-309.
170. Boschwitz H, Milner Y, Keynan A, Halvorson HO, & Troll W (1983) Effect of inhibitors of trypsin-like proteolytic enzymes *Bacillus cereus* T spore germination. *J Bacteriol* 153(2):700-708.
171. Cortezzo DE, Setlow B, & Setlow P (2004) Analysis of the action of compounds that inhibit the germination of spores of *Bacillus species*. *J Appl Microbiol* 96(4):725-741.
172. Igarashi T & Setlow P (2005) Interaction between individual protein components of the GerA and GerB nutrient receptors that trigger germination of *Bacillus subtilis* spores. *Journal of Bacteriology* 187(7):2513-2518.
173. Li Y, *et al.* (2014) Structural and functional analysis of the GerD spore germination protein of *Bacillus species*. *J Mol Biol* 426(9):1995-2008.
174. Petersen LC, Olsen OH, Nielsen LS, Freskgard PO, & Persson E (2000) Binding of Zn^{2+} to a Ca^{2+} loop allosterically attenuates the activity of factor VIIa and reduces its affinity for tissue factor. *Protein Sci* 9(5):859-866.
175. Wakabayashi H, Zhen Z, Schmidt KM, & Fay PJ (2003) Mn^{2+} binding to factor VIII subunits and its effect on cofactor activity. *Biochemistry* 42(1):145-153.
176. Krojer T, *et al.* (2008) Interplay of PDZ and protease domain of DegP ensures efficient elimination of misfolded proteins. *Proc Natl Acad Sci U S A* 105(22):7702-7707.
177. Murwantoko, *et al.* (2004) Binding of proteins to the PDZ domain regulates proteolytic activity of HtrA1 serine protease. *Biochem J* 381(Pt 3):895-904.